2013

Application of Silver Nanoparticles in Drinking Water Purification

Hongyin Zhang
University of Rhode Island, hongyin1983@gmail.com

APPLICATION OF SILVER NANOPARTICLES IN DRINKING WATER PURIFICATION

BY

HONGYIN ZHANG

A DISSERTATION SUBMITTED IN PARTIAL FULFILLMENT OF THE REQUIREMENTS FOR THE DEGREE OF

DOCTOR OF PHILOSOPHY

IN

CIVIL AND ENVIRONMENTAL ENGINEERING

UNIVERSITY OF RHODE ISLAND

2013

DOCTOR OF PHILOSOPHY

OF

HONGYIN ZHANG

APPROVED:

Thesis Committee:

Major Professor Vinka Oyanedel-Craver

Leon Thiem

Thomas Boving

Geoffrey Bothun

Aaron Bradshaw

Nasser H. Zawia
DEAN OF THE GRADUATE SCHOOL

UNIVERSITY OF RHODE ISLAND
2013

ABSTRACT

Nanotechnology is an emerging and fast-growing technology. Currently, there are more than 1,317 nanotechnology-based products on the market. Silver nanoparticles account for more than 23% of all nano-products. The extensive application of the silver nanoparticle (AgNP) results in their inevitable release into the environment. Silver nanoparticles are known as excellent antimicrobial agents, and therefore they could be used as alternative disinfectant agents. On the other hand, released silver nanoparticles could pose a threat to naturally occurring microorganisms.

In Chapter 1, we introduce the background information on the environmental fate, toxicological effects, and application of AgNP and review the current knowledge on the physicochemical and antimicrobial properties of AgNP in different aqueous solutions, as well as their application as alternative disinfectants in water-treatment systems.

In Chapter 2 of this dissertation, we discuss the evaluation of AgNP's antimicrobial properties at different water chemistry conditions. It was found that the aggregation of silver nanoparticles depends on the properties of the background ions, such as Na^{+} and Ca^{2+}, at different water chemistry conditions. Divalent cations can significantly enhance the aggregation, while monovalent cations and anions do not have such a significant influence. A saturation-type fitting curve was established, showing the survival of bacteria under different water chemistry conditions as a function of the size of the nanoparticles.

In Chapter 3, we talk about the evaluation of the antimicrobial properties of AgNP when coated with different organic compounds using natural water conditions.

The results obtained showed that silver nanoparticles in surface water, ground water, and brackish water are stable. However, in seawater conditions, AgNP tend to aggregate. This study also shows that the antimicrobial activity of AgNP can be impaired by the presence of a humic substance and high concentrations of divalent cations. These results are helpful in explaining how discharged AgNP behave in natural aquatic systems as well as their environmental toxicological effects on naturally occurring microorganisms.

In Chapter 4, we discuss the investigation of the effect of silver nanoparticles on a model virus-MS2 bacteriophage. A negligible deactivation effect on MS2 phage was found regardless of the type of AgNP and the water chemistry conditions used.

In Chapter 5, we talk about the comparison of AgNP-impregnated point-of-use ceramic water filters and ceramic filters impregnated with silver nitrate. This study was performed using different water chemistry conditions and different manufacturing materials. The results showed that AgNP-impregnated ceramic water filters are more appropriate for this application due to the lesser amount of silver desorbed compared with silver nitrate-treated filters. The bacterial removal performance of the silver-treated ceramic filters and concentration of viable bacteria in the filters are dose-dependent on the amount of silver applied. However, the data showed that influent water chemistry conditions did not have a significant effect on the performance of the filters. This study established evidence-based silver application guidelines for the ceramic water filter manufacturers around the world.

In Chapter 6, the discussion centers in the comparison of a polymer-based quaternary amine functionalized silsesquioxanes compound and AgNP. The results

showed that the quaternary ammonium functionalized silsesquioxanes-treated ceramic water filter desorbed less from the filters and achieved higher bacteria removal than the filters impregnated with AgNP. This indicates that the quaternary ammonium functionalized silsesquioxanes compound could be considered as a substitute for silver nanoparticles due to its lower price and higher performance. However, more information regarding the possible chronic health effects of the silsesquioxanes compound is needed.

In Chapter 7, we present the main conclusions and recommended future work based on the dissertation results.

ACKNOWLEDGMENTS

I would like to first thank Dr. Vinka Oyanedel-Craver for her inculcation over the last four years. She has endowed me with valuable knowledge that will benefit me throughout my life. She also set up an example with meticulous spirit and enthusiasm to explore. I would also like to express my thanks to Dr. Geoffrey Bothun for his useful suggestions, advices, and his permission to access to the instruments in his laboratory. Dr. Thomas Boving and Dr. Thiem have provided constructive advices and conferred the very helpful knowledge in the environmental field. I would like to thank Dr. Aaron Bradshaw for his commitment to the Dissertation committee and his valuable comments and suggestions.

My thanks also go to my family. Thanks to my parents who supported me in my overseas life. I am also very grateful to my lovely wife, who always encourages me to go forward.

PREFACE

This dissertation is in manuscript format.

Chapter 2 was originally published by H. Zhang and V. Oyanedel-Craver, *Journal of Environmental Engineering* 138 (1) (2012) 58-66.

Chapter 3 was published by H. Zhang, J. Smith, and V. Oyanedel-Craver, Water Research (2012) 691-699. In addition to the published manuscript text, supplementary text and figures have been included.

Chapter 4 is a manuscript in preparation to be submitted by H. Zhang and V. Oyanedel-Craver to Water Research.

Chapter 5 was submitted for publication in ACS Sustainable Chemistry and Engineering by J. Rayner, H. Zhang, D. Lantagne, J. Schubert, P. Lennon, and V. Oyanedel-Craver. In addition to the published manuscript text, supplementary text and figures have been included.

Chapter 6 was submitted for publication in Journal of Hazardous Materials by H. Zhang and V. Oyanedel-Craver.

TABLE OF CONTENTS

LIST OF TABLES

LIST OF FIGURES

CHAPTER 1

INTRODUCTION

Nanoparticles are defined as small particles sized between 1 to 100 nanometers in at least one dimension. Currently there are more than 1,317 nanotechnology-based consumer products according to an analysis by Nanotechproject.com [1]. Compared to their counterparts in bulk states, manufactured nanomaterials have the merits of better adjustable electronic properties, better tunable optical properties, and higher reactivity. Among all the nano-products, 313 products (23%) are impregnated with nano-sized silver. Silver nanoparticles (AgNP) are used in a wide range of applications, including pharmaceuticals, cosmetics, medical devices, foodware, clothing and water purification, among others uses, due to their antimicrobial properties [2].

1 AgNP synthesis

AgNP can be prepared by various methods including chemical reduction, electrochemical techniques, and photochemical reduction [3]. Among all the synthetic methods, chemical reduction is most commonly used. However, toxic compounds such as borohydride are usually involved. Studies have focused on "green" synthesis approaches to avoid using hazardous materials. The Tollens method is widely applied for AgNP synthesis. Environmentally benign monosaccharides and polysaccharides are used to reduce the $Ag(NH_3)_2^+$ complex formed by reacting $AgNO_3$ with ammonia to AgNP. Previous studies have produced AgNP with sizes ranging from 50-200 nm and silver hydrosols ranging from 20-50 nm [4-6]. Panacek et al. [4] synthesized AgNP by reduction of the $Ag(NH_3)_2^+$ complex with two monosaccharides, glucose

and galactose, and two disaccharides, maltose and lactose, and found the average particle size ranged from 25 to 450 nm at various ammonia concentrations (0.005-0.2 M) and pH conditions (11.5-13.0) [4].

Aggregation during synthesis can hinder the production of AgNP with small and uniform sizes. For antimicrobial purposes, formation of aggregates can reduce the antimicrobial ability of AgNP [7-9]. Stabilizers are incorporated in the AgNP manufacturing process to ensure their stability in aqueous solutions. Absorption of the stabilizing molecules onto the nanoparticle surface depends on the molecular weight, ionization, and charge density of the stabilizing molecules [3, 4, 10, 11]. Stabilizing layers can increase the electrostatic and steric repulsion between nanoparticles and therefore enhance the stability of the nanosuspension [3, 12]. Commonly used stabilizing agents include different surfactants (such as sodium dodecyl sulfate (SDS) and Tween) and polymers including Polyvinylpyrrolidone (PVP) [13], Polyvinyl Achohol (PVA) [12], starch [8, 14], and various proteins [9, 15] .

2 Environmental fate and antimicrobial properties of AgNP in different water chemistry conditions

The use of AgNP in a wide variety of consumer products will inevitably lead to the release of the nanoparticles into natural water, which are the final receptacles [16]. Therefore, knowing the fate and reactivity of AgNP under environmentally relevant conditions is essential to prevent possible negative impacts on microorganisms commonly found in aquatic ecosystems.

2.1 Aggregation of AgNP in different water chemistry conditions

Previous studies have shown that different water chemistry conditions affect the

toxicity of AgNP on microorganism communities [17].

It is widely accepted that the aggregation of AgNP follows the Derjaguin-Landau-Verwey-Overbeek (DLVO) theory [18-20], which combines the effects of the van der Waals attraction force and the electrostatic repulsion force created by the double layer of counterions [8, 20, 21]. In an aqueous solution, AgNP are electrostatically stabilized when the energy barrier is formed, because the electrostatic repulsion force is in excess of the van der Waals attraction force. AgNP are stable under this condition. However, when electrolytes are introduced into the system, the counterions in the aqueous solution neutralize the surface charges and disrupt the energy barrier, leading to aggregation [19, 21-25]. Figure 1-1 is an example of AgNP aggregation at increasing concentrations of NaCl [13]. When addition of the electrolyte solution results in complete removal of the energy barrier, fast aggregation occurs and the cluster size increases regardless of the electrolyte concentration [19, 20, 26].

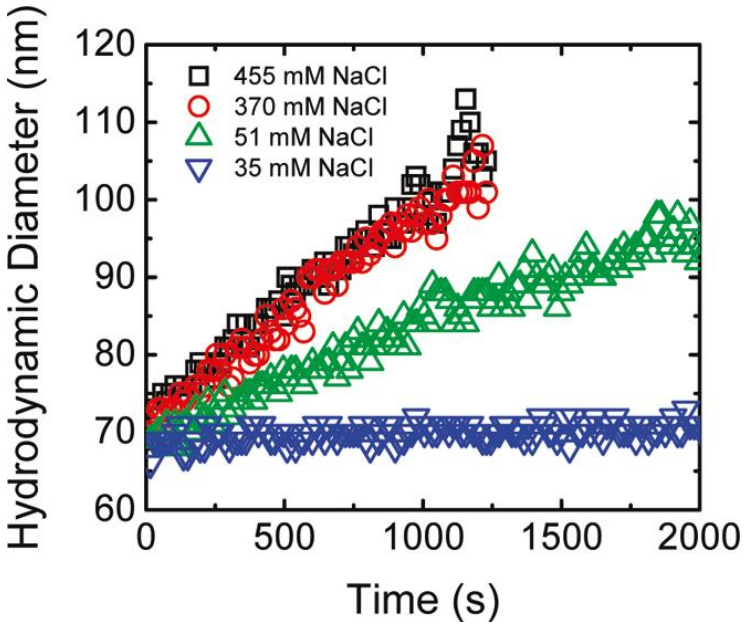

Figure 1-1 Aggregation kinetics of AgNP in different concentrations of NaCl solution [13].

ξ-potential is used to quantify the stability of the colloidal systems. Its value (negative or positive) indicates the degree of repulsion between charged particles in a nanosuspension. For AgNP suspension, high ξ-potential indicates the AgNP are electrically stabilized, while AgNP with low ξ-potential tend to aggregate. AgNP, in aerobic aqueous systems, carry negative charges because $Ag(OH)_2$ species at the surface can be formed due to the oxidation of metallic silver in the presence of O_2 in an aqueous solution [9, 19, 20]. In an aqueous solution containing ions, adsorption of anions can impart negative surface charges. More negative ξ-potential values indicate stronger electrostatic repulsion force between nanoparticles. Previous studies have also examined the effects of pH on the ξ-potential of AgNP. Li et al. [20] found that increasing pH (from 4-10) can better help stabilize the uncoated nanoparticles. Other studies [22] found similar trends using citrate coated AgNP across a wide pH range (2-10). As the silver atoms at the surface of AgNP are coordinately unsaturated, the OH^-

group can donate a pair of electrons. Therefore, when pH increases from 2- 10, the concentration of OH^- increases, thus allowing the OH^- to more effectively compete for surface sits, which generates a negative surface charge in alkaline pH conditions [22]. As the commonly used AgNP are negatively charged, increasing electrolyte concentration can increase the neutralization by the cations present in the electrolytes, which results in a decreasing ξ-potential (less stable) colloidal system [8].

Another mechanism of stabilization is steric repulsion [8, 9, 17, 18, 27]. Neutral organic coatings such as PVP and starch can also sterically prevent AgNP from aggregating [17, 20, 28]. Similarly, in water solutions containing natural organic matter (NOM), the NOM can absorb onto the AgNP surface, creating a physical barrier that hinders the contact between nanoparticles, and thus sterically stabilizing the nanoparticles.

Numerous studies have focused on the aggregation behavior of AgNP and have been summarized in Table 1-1.

Table 1-1 Recent studies investigated AgNP aggregation

AgNP types	Water matrices	References	Main findings
Casein coated AgNP	Electrolyte solution	[9]	Aggregation of casein coated AgNP agrees with DLVO theory; Humic acid introduces steric repulsion
Casein, dextrin, and PVP coated AgNP	Electrolyte solutions and natural water conditions	[8]	Aggregation of AgNP agrees with DLVO theory; Humic acid and PVP coating introduces steric repulsion
Bare, citrate, PVP, and BPEI coated AgNP	Electrolyte solution	[29]	Aggregation of AgNP agrees with DLVO theory
Citrate, SDS, Tween coated AgNP	Electrolyte solutions	[10]	Aggregation of AgNP agrees with DLVO theory
Citrate and PVP coated AgNP	Electrolyte solution	[13]	Aggregation of AgNP agrees with DLVO theory; Humic acid and PVP coating introduces steric repulsion
Bare AgNP	Electrolyte solutions	[20]	Aggregation of AgNP agrees with DLVO theory
Bare AgNP	Natural water conditions	[17]	Aggregation of AgNP agrees with DLVO theory; Humic acid introduces steric repulsion

2.2 Dissolution of AgNP in different water chemistry conditions

Dissolution of AgNP is an important parameter in determining their environmental fate. Recent studies have attempted to quantify the dissolution of AgNP in different water matrices. For aqueous solutions with different pHs, Liu and Hurt [28]and Elzey et al. [30] have found that lower pH can enhance the dissolution of AgNP. Figure 1-2 shows the dissolution of AgNP in the presence of DI and electrolyte solutions.

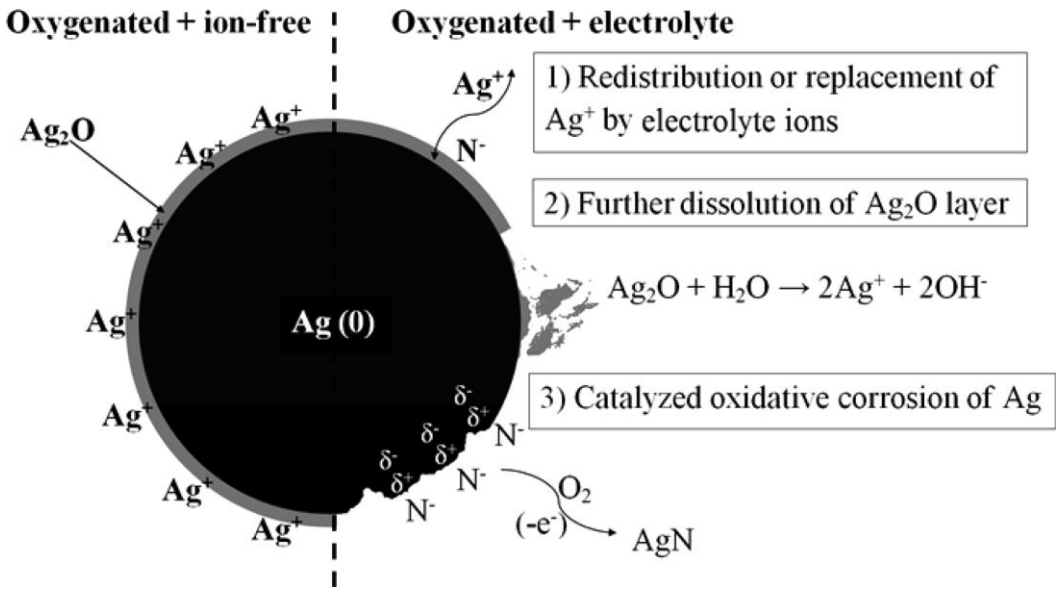

Figure 1-2 Schematic illustration of dissolution of the oxide layer coated AgNP [19].

In different environmental aqueous conditions, Liu and Hurt [28] investigated the dissolution kinetics of AgNP and reported that the number of dissolved silver ions from AgNP coated with sodium citrate (average particle size: 4.8±1.6 nm; initial concentration: 0.05 mg/L) in diluted synthetic seawater is more than that in seawater (ionic strength: 0.7 M). This study also showed that ionic strength and NOM may inhibit AgNP dissolution [28].

Effect of size of AgNP on the dissolution was also study. It was shown that the dissolution of smaller AgNP (coated with sodium citrate; particle size: 4.8 nm) is much higher than that of large AgNP (coated with sodium citrate; particle size: 60 nm).

Several studies have modeled the dissolution kinetics of AgNP. Lee et al. [31] has established a first-order dissolution rate in solutions with various AgNP concentrations, and the rate constants of first-order kinetics were calculated to

0.0734/h, 0.0709/h, and 0.0278/h for initial AgNP concentrations of 0.05 mg/L, 0.1 mg/L, and 1 mg/L [31]. A different AgNP dissolution model was established by Zhang et al. [32] using citrate coated AgNP (particle size ranges from 20-80 nm) indicating the dissolution kinetics agree with the Arrhenius equation [32].

2.3 Antimicrobial property of AgNP in different water chemistry conditions

Antimicrobial ability is a well-known property of AgNP. AgNP can inactivate a broad spectrum of microorganisms. Previous studies have proposed three mechanisms of the antimicrobial activities of AgNP (Figure 1-3): (i) Could attach to cell membrane and disrupt the permeability and respiration functions of the cell and thus kill the cells [7, 33, 34]; (ii) Reactive oxygen species (ROS) can be generated on the surface of nanoparticles and cause damage of DNA by exerting oxidative stress [35]; (iii) Silver ions released from AgNP can also cause disruption of ATP production and DNA replication [36, 37].

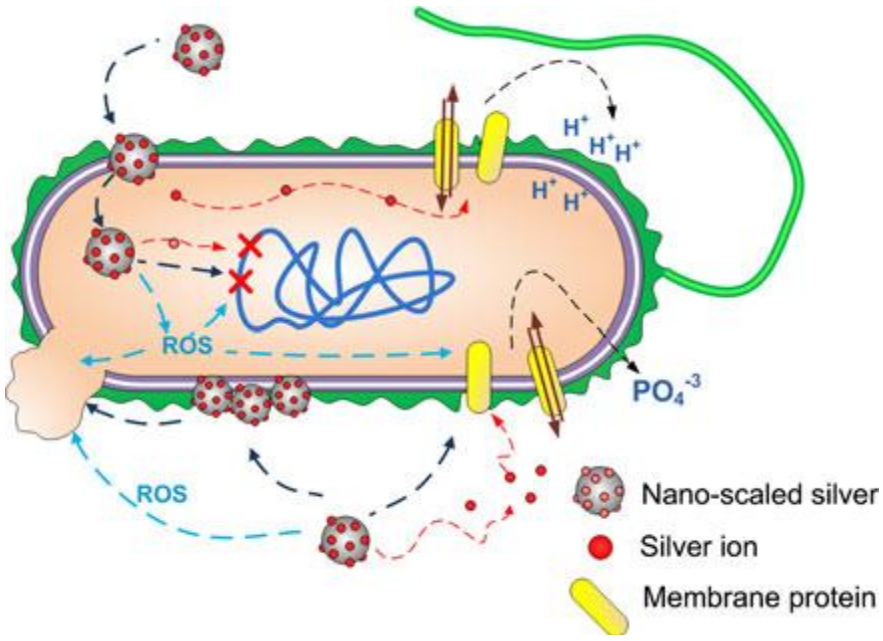

Figure 1-3 Mechanisms of interaction between AgNP and bacterial cells [38].

Previous studies have evaluated the toxicity of AgNP toward different microorganisms in aquatic systems. Gao et al. [17] have reported that the LC_{50} (μg/L) of AgNP against *Escherichia coli* (*E. coli*) and *Ceriodaphnia dubia* (*C. dubia*) are less than 112.14 and 6.18 μg/L, respectively. Studies on the toxicity of AgNP against other microorganisms, such as *Staphylococcus aureus* [39], *Leuconostoc mesenteroides* [40], *Bacillus subtilis* [41], and *Pseudomonas aeruginosa* [42] were also reported. Recent studies also focus on viruses, a smaller microorganism, as viruses are responsible for a wide spectrum of diseases in bacteria, plants, and animals and they play important role in aquatic food webs as active constituents of the microbial loop [43]. A recent study reported that AgNP (particle size: 21 nm) could not inactivate an MS2 bacteriophage in a phosphate buffer solution (PBS) even at their highest concentration (5 mg/L) [44]. Another study shows that IC_{50} of AgNP on different strains of HIV-1 virus ranged from 0.19-0.91 mg/mL [45]. However, more research is needed to determine the antiviral activity of AgNP in environmental relevant conditions and their antiviral mechanisms.

In environmental conditions, the antimicrobial property of AgNP can be affected by their stability in different water chemistry conditions. Environmental factors such as the presence of O_2, complexing agents (such as Cl^- and SO_4^{2-}, etc), and ionic strength influence the particle size, surface chemistry, and silver dissolution [46] of AgNP.

Under various oxidation conditions, Lok et al. [47] showed that *E. coli* colony formation was not affected by a treatment of 9.2 nm AgNP prepared under reducing conditions compared with the control group (*E. coli* without AgNP treatment).

However, after air saturation, aqueous solutions containing AgNP with O_2 for 30 min showed a strong antimicrobial effect on *E. coli*. Xiu et al. [48] revealed that the toxicity of AgNP was 20 times less toxic to *E. coli* than silver ions (EC_{50}: 2.04±0.07 vs 0.10±0.01mg/L) and the toxicity of AgNP increased 2.3-fold after exposure to air for 0.5 h. In these studies, the presence of a soluble Ag_2O layer was the key to the antimicrobial property of silver.

Several studies have investigated the antimicrobial activity of AgNP in different environmentally relevant conditions. Jin et al. [49] investigated the antibacterial properties of AgNP in different synthetic electrolyte solutions and elucidated that the antibacterial activity of AgNP was much lower than with silver ions when compared on the basis of total mass of AgNP added across all water conditions. However, bacterial inactivation also depended on the bacteria cell type as well as the hardness and alkalinity of the synthetic media. A similar study [50] investigated the effects of ligands (S^{2-}, Cl^-, SO_4^{2-}, PO_4^{3-}, and EDTA) on the toxicity of AgNP (1 mg/L). The study revealed that Cl^-, SO_4^{2-}, PO_4^{3-} can decrease bacterial inhibition by 20%; however, sulfide appeared to be more effective to reduce AgNP toxicity by 80%.

Natural organic matter has a negative impact of the antimicrobial performance of AgNP. Studies have shown that the organic matter can adsorb on the surface of AgNP and reduce the physical contact between AgNP and bacterial cells [8, 9, 17, 51]. In addition, the adsorption of organic matters can also inhibit their dissolution, resulting in a decreasing antimicrobial property [28].

The abovementioned studies focused on investigating the isolated water compositions, such as individual electrolytes or humic substances. However, more

comprehensive studies on the antimicrobial properties of AgNP in natural water conditions are needed for their environmental risk evaluations.

3 Application of AgNP in low cost drinking water purification systems

Currently, WHO/UNICEF estimated that 783 million people in the world do not have access to safe drinking water [52]. Boschi-Pinto et al. [53] reported 1.87 million childhood deaths are due to water-borne diseases [53]. Conventional water treatment and delivery approaches are considered unfeasible in these under-developed areas because they need high capital investments, a high cost of maintenance, a high-quantity water source, and these require users to pay for the treated water [54]. People have to collect their own water outside their homes and then store the water in the household due to the lack of water supply, and contaminations could occur during the water collection, transport, and storage, which cause a high chance of water-borne disease infection [54]. A point-of-use (POU) ceramic water filter (CWF) provides an option to purify the water.

A ceramic water filter (CWF) is a simple device that can eliminate water-borne pathogens. Currently, CWFs are manufactured by pressing and firing a mixture of clay and a burnable organic material such as flour, rice husks, or sawdust before treatment with AgNP [55]. The filter is formed using a filter press, after which it is air-dried and fired in a kiln. This forms the ceramic material and burns off the sawdust, flour, or rice husk in the filters, making it porous and permeable to water. CWFs are reported as effective in removing more than 99% of protozoa and 90-99.99% of bacteria from drinking water [56-58]. However, a high removal of viruses is not achieved. AgNP and silver nitrate ($AgNO_3$, Ag^+) are added to filters at all CWF factories to achieve

higher pathogen removal due to their antimicrobial properties [59, 60]. The silver solutions are applied to CWF either by brushing or dipping [61]. It was reported that 83% of CWF factories apply AgNP and 17% use Ag^+ [61]. The concentration of silver applied at CWF factories varies. Reported amounts of AgNP applied on CWFs ranges from 32 to 96 mg per CWF [62]. Current guidelines recommend 64 mg of AgNP per CWF [62].

Two mechanisms of microorganism disinfection by CWFs were suggested. (i) CWFs can remove microorganisms by size exclusion or adsorption; (ii) AgNP or Ag^+ inside of CWFs can inactivate pathogens [63]. Figure 1-5 shows the bacteria trapped inside of CWFs coated with AgNP or Ag^+.

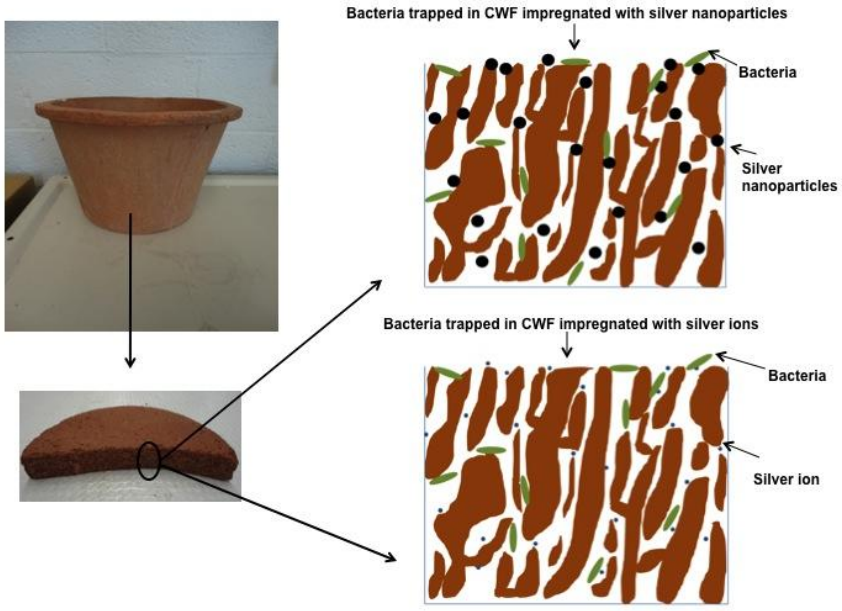

.

Figure 1-4 Bacteria trapped in CWF impregnated with AgNP or Ag^+

Numerous studies have investigated the pathogen removal performance of silver-impregnated CWFs. Table 1-2 summarizes these studies, including the types of silver and pathogens as well as the removal performances.

Table 1-2 Summary of pathogen removal performance of silver coated CWFs manufactured with different clay materials

References	Pathogen types	Pathogen reduction performance		Types of silver	Type of clay
		%	LRV		
[64]	*E. coli*		>2	AgNP	Nicaraguan
	Cryptosporidium parvum		4.3		
	MS2 bacteriophage		<1		
[65]	*E. coli*		2.9	AgNP	Nicaraguan
[66]	*E. coli*		>3	AgNP	Nicaraguan
[54]	*E. coli*		7	AgNP	Nicaraguan
	Clostridium spores		3.3-4.9		
	MS2 bacteriophage		<1		
[67]	*E. coli*		3	AgNP	Nicaraguan
[55]	*E. coli*	>97.8		AgNP	Guatemalan, Redart, Mexican
[63]	*E. coli*		4.5	AgNP	Nicaraguan
[56]	*E. coli*	99		Ag^{+}	Cambodian
	MS2 bacteriophage	90-99			
[68]	*E. coli*		4.56	AgNP	Guatemalan

Although studies have addressed the pathogen reduction of silver-coated CWFs manufactured with different materials, other manufacturing conditions may affect the performance of CWFs. When applying silver on CWFs, a variety of water sources is used at factories to prepare silver solutions, from untreated surface water to treated water. Water characteristics at the filter user's home also vary with location. Previous studies have reported a reduction in antibacterial properties of AgNP with increased size of the nanoparticle clusters due to aggregation in the presence of divalent ions such as Ca^{2+} and Mg^{2+} [8]. In addition, environmental waters usually contain organic

compounds, such as humic acids (HA) [8, 51]. These natural organic matter compounds can rapidly coat the nanoparticle surfaces, creating a physical barrier that prevents interaction between nanoparticles and bacteria. While previous studies have reported that different water chemistry conditions can have an impact on the disinfection performance of AgNP in the aqueous phase[8], these parameters have not been evaluated on CWFs either in the field or in laboratory tests.

Due to the silver application, desorption of silver from coated CWFs has been reported during the first flushes of water. Previous studies using a phosphate buffer as an influent solution reported a decrease in silver concentration in effluent from AgNP-impregnated CWFs to below the United States Environmental Protection Agency (USEPA) maximum contaminant level (MCL) for silver in drinking water (0.1 mg/L or 100 ppb) within few flushes [69]. However, no comprehensive study has evaluated the desorption of either AgNP or Ag^{+} from CWFs using different clays and water chemistry conditions.

Silver application in CWFs has advantages in reducing pathogens. However, the price of silver has increased significantly in the past few years, from approximately $10 to $30 per ounce (Figure 1-6) [70].

Figure 1-5 Price of silver per ounce during the last 5 years [70].

The increase in the price of silver is threatening the sustainability of CWFs. Therefore, alternative disinfectants are needed to ensure the antimicrobial efficacy of the CWF system. One promising disinfectant agent candidate is 3-(trihydroxysilyl) propyldimethyloctadecyl ammonium chloride (TPA), which is a quaternary amine functionalized silsesquioxane compound. Getman [71] compared the antimicrobial performance between TPA and silver and found that TPA can deactivate 99.99% of *E. coli* in a nylon-thin film, while silver does not exhibit any performance during a one-hour antimicrobial test [71]. In addition to its high antimicrobial properties, TPA powder is less expensive (~ $222 per kg) than silver (~ $1024 per kg). TPA is currently applied as an antibacterial or anti-mold reagent. Its applications include integration into thermoplastics or thermoset; dissolution in water and other solvents for use in coating, as with caulk or adhesive formulations; and application as a surface treatment for disinfection purposes [71].

Currently, no studies have applied TPA in CWFs. This dissertation provides a comparative study on the antimicrobial properties of TPA and AgNP in aqueous phases and evaluates their application in CWFs.

4 Dissertation objectives

Evaluating the reactivity of AgNP is essential to support their application in water treatment technologies. Reactivity of nanoparticles is also important in order to address their environmental impacts once released in natural systems. Therefore, considering the gaps in the literature, the following objectives were developed:

- Determine the effect of natural water composition on the bactericidal and antiviral activity of AgNP stabilized with different coatings. This goal is important, since few studies have focused on studying their antimicrobial properties (especially their antiviral properties) [17] and physicochemical properties [17, 72] in natural water conditions. This study will provide new evidence of how natural waters affect the abovementioned properties of AgNP, which is helpful in explaining their environmental fate.
- Determine the performance of silver nanoparticles applied to ceramic water filters used for water treatment in developing communities. This goal is important, since previous literature has only focused on the effects of silver concentration and CWF manufacturing materials on the bacterial removal of AgNP-impregnated CWFs. This study will provide new evidence on how different water chemistries influence the bacterial removal and biofilm formation inside CWFs.

- Compare the disinfection performance of ceramic water filters impregnated with two antibacterial compounds: AgNP and TPA. This goal is important, since previous literature has only focused on how the application of different silver species (AgNP and $AgNO_3$) affects CWF performance. This study will provide new evidence of the feasibility in applying cheaper but more effective alternative disinfectants on CWFs.

5 Dissertation overview

Chapter 1 provides a background and literature review of the environmental fate of AgNP, their antimicrobial properties, their application in CWFs, and potential alternative candidates in place of AgNP.

Chapter 2 is entitled "Evaluation of the disinfectant performance of silver nanoparticles in different water chemistry conditions." It was published in the *Journal of Environmental Engineering* (2012) volume 138 by Hongyin Zhang and Vinka Oyanedel-Craver. This manuscript evaluated the physicochemical properties and antimicrobial performance of AgNP over a range of electrolyte types and concentrations. The effects of natural organic matter were also investigated using humic acid as a surrogate.

Chapter 3, "The effect of natural water conditions on the anti-bacterial performance and stability of silver nanoparticles capped with different polymers" was published in *Water Research* (2012) volume 46 by Hongyin Zhang, James A. Smith, and Vinka Oyanedel-Craver. This chapter describes the significance of different natural water conditions in affecting the physicochemical properties (including particle

size, aggregation behavior, ξ-potential, dissolution) and antimicrobial performance of AgNP coated with dextrin, casein, and PVP.

Chapter 4, "Antiviral effect and physicochemical characteristics of silver nanoparticles in different water conditions" is a manuscript in preparation by Hongyin Zhang and Vinka Oyanedel-Craver. This chapter investigates the physicochemical behavior and antiviral effect of AgNP (coated with sodium citrate and PVP) in different synthetic aqueous solutions and natural water conditions.

In Chapter 5, we investigated the performance of ceramic disks manufactured with clays from three different factories and two types of burn-out materials. Firstly, the ceramic disks were coated with three different concentrations of either AgNP or Ag^{+}. Effluent silver concentration, silver retention, *E. coli* removal, and biofilm formation were evaluated. Then, the influence of three water chemistries including NaCl, $CaCl_2$, and humic acid on AgNP and Ag^{+} were evaluated on disks against the same abovementioned parameters. The manuscript is authored by Justine Rayner, Hongyin Zhang, Jesse Schubert, Pat Lennon, Daniele Lantagne, and Vinka Oyanedel-Craver and was submitted to *ACS Sustainable Chemistry and Engineering* for possible publication.

Chapter 6 is entitled "Comparison of the bacterial removal performance of point-of-use ceramic water filters impregnated with silver nanoparticles and quaternary ammonium functionalized silane as an alternative disinfectant." The manuscript is authored by Hongyin Zhang and Vinka Oyanedel-Craver and has been submitted to the *Journal of Hazardous Materials*. This chapter investigated the antimicrobial performance of AgNP and TPA in an aqueous solution using a respirometric technique

and determined the bacterial removal performance of CWFs coated with AgNP or TPA. The release of AgNP and TPA from ceramic material was also measured to determine their potential health impacts.

Finally, the conclusion and recommended future research are summarized in Chapter 7.

REFERENCE

1. *Woodrow Wilson Center*. 2011; Available from: http://www.nanotechproject.org/inventories/consumer/analysis_draft/.
2. Choi, O., et al., *The inhibitory effects of silver nanoparticles, silver ions, and silver chloride colloids on microbial growth.* Water Res, 2008. **42**(12): p. 3066-3074.
3. Sharma, V.K., R.A. Yngard, and Y. Lin, *Silver nanoparticles: green synthesis and their antimicrobial activities.* Adv Colloid Interface Sci, 2009. **145**(1-2): p. 83-96.
4. Panacek, A., et al., *Silver colloid nanoparticles: synthesis, characterization and their antibacterial activity.* J. Phys. Chem. C, 2006. **110**: p. 16248-16253.
5. Yu, D. and V. Yam, *Controlled synthesis of monodisperse silver nanocubes in water.* J Am Chem Soc, 2004. **126**: p. 13200–13201.
6. Saito, Y., et al., *Simple chemical method for forming silver surfaces with controlled grain sizes for surface plasmon experiments.* Langmuir, 2003. **19**: p. 6857–6861.
7. Morones, J.R., et al., *The bactericidal effect of silver nanoparticles.* Nanotechnology, 2005. **16**(10): p. 2346-2353.
8. Zhang, H., J.A. Smith, and V. Oyanedel-Craver, *The effect of natural water conditions on the anti-bacterial performance and stability of silver nanoparticles capped with different polymers.* Water Res., 2012. **46**(3): p. 691-699.
9. Zhang, H. and V. Oyanedel-Craver, *Evaluation of the disinfectant performance*

of silver nanoparticles in different water chemistry conditions. J. Environ. Eng., 2012. **138**: p. 58-66.

10. Kvitek, L., et al., *Effect of surfactants and polymers on stability and antibacterial activity of silver nanoparticles (NPs).* J. Phys. Chem. C, 2008. **112**: p. 5825-5834.
11. Ren, D. and J.A. Smith, *Proteinate-Capped Silver Nanoparticle Transport in Water-Saturated Sand.* Journal of Environmental Engineering, 2012: p. 121119223630003.
12. Rai, M., A. Yadav, and A. Gade, *Silver nanoparticles as a new generation of antimicrobials.* Biotechnol Adv, 2009. **27**(1): p. 76-83.
13. Huynh, K.A. and K.L. Chen, *Aggregation kinetics of citrate and polyvinylpyrrolidone coated silver nanoparticles in monovalent and divalent electrolyte solutions.* Environ Sci Technol, 2011. **45**(13): p. 5564-5571.
14. Tai, C.Y., et al., *Synthesis of silver particles below 10nm using spinning disk reactor.* Chemical Engineering Science, 2009. **64**(13): p. 3112-3119.
15. Navarro, E., et al., *Toxicity of silver nanoparticles to Chlamydomonas reinhardtii.* Environ Sci Technol, 2008. **42**: p. 8959-8964.
16. Colvin, V.L., *The potential environmental impact of engineered nanomaterials.* Nature Biotechnol., 2003. **21**: p. 1166-1170.
17. Gao, J., et al., *Dispersion and toxicity of selected manufactured nanomaterials in natural river water samples: effects of water chemical composition.* Environ Sci Technol, 2009. **43**: p. 3322-3328.
18. Chen, K.L. and M. Elimelech, *Influence of humic acid on the aggregation*

kinetics of fullerene (C60) nanoparticles in monovalent and divalent electrolyte solutions. J Colloid Interface Sci, 2007. **309**(1): p. 126-134.

19. Li, X. and J.J. Lenhart, *Aggregation and dissolution of silver nanoparticles in natural surface water.* Environ Sci Technol, 2012. **46**(10): p. 5378-5386.
20. Li, X., J.J. Lenhart, and H.W. Walker, *Dissolution-accompanied aggregation kinetics of silver nanoparticles.* Langmuir, 2010. **26**(22): p. 16690-16698.
21. Li, M. and C.P. Huang, *Stability of oxidized single-walled carbon nanotubes in the presence of simple electrolytes and humic acid.* Carbon, 2010. **48**(15): p. 4527-4534.
22. El Badawy, A.M., et al., *Impact of Environmental Conditions (pH, Ionic Strength, and Electrolyte Type) on the Surface Charge and Aggregation of Silver Nanoparticles Suspensions.* Environ Sci Technol, 2010. **44**: p. 1260-1266.
23. Piccapietra, F., L. Sigg, and R. Behra, *Colloidal stability of carbonate-coated silver nanoparticles in synthetic and natural freshwater.* Environ Sci Technol, 2012. **46**(2): p. 818-825.
24. Gebauer, J.S. and L. Treuel, *Influence of individual ionic components on the agglomeration kinetics of silver nanoparticles.* J Colloid Interface Sci, 2011. **354**(2): p. 546-554.
25. Van Hoecke, K., et al., *Aggregation and ecotoxicity of CeO(2) nanoparticles in synthetic and natural waters with variable pH, organic matter concentration and ionic strength.* Environ Pollut, 2011. **159**(4): p. 970-976.
26. Liu, X., et al., *Influence of Ca(2+) and Suwannee River Humic Acid on*

aggregation of silicon nanoparticles in aqueous media. Water Res, 2011. **45**(1): p. 105-112.

27. Illes, E. and E. Tombacz, *The effect of humic acid adsorption on pH-dependent surface charging and aggregation of magnetite nanoparticles.* J Colloid Interface Sci, 2006. **295**(1): p. 115-123.

28. Liu, J. and R.H. Hurt, *Ion release kinetics and particle persistence in aqueous nano-silver colloids.* Environ. Sci. Technol., 2010(44): p. 2169-2175.

29. Li, X., J.J. Lenhart, and H.W. Walker, *Aggregation kinetics and dissolution of coated silver nanoparticles.* Langmuir, 2012. **28**(2): p. 1095-1104.

30. Levard, C., et al., *Environmental transformations of silver nanoparticles: impact on stability and toxicity.* Environ Sci Technol, 2012. **46**(13): p. 6900-6914.

31. Lee, Y.J., et al., *Ion-release kinetics and ecotoxicity effects of silver nanoparticles.* Environ Toxicol Chem, 2012. **31**(1): p. 155-159.

32. Zhang, W., et al., *Modeling the primary size effects of citrate-coated silver nanoparticles on their ion release kinetics.* Environ Sci Technol, 2011. **45**(10): p. 4422-4428.

33. Sondi, I. and B. Salopek-Sondi, *Silver nanoparticles as antimicrobial agent: a case study on E. coli as a model for Gram-negative bacteria.* J. Colloid Interface Sci., 2004. **275**(1): p. 177-182.

34. Park, M.V., et al., *The effect of particle size on the cytotoxicity, inflammation, developmental toxicity and genotoxicity of silver nanoparticles.* Biomaterials, 2011. **32**(36): p. 9810-9817.

35. Feng, Q.L., et al., *A mechanistic study of the antibacterial effect of silver ions on Escherichia coli and staphylococcus aureus.* J. Biomed. Mater., 2000. **52**(4): p. 662-668.

36. Cumberland, S.A. and J.R. Lead, *Particle size distributions of silver nanoparticles at environmentally relevant conditions.* J. Chromatogr. A, 2009. **1216**(52): p. 9099-9105.

37. Kittler, S., et al., *Toxicity of Silver Nanoparticles Increases during Storage Because of Slow Dissolution under Release of Silver Ions.* Chemistry of Materials, 2010. **22**(16): p. 4548-4554.

38. Marambio-Jones, C. and E.M.V. Hoek, *A review of the antibacterial effects of silver nanomaterials and potential implications for human health and the environment.* Journal of Nanoparticle Research, 2010. **12**(5): p. 1531-1551.

39. Kim, J., *Antibacterial activity of Ag+ ion-containing silver nanoparticles prepared using the alcohol reduction method.* J. Ind. Eng. Chem., 2007. **13**: p. 718-722.

40. Vertelov, G., et al., *A versatile synthesis of highly bactericidal myramistin stabilized silver nanoparticles.* nanotechnology, 2008. **19**(355707-355708).

41. Yoon, K., et al., *Antimicrobial effect of silver particles on bacterial contamination of activated carbon fibers.* Environ. Sci. Technol., 2008. **42**: p. 1251-1255.

42. Balogh, L., et al., *Dendrimer-silver complexes and nanocomposites as antimicrobial agents.* Nano. Lett., 2001. **1**: p. 18-21.

43. Hewson, I., C. Chow, and J. Fuhrman, *Ecological role of viruses in aquatic*

ecosystems. 2010, Chichester: eLS. John Wiley & Sons Ltd.

44. You, J., Y. Zhang, and Z. Hu, *Bacteria and bacteriophage inactivation by silver and zinc oxide nanoparticles.* Colloids Surf B Biointerfaces, 2011. **85**(2): p. 161-167.

45. Lara, H.H., et al., *Mode of antiviral action of silver nanoparticles against HIV-1.* J Nanobiotechnology, 2010. **8**: p. 1.

46. Suresh, A.K., D.A. Pelletier, and M.J. Doktycz, *Relating nanomaterial properties and microbial toxicity.* Nanoscale, 2013. **5**: p. 463-474.

47. Lok, C.N., et al., *Silver nanoparticles: partial oxidation and antibacterial activities.* J Biol Inorg Chem, 2007. **12**(4): p. 527-534.

48. Xiu, Z.M., J. Ma, and P.J. Alvarez, *Differential effect of common ligands and molecular oxygen on antimicrobial activity of silver nanoparticles versus silver ions.* Environ Sci Technol, 2011. **45**(20): p. 9003-9008.

49. Jin, X., et al., *High-through screening of silver nanoparticle stability and bacterial inactivation in aquatic media: Influence of specific ions.* Environ Sci Technol, 2010. **44**: p. 7321-7328.

50. Choi, O., et al., *Role of sulfide and ligand strength in controlling nanosilver toxicity.* Water Res, 2009. **43**(7): p. 1879-1886.

51. Fabrega, J., et al., *Silver nanoparticle impact on bacterial growth: effect of pH, concentration, and organic matter.* Environ Sci Technol, 2009. **43**: p. 7285-7290.

52. WHO/UNICEF, *Progress on Drinking Water and Sanitation: 2012 Update*. 2012.

53. Boschi-Pinto, C., L. Velebit, and K. Shibuya, *Estimating child mortality due to diarrhea in developing countries.* World Health Organization Bulletin, 2008. **86**: p. 710-717.

54. Van Halem, D., *Ceramic silver impregnated pot filters for household drinking water treatment in developing countries*. 2006, Delft University of Technology.

55. Oyanedel-Craver, V.A. and J.A. Smith, *Sustainable colloidal-silver-impregnated ceramic filter for point-of-use water treatment.* Environ. Sci. Technol., 2008. **42**: p. 927-933.

56. Brown, J. and M.D. Sobsey, *Microbiological effectiveness of locally produced ceramic filters for drinking water treatment in Cambodia.* J Water Health, 2010. **8**(1): p. 1-10.

57. van Halem, D., et al., *Assessing the sustainability of the silver-impregnated ceramic pot filter for low-cost household drinking water treatment.* Phys. Chem. Earth, 2009. **34**(1-2): p. 36-42.

58. Lantagne, D.S., *Investigation of the potters for peace colloidal silver impregnated ceramic filter. Report 1: Intrinsic Effectiveness*. 2001.

59. Pradeep, T. and Anshup, *Noble metal nanoparticles for water purification: A critical review.* Thin Solid Films, 2009. **517**(24): p. 6441-6478.

60. Lv, Y., et al., *Silver nanoparticle-decorated porous ceramic composite for water treatment.* Journal of Membrane Science, 2009. **331**(1-2): p. 50-56.

61. Rayner, J., *Current practices in manufacturing locally-made ceramic pot filters for water treatment in developing countries.* Journal of Water, Sanitation

and Hygiene for Development 2013. **(in press)**.

62. CMWG, *Best Practice Recommendations for Local Manufacturing of Ceramic Pot Filters for Household Water Treatment*. 2011: Atlanta, GA, USA.

63. Bielefeldt, A.R., K. Kowalski, and R.S. Summers, *Bacterial treatment effectiveness of point-of-use ceramic water filters.* Water Res., 2009. **43**(14): p. 3559-3565.

64. Lantagne, D.S., *Investigation of the Potters for Peace Colloidal Silver Impregnated Ceramic Filter, Report 1: Intrinsic Effectiveness*. 2001: Alethia Environmental, Allston.

65. Fahlin, C.J., *Hydraulic Properties Investigation of the Potters for Peace Colloidal Silver Impregnated, Ceramic Filter*. 2003, University of Colorado at Boulder College of Engineering.

66. Campbell, E., *Study on Life Span of Ceramic Filter Colloidal Silver Pot Shaped (CSP) Model*. 2005: Managua, Nicaragua.

67. Duke, W.F., R. Nordin, and A. Mazumder, *Comparative Analysis of the Filtron and Biosand Water Filters.* 2006, University of Victoria: British olumbia.

68. Kallman, E., V. Oyanedel-Craver, and J. Smith, *Ceramic Filters Impregnated with Silver Nanoparticles for Point-of-Use Water Treatment in Rural Guatemala.* Journal of Environmental Engineering, 2011. **137**: p. 407-415.

69. USEPA. Available from: http://water.epa.gov/drink/contaminants/index.cfm.

70. Ebullionguide. Available from: www. Ebullionguide.com/price-chart-silver-last-5-years.aspx.

71. Getman, G.D., *An advanced non-toxic polymeric antimicrobial for consumer products,* in *Rubber World* 2011. p. 22-25.

72. Chinnapongse, S.L., R.I. MacCuspie, and V.A. Hackley, *Persistence of singly dispersed silver nanoparticles in natural freshwaters, synthetic seawater, and simulated estuarine waters.* Sci Total Environ, 2011. **409**(12): p. 2443-2450.

CHAPTER 2

EVALUATION OF THE DISINFECTANT PERFORMANCE OF SILVER NANOPARTICLES IN DIFFERENT WATER CHEMISTRY CONDITIONS

By

Hongyin Zhang and Vinka Oyanedel-Craver*

is published in Journal of Environmental Engineering, 138, 58-66

[1]Department of Civil and Environmental Engineering, University of Rhode Island, Bliss Hall 213, Kingston, RI 02881

1 Abstract

This study aimed to determine the effect of different water chemistry conditions on the bactericidal properties of silver nanoparticles (AgNP). Lower disinfection performance of AgNP was obtained in divalent cationic solutions in comparison with monovalent solutions with the same concentration. Average particle size of AgNP increased with increasing electrolyte concentration as divalent cations (Ca^{2+} and Mg^{2+}) produced larger AgNP aggregates than those formed with monovalent solutions. ξ-potential measurements showed that AgNP in divalent cationic solutions had low absolute ξ-potential values (-9.8- -23.2 mV) while the values obtained in monovalent solutions were considerable higher. The measurements of the concentration of ionic silver released indicated that the fraction of dissolved Ag^{+} (5.9-18.8 ppb) was around 0.1% of the total mass of Ag^{0} added. The contribution of Ag^{+} to the overall disinfection performance was negligible at the conditions tested. In this study, we have analyzed different physco-chemical properties of silver nanoparticles and the survival rate of *Escherichia coli* (*E. coli*)in different AgNP solutions. The data we collected lead to a correlation between survival rate of of *E. coli* and average size of AgNP. We found a strong correlation between this two parameters tha can be fitted to a saturation type curve, reaching a survival plateau around 20% survival at an average particle size of 200 nm for all the water chemistry conditions tested.

2 Introduction

AgNP are commonly used in a wide range of applications, including solar energy absorption and chemical catalysis and disinfection [1-5]. Consumer products containing AgNP accounted for more than 25% of the 1,015 nanotechnology-based

consumer products available on the market in 2009 [6]. AgNP have large surface areas per volume ratio and high reactivity compared with the bulk solid. This feature gives AgNP antimicrobial properties.

Three possible antimicrobial mechanisms of AgNP have been raised: (1) AgNP can damage cell membrane and intracellular components [7, 8], (2) silver ions released from AgNP can be sorbed into the cell wall and cause lysis and death [7, 9, 10], and (3) reactive oxygen species (ROS) can be formed in AgNP solution [11-14]. While the antibacterial properties of AgNP have been extensively demonstrated [15-18],their performance at different water chemistries have not been fully understood yet. Some evidence shows that the disinfection effectiveness of AgNP is size dependent [19], and that the process of aggregation reduces their surface area, reducing the cell-particle interaction, membrane penetration, and the rate of silver ion release [6].

Studies measuring the rate of silver ions release at different dilutions of seawater showed that the salt concentration did not affect the AgNP' oxidation kinetics; however, high ionic strength increased the size of the particles from 1.9 to 200 nm after 24 hours [6]. Gao et al. [20] also found that fresh water samples with higher ionic strength produced large AgNP [20]. Jin et al. [21] studied the effect of different water matrices on the AgNP size, silver ions release, and antimicrobial activity using a fixed concentration of Ca^{2+} and Mg^{2+}. The study revealed that Ca^{2+} and Mg^{2+} increased the AgNP aggregation in different electrolyte solutions with the same ionic strength in comparison with mono-valent ions. The antimicrobial test showed that Gram-negative bacteria *Pseudomonas putida* was more resistant to AgNP compared to Gram-positive bacteria *Bacillus subtilis* [21].

In this work, we used seven different electrolyte solutions to study systematically the influence of different cations and anions on physico-chemical characteristic of the particles and disinfection performance. One objective of this study was to establish a correlation between survival rate of bacteria and particle characteristics that could easily predict the disinfection performance of AgNP at different water chemistry conditions.

3 Materials and methods

3.1 Synthetic water solutions

Synthetic water solutions were prepared using eight different solutions, four mono-valent and three divalent salts in addition to one solution containing humic acids (HA). These different solutions were prepared using cations concentrations ranging from 10 to 1000 mg/L (ionic strength range 0.16-167 mM/L) and HA concentrations ranging from 0.2-20 mg/L [22, 23]. These ranges of concentrations were selected to mimic the ionic strength and dissolved organic carbon (DOC) content in natural waters (seawater conditions were not included). Table A-1 (Appendix A) presents the complete list of solutions tested. The effect of cations with different valence and anions on the disinfection performance and average particle size of AgNP was evaluated using a statistical test using a general linear model in PASW SPSS 18.0. All salts and other reagents were ACS reagent grade and used as received.

3.2 Preparation and characterization of AgNP

AgNP (70.37% w/w Ag^0) stabilized with casein were obtained from Argenol laboratories. The nanoparticles are proposed to bind to casein polymers surface via complexation with the carboxylate or amino group of casein [24]. A fresh AgNP stock

solution of 4 mM was prepared immediately before testing using deinozed (DI) water and the respective electrolyte as presented in Table A-1. Transmission Electron Microscopy (TEM) observations of AgNP were performed with a JEM-2100 TEM transmission electron microscope (Jeol) (Figure 1). The surface charge and average size distribution were determined by zeta potential and dynamic light scattering (DLS) using a Zetasizer (Nano ZS, ZEN 3600, Malvern) at 25 ^{o}C. Silver nitrate (ACS reagent grade) was used to compare the antimicrobial activity between AgNP and Ag^{+} ion. Silver ions released in each batch test concentrations were measured after 20 h (the same duration as described in the Antibacterial assay) by passing a sample through an 10,000 nominal molecular weight cut-off (NMWCO) ultrafiltration membrane (Millipore, NMWCO: 10,000) using a stirred ultrafiltration cell (Millipore, Model 8200) in dark condition [21, 25]. Concentrations of silver ion were analyzed using ICP-MS (X series, Thermo Elemental).

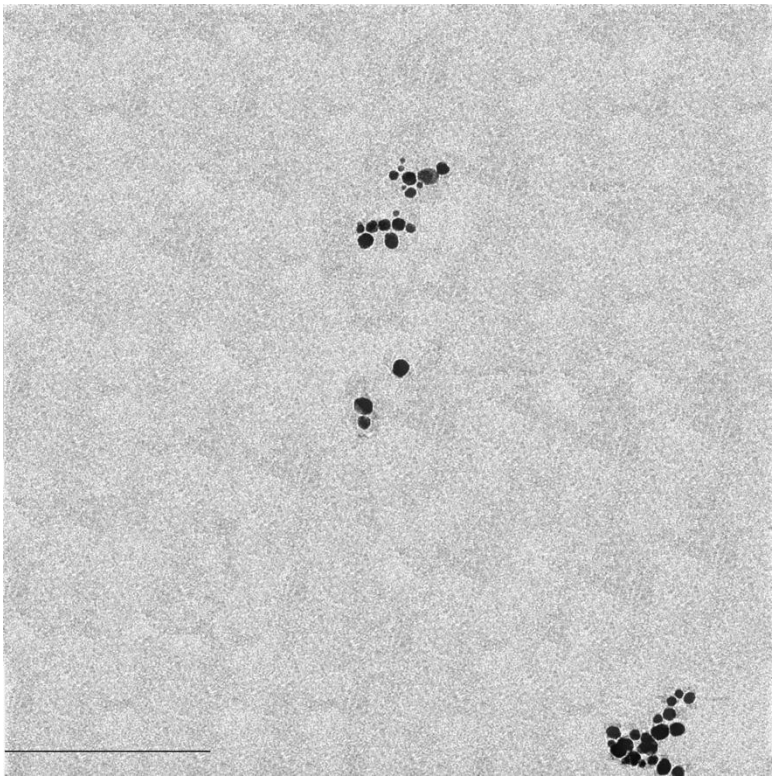

Figure 2-1 TEM image of AgNP (line=200 nm).

3.3 Microbial cultures

A non-pathogenic wild strain of *E.coli* provided by IDEXX laboratories was used for bacteria transport experiment through ceramic filter [26]. This organism was selected because of its use as specific indicator of fecal contamination in drinking water and its extensive use in several studies on AgNP, which will allow us to compare our results with previously published work. Bacteria were grown as described by Vigeant et al. [27]. Cells were re-suspended in a sterilized solution prepared with the respective electrolyte solution (Table A-1) to a concentration of $(1 \pm 4) \times 10^{10}$ CFU/ml. Determination of the *E. coli* concentrationwas performed using the membrane filtration technique, applying m-FC with Rosolic Acid Broth

(Millipore) and incubation at 44.5 ^{0}C for 24 h. Blue colonies were counted and recorded as individual *E. coli*.

3.4 Antibacterial assay

Different solutions were prepared with mono-valent and divalent salt and organic matter compounds to mimic different natural water chemistries. Bacteria deactivation batch tests were performed using manometric respirometric equipment (OxiTop control system, WTW Weilheim, Germany). An OxiTop control system includes a sample bottle sealed with a measuring head, a small container for CO_2 absorbent fixed at the neck of the bottle, and an OxiTop controller for data recording. The test is based on automated pressure measurements conducted via piezoresistive electronic pressure sensors in a closed bottle under constant temperature. Different amount of salts, DI water, and 10 ml *E. coli* (total 100 ml mixture, *E. coli* concentration: 10^9 CFU/ml) were inoculated into sample bottles. The sample bottles were sealed with the measuring heads and placed in the incubator at 25 ^{0}C. The endogeneous respiration was determined by measuring the pressure drop within 2-3 h without adding carbon source or nanoparticles. Then, 0.5 ml glucose of a 70 g/L (glucose was sufficient for *E. coli* over 20 h, data not shown) was injected to determine the oxygen uptake rate (OUR) without AgNP . Finally, after about 2-3 h, 0.25 ml AgNP stock solution was injected into the bottles to determine the alteration of the OUR due to the reduction of bacteria. The total duration of the experiments was 20 h. The percentage of the bacteria reduction using a modified equation from Tzoris et al. was calculated using the following equation [28]:

$$Survival\ rate\ (\%) = \frac{P_t - P}{P_c - P} \times 100$$

Where P_c is the pressure drop after the injection of glucose, P_t is the OUR after the injection of AgNP, P is the OUR during the endogenous respiration without the addition of carbon source or nanoparticles. Figure 2-2 presents a typical respiration curve. Compared to the conventional deactivation methods based on microbial growth (such as plate count method), the manometric respirometric method determined the activity of all active bacteria (not only those that are able to grow). Other advantage is that this method is based on the total oxygen uptake rate of all bacteria while the plate count method could miscount colonies grown from bacteria aggregates, considering only individual bacteria.

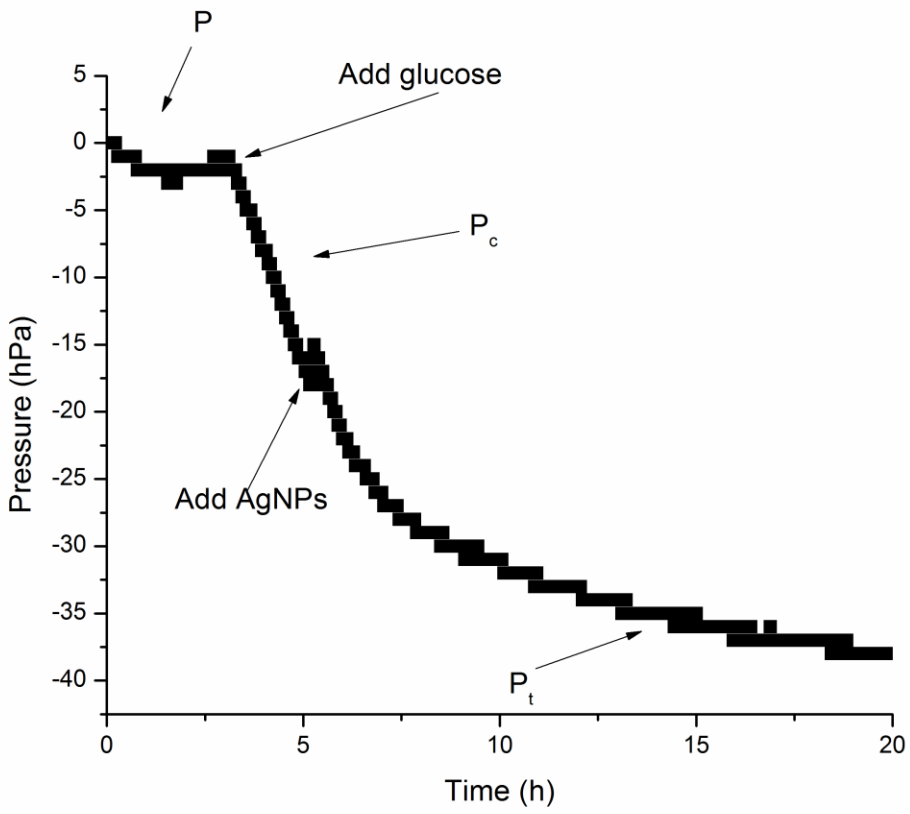

Figure 2-2 A typical respiration curve after 20 h incubation at 25 ^{0}C with glucose injection: 35 mg and AgNP concentration: 11.5 mg/L. P: Oxygen uptake rate during endogenous respiration; P_c: Oxygen uptake rate after the injection of glucose; P_t: Oxygen uptake rate after injection of AgNP.

3.5 Data analysis

The data acquired were fitted using the Origin 8 software, minimizing the weighted sum of squared errors of determined parameters between the calculated values and the experimental data. Linear regression analysis with a dummy variable to compare the survival rate of *E. coli* and particle size in the presence of different ions was performed using PASW SPSS 18.0. F statistic values and *p* values were calculated. *p* values of less than 0.05 were considered significant.

4 Results

The shape and sizes of AgNP in DI water determined by TEM are presented in Figure 2-1. AgNP exhibited spherical shape, commonly observed in other studies [6, 29]. Average size of AgNP was 75.5 ± 2.56 nm using DLS which is larger than sizes determined by TEM (12.6 ± 5.7 nm). The discrepancy is likely due to the formation of AgNP aggregates.In addition, DLS measurement is volume-squared weighted distributions and it can be influenced by small numbers of large aggregates compared to TEM size measurement.

Figure 2-3 shows that the survival rate of *E. coli* (0-20%) increased with increasing ion concentration across all conditions tested. The survival rates of *E. coli* were 18.3% and 20.2% at 1000 mg/L for Mg^{2+} and Ca^{2+}, respectively, while survival rate for most mono-valent cations and anions at 1,000 mg/L was below 10% (with the exception of sulfate mono-valent salts). Humic acid (HA) was used as natural organic matter in this antimicrobial assay. The survival rate of *E. coli* in HA was between 4 to 5%. Similarly, Gao et al. [20] showed that the toxicity of AgNP of bacteria and microinvertebrate decreased with increasing concentration of natural organic matter as total organic carbon (10^{-4}-10 mg/L)[20].

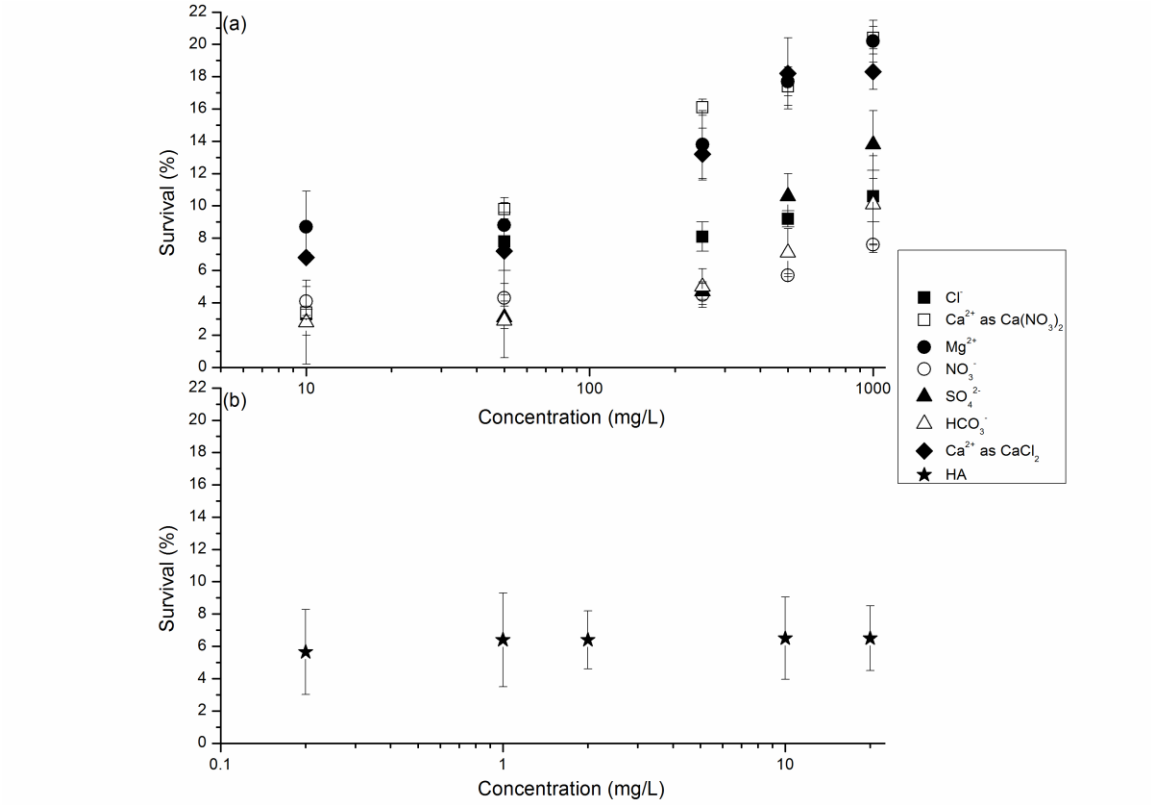

Figure 2-3 Plot of viability of *E. coli* cells in the presence of AgNP in (a) salts solutions, (b) HA solutions. Incubation time: 20h, temperature: 25 ^{o}C, AgNP concentration in each sample: 11.5 mg/L. The concentrations of the ions are listed in Table A-1. It is clear that Ca^{2+} and Mg^{2+} increase the survival rate of *E. coli*.

Figure 2-4 presents the sizes of AgNP across different water chemistry conditions. The average size of AgNP increased when the concentration of salts increased. Our result showed that Mg^{2+} and Ca^{2+} cations produce a large aggregation of AgNP. At 1000 mg/L, sizes of AgNP reached over 1000 nm for Mg^{2+} and Ca^{2+} cations while aggregates produced by mono-valent cations at the same concentration were about ten times smaller. These observations agree with the Schulze-Hardy rule [30], which indicates that the critical coagulationconcentration of a typical colloidal system is extremely sensitive to the valence of the counter-ions. Sizes of AgNP in HA

solutions decreased with increasing HA concentration except at the point of 1 mg/L (32.5 nm). At 10 mg/L, AgNP sizes in HA solution reached 31.3 nm, which was similar to the sizes for mono-valent cations at the same concentration. The aggregates produced by mono-valent cations at 10 mg/L were below 40 nm.

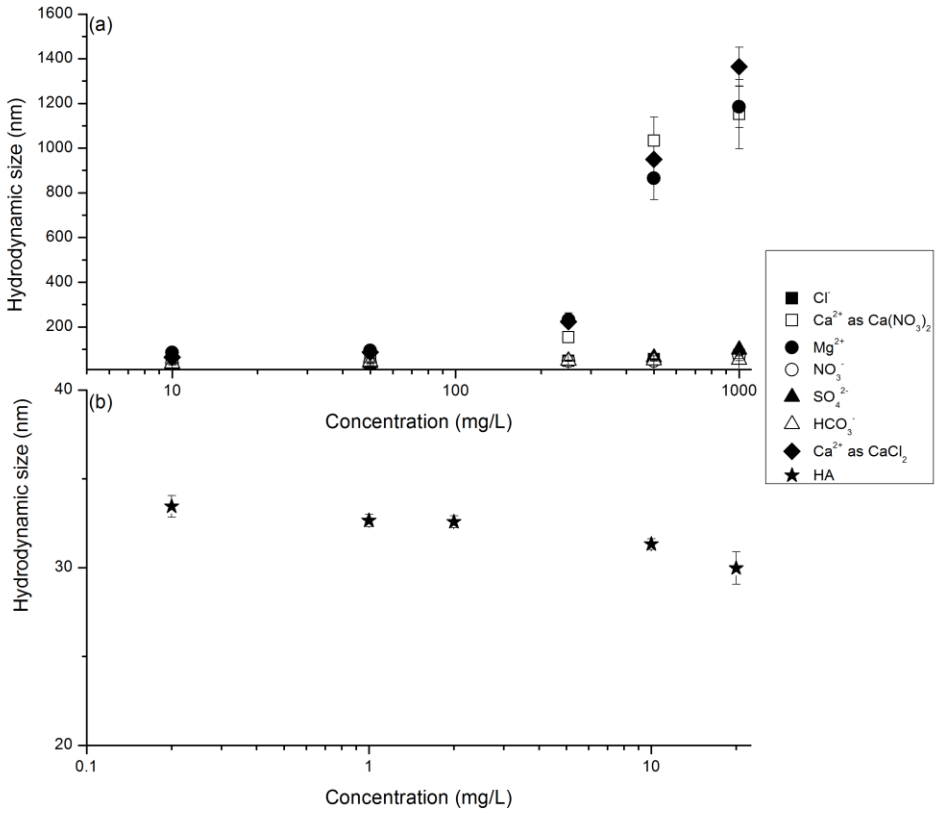

Figure 2-4 Plot of hydrodynamic particle sizes of AgNP in different water chemistry conditions. (a) Hydrodynamic particle sizes in salts solutions. (b) Hydrodynamic particle sizes in HA solutions. Incubation time: 20h, temperature: 25 ^{o}C, AgNP concentration in each sample: 11.5 mg/L. The concentrations of the ions are listed in Table A-1.

ξ-potential is related to the stability of the colloidal systems. Its value (negative or positive) indicates the degree of repulsion between adjacent or charged particles in a colloidal system. As Figure 2-5 shows, AgNP had negative ξ-potentials across all

water chemistry conditions, which is attributed to the adsorption of various anions onto the AgNP surface. The data also showed that ξ-potential of AgNP solutions became less negative as the salt concentration increased. However, AgNP in divalent cationic solution exhibited lower absolute ξ-potential values (-9.8 mV to -23.2 mV) in comparison with mono-valent cations (-15.6 mV to -39.8 mV). Our values are smaller than those obtained by Jin et al. [30] who found that the ξ-potentials of AgNP at different fixed ionic strength solutions (5.6 mM) ranged from -10mV to -60 mV and with the addition of divalent cationic to the solutions (7 mg/L Mg^{2+} and 40 mg/L Ca^{2+}), the range decreased to between -10 mV to -40 mV [21]. A different surface modification of the nanoparticle and, in our case, higher concentration of electrolyte can explain the difference in the results. However, both studies showed that the attractive interaction between divalent cations and negative charged AgNP increased led to higher aggregation and large particles. For AgNP in HA solutions, ξ-potentials decreased (-29.1- -35.2 mV) with increasing concentration. At 10 ppm, ξ-potentials of AgNP in HA solution exhibited similar values to those in the mono-valent cationic solutions, except NaCl solution.

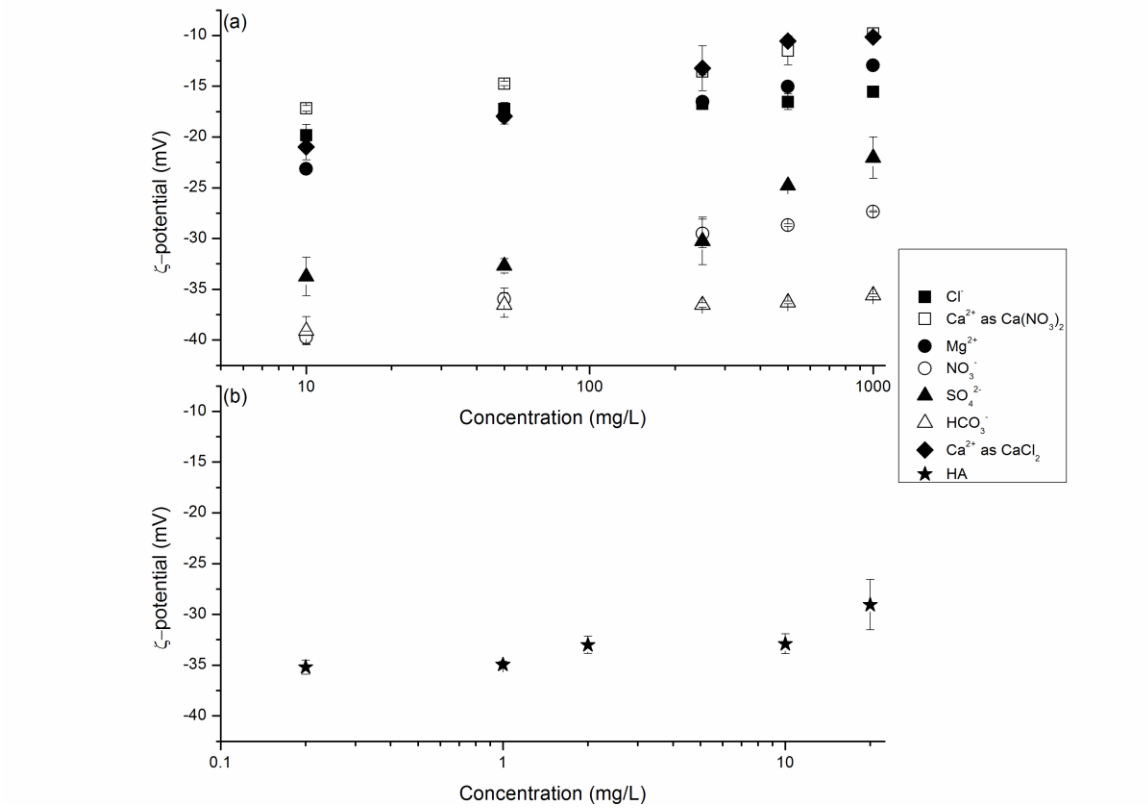

Figure 2-5 Plot of ξ-potential of AgNP in (a) salts solutions, (b) HA solutions. Incubation time: 20h, temperature: 25 ^{o}C, AgNP concentration in each sample: 11.5 mg/L. The concentrations of the ions are listed in Table A-1.

Figure 2-6 shows that the absolute ξ-potential values for *E. coli* solutionswere lower compared to those for AgNP solutions at the same electrolyte concentration. Similarly to the AgNP, *E. coli* in divalent cationic solutions had less negative values, ranging from -0.71 mV to -5.44 mV, while in $NaHCO_3$ solutions, the most negative values were obtained (-7.7 mV to -11.6 mV). Divalent cations were more likely to be adsorbed to the *E. coli* membrane, reducing the absolute ξ-potential values. Consequently, less electrostatic repulsion was produced when AgNP were mixed with the bacteria in solutions containing divalent cations, making the AgNP-bacteria interaction easier to happen; thus, decreasing the survival rate of *E. coli*.

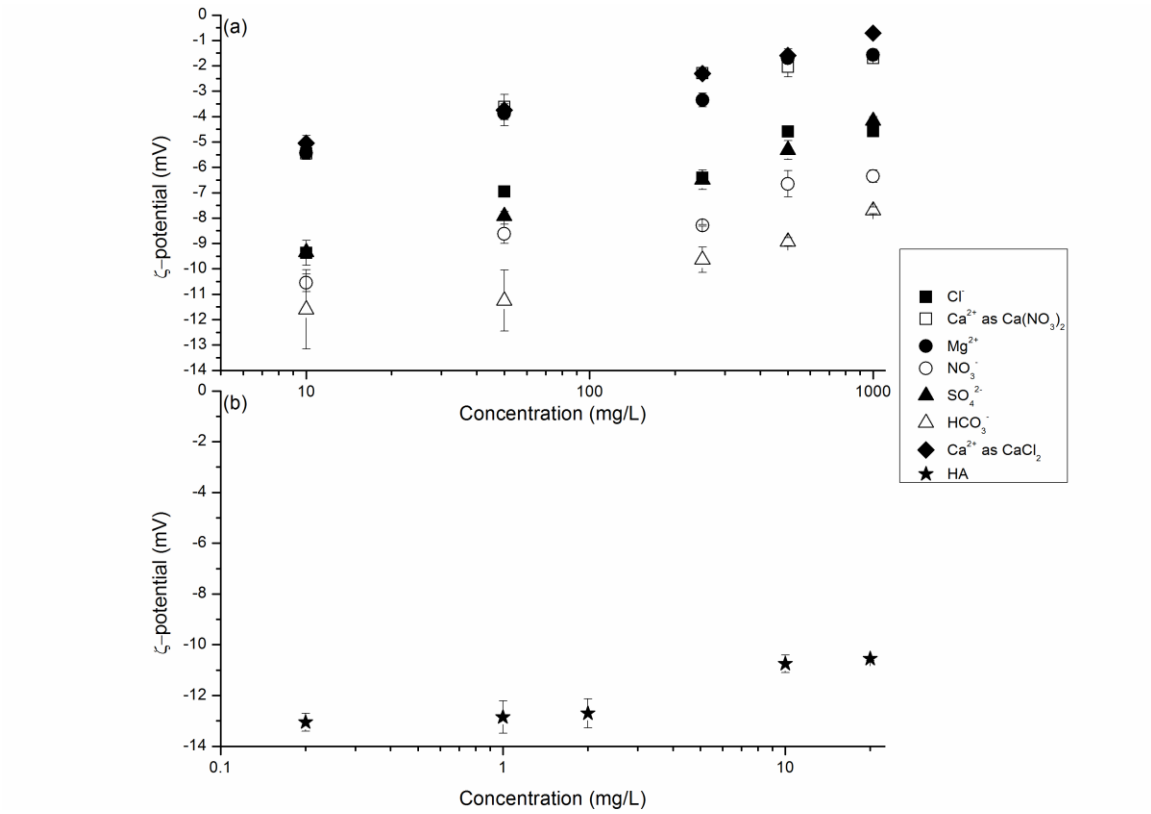

Figure 2-6 Plot of ξ-potential of *E. coli* in (a) salts solutions, (b) HA solutions. Incubation time: 20h, temperature: 25 ^{o}C, *E. coli* concentration: 10^{9} CFU. The concentrations of the ions are listed in Table A-1.

The silver ionic release (Figure 2-7) measured during the tests was about 0.1% of the total mass of silver added as AgNP (5.9-18.8 ppb). Discrepancies in the silver ionic release have been found in previous studies. Liu & Hurt, [6] reported that the silver ionic release of AgNP coated with trisodium citrate (average particle size: 4.8±1.6 nm; initial concentration: 0.05 mg/L) in seawater (ionic strength: 0.7 M) and deionized (DI) water after 24 h were 20 wt% and 50 wt%, respectively [6]. On the other hand, percentages of silver ionic release from two types of AgNP (applied without coating, average particle size: 9±2 nm; coated with oleate, average particle size: 4±1 nm) after 18 h reported by Suresh et al. [31]and from AgNP (coating not

specified; average particle size in DI water: not specified) after 24 h reported by Jin et al, (2010) [21]were below 1% under conditions similar to the one used in this study. To determine the contribution of the silver ions released to the overall disinfection performance of the AgNP, several $AgNO_3$ solutions were prepared ranging from 1 to 20 ppb (as Ag^+), and the survival rate of *E coli* was determined following the same abovementioned manometric respirometric method. At all the concentrations tested, 100% *E. coli* survival was obtained, which indicated that silver ions in solution have a negligible effect on the disinfection performance of AgNP.

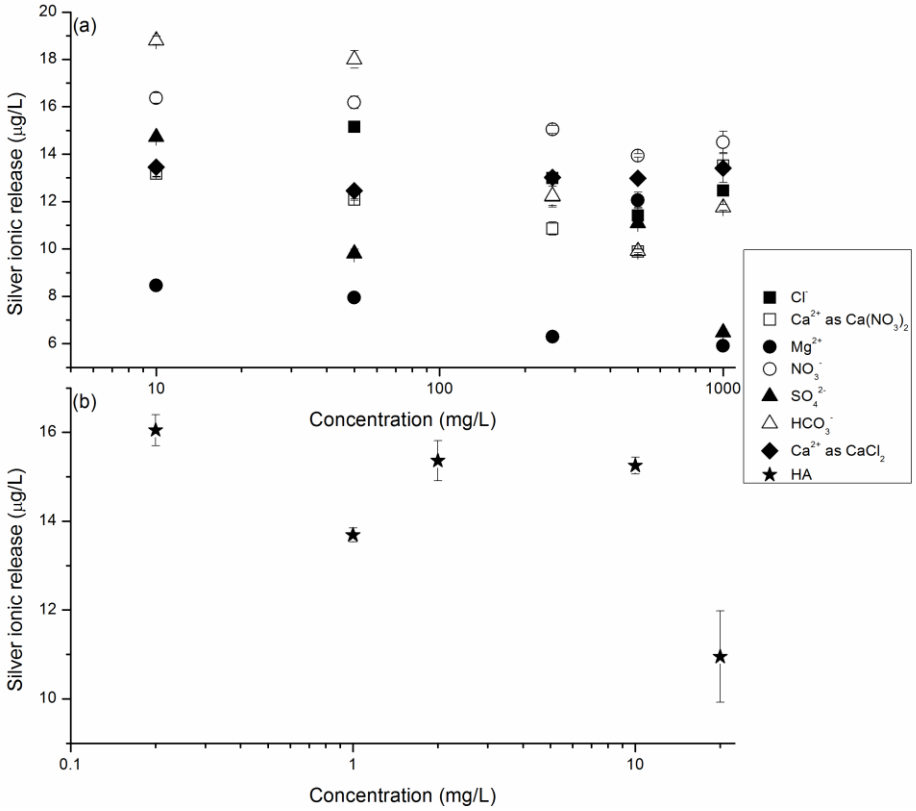

Figure 2-7 Silver ionic release in (a) salts solutions, (b) HA solutions. Incubation time: 20h, temperature: 25 ^oC, AgNP concentration in each sample: 11.5 mg/L. The concentrations of the ions are listed in Table A-1.

5 Discussion

Our results showed that AgNP exhibited high antimicrobial activity across several water chemistry conditions (20% survival and below). Figure 2-8 presents the results for the survival rate of *E.coli* as a function of the average AgNP particle size in all solutions tested. Survival rate of *E.coli* increased sharply with the increase of the AgNP average particle size up to 200 nm. After achieving this threshold, the survival rate seemed to converge to a value close to 20%. A modified saturation type equation was proposed to tentatively describe the relation between particle size and survival rate (AgNP concentration: 11.5 mg/L).

$$y = y_{max} \frac{x}{k_m + x} \quad \text{(eq. 2)}$$

Where y is the survival rate of *E. coli*; x is the particle size of AgNP (nm); y_{max} is the maximum survival rate of *E. coli* (%); k_m is the particle size at which y is half of y_{max} (nm).

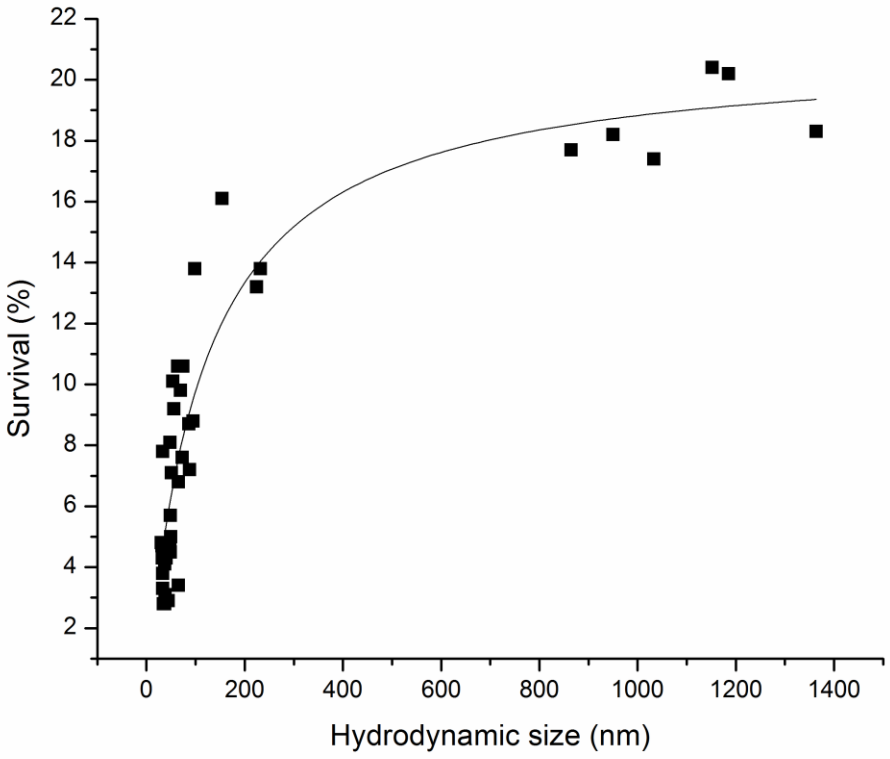

Figure 2-8 The survival rate of *E. coli* as a function of hydrodynamic particle sizes. The curve line is the least-squares fitted to the data collected. Coefficient y_{max} is the predicted maximum survival rate of *E. coli,* where y_{max}=21.0 and its standard error is 1.04. Coefficient k_m is the calculated value of particle size at which the survival rate of *E. coli* is half of its maximum value, where k_m=114.6 and its standard error is 13.8. The adjusted R^2 for the fitted line reached 0.87.

Statistical analysis compared survival rate and particle size in the presence of different representative ions. Table 2-1 and 2-2 shows the F and *p* values calculated for the particle sizes and survival rates in solutions of different ionic compositions. The null hypothesis proposed that different ions have no significant effect on the AgNP particle size or survival rate of *E.coli*. Any *p* value smaller than 0.05 implies

that the null hypothesis is false that different ions have significantly different effect on particle size and/or survival rate. The results of the statistical analysis indicated that anions can affect the particle size and survival rate if there are paired with a mono-valent cation. When divalent cations are present, anions showed no significant effect on the particle size and survival rate, indicating the divalent cations are the dominant influencing factor.

Table 2-1 F and *P* values obtained from linear regression analysis with a dummy variable to compare survival rate of *E. coli* in different water chemistry conditions; *P*<0.05 indicatingsignificant difference.

Ionic composition		Slope		Intercept	
		F value	Significance	F value	Significance
Na^+	Cl^-	6.35	0.05	3.63	0.1
	HCO_3^-				
K^+	NO_3^-	10.19	0.02	2.09	0.19
	SO_4^{2-}				
Ca^{2+}	Cl^-	0.24	0.64	1.44	0.27
	NO_3^-				
SO_4^{2-}	Mg^{2+}	1.33	0.29	14.88	0
	K^+				
Cl^-	Ca^{2+}	0.69	0.44	6.11	0.04
	Na^+				

Table 2-2 F and *P* valuesobtained from linear regression analysis with a dummy variable to compare particle sizes of AgNP in different water chemistry conditions; *P*<0.05 indicating significant difference.

Ionic composition		Slope		Intercept	
		F value	Significance	F value	Significance
Na^+	Cl^-	6.78	0.040	1.07	0.34
	HCO_3^-				
K^+	NO_3^-	13.31	0.01	0.46	0.52
	SO_4^{2-}				
Ca^{2+}	Cl^-	0.22	0.66	0.36	0.57
	NO_3^-				
SO_4^{2-}	Mg^{2+}	167.80	0	7.15	0.03
	K^+				
Cl^-	Ca^{2+}	7.57	0.03	1.06	0.34
	Na^+				

The antimicrobial performance of AgNP has been related to the collision frequency between bacteria and AgNP [32]. Other studies suggested that the antimicrobial performance is size-dependent [16, 29, 33]. Smaller particles can more easily attach to and penetrate the cell membrane compared to larger particles, damaging the cell membrane by impairing its permeability and respiration [8, 19, 29, 34]. Morones et al. [29] indicated that AgNP with a diameter smaller than 10 nm were able to interact with *E. coli* and *Pseudomonas aeruginosa* [29]. However, Xu et al. [35] observed that AgNP with a particle size up to 80 nm could also accumulate inside *Pseudomonas aeruginosa* cells [35]. In this study, we proposed that the disinfection performance of AgNP is size-dependent as shown in Figure 2-8. Survival rate of *Escherichia coli (E. coli)* and average size of AgNP showed a strong correlation that can be fitted to a saturation type curve, reaching a survival plateau around 20% survival at average particle size of 200 nm. However, it should be noticed that low

survival rates are achieved (about 20%) even at large particle sizes (200nm < X<1000nm). This is could be because the presence of Ca^{2+} and Mg^{2+} could promote the formation of ion bridges between the negatively charged AgNP and the lipopolysaccharide molecules on the cell membrane. This interaction could decrease the electrostatic repulsion and enhance the aggregation of AgNP with *E. coli* [21]. The AgNP-*E. coli* aggregates can impair the permeability of the cell membrane, causing membrane leakage and cell death. In addition, particle size distribution showed that the sizes of AgNP in divalent cationic solutions were monodispersed, with few small nanoparticles capable to penetrate the cell membrane. Therefore, our results showed that the AgNP-*E. coli* interaction played a major role in the antimicrobial activity in divalent cationic solutions.

In our study, the levels of silver ions detected did not significantly contribute to the overall disinfection performance. Low concentration of silver ions (5.9-18.8 ppb) and high concentration of E. coli (10^9 CFU/ml) could explain the observed phenomena. Other studies, such as Choi et al. [2] reported 100% inhibition of *E. coli* PHL628-gfp with concentration of silver ions of 0.5 mg/L. Jin et al. [21] reported an IC_{50} of 0.1 mg/L to 50 mg/L for Gram-negative bacteria *Pseudomonas putida* (initial concentration: 10^8 cells/ml) [21]. Suresh et al. [31] indicated that the concentration of 0.48 mg/L Ag^+ released from AgNP (initial concentration: 100 mg/L) had no significant effect on *E. coli* (initial concentration: 10^5 CFU/ml) [31].

ROS generation has been proposed to be one of the AgNP antimicrobial mechanisms [36]. Recent studies revealed that AgNP in dark conditions (the same conditions as in our experiments) cannot produce ROS. In natural light conditions,

ROS generated by AgNP exhibited no relationship with intracellular ROS concentration and bacterial inhibition [37, 38]. Simon-Deckers et al. [38] also showed that ROS production did not correlate with their observed antimicrobial activity. Instead, they suggested that the antimicrobial activity of AgNP is due to the impaired cell membrane [38]. Our experiments were performed in dark conditions; therefore, ROS contribution to the disinfection processes could be considered negligible. Conclusively, this study suggests several implications. (1) The antimicrobial performance of AgNP is mainly size-dependent. (2) Aggregation of AgNP depends on the ions at different water chemistry conditions. Divalent cations can significantly enhance the aggregation while mono-valent and anions do not have such significant influence. (3) Silver ionic release exhibited negligible contributions to the antimicrobial activity of AgNP in this study.

REFERENCE

1. Tiwari, D.K., J. Behari, and P. Sen, *Application of nanoparticles in waste water treatment.* World Applied Sciences Journal, 2008. **3**: p. 417-433.
2. Choi, O., et al., *The inhibitory effects of silver nanoparticles, silver ions, and silver chloride colloids on microbial growth.* Water Res, 2008. **42**(12): p. 3066-3074.
3. Carlson, C., et al., *Unique cellular interaction of silver nanoparticles: Size-dependent generation of reactive oxygen species.* J. phys. Chem, 2008. **112**: p. 13608-13619.
4. Gurunathan, S., et al., *Biosynthesis, purification and characterization of silver nanoparticles using Escherichia coli.* Colloids Surf B Biointerfaces, 2009. **74**(1): p. 328-335.
5. Pradeep, T. and Anshup, *Noble metal nanoparticles for water purification: A critical review.* Thin Solid Films, 2009. **517**(24): p. 6441-6478.
6. Liu, J. and R.H. Hurt, *Ion release kinetics and particle persistence in aqueous nano-silver colloids.* Environ. Sci. Technol., 2010(44): p. 2169-2175.
7. Feng, Q.L., et al., *A mechanistic study of the antibacterial effect of silver ions on Escherichia coli and staphylococcus aureus.* J. Biomed. Mater., 2000. **52**(4): p. 662-668.
8. Sondi, I. and B. Salopek-Sondi, *Silver nanoparticles as antimicrobial agent: a case study on E. coli as a model for Gram-negative bacteria.* J. Colloid Interface Sci., 2004. **275**(1): p. 177-182.

9. Navarro, E., et al., *Toxicity of silver nanoparticles to Chlamydomonas reinhardtii.* Environ Sci Technol, 2008. **42**: p. 8959-8964.

10. Cumberland, S.A. and J.R. Lead, *Particle size distributions of silver nanoparticles at environmentally relevant conditions.* J. Chromatogr. A, 2009. **1216**(52): p. 9099-9105.

11. Hamasaki, T., et al., *Kinetic analysis of superoxide anion radical-scavenging and hydroxyl radical-scavenging activities of platinum nanoparticles.* Langmuir, 2008. **24**: p. 7354-7364.

12. Lok, C., et al., *Silver nanoparticles: Partial oxidation and antibacterial activities.* J. Biol. Inorg. Chem., 2007. **12**: p. 527-534.

13. Watts, R.J., et al., *Comparative toxicity of hydrogen peroxide, hydroxyl radicals, and superoxide anion to Escherichia coli.* Advances in Environmental Research, 2003. **7**(4): p. 961-968.

14. Park, M.V., et al., *The effect of particle size on the cytotoxicity, inflammation, developmental toxicity and genotoxicity of silver nanoparticles.* Biomaterials, 2011. **32**(36): p. 9810-9817.

15. Ju-Nam, Y. and J.R. Lead, *Manufactured nanoparticles: an overview of their chemistry, interactions and potential environmental implications.* Sci Total Environ, 2008. **400**(1-3): p. 396-414.

16. Panacek, A., et al., *Silver colloid nanoparticles: synthesis, characterization and their antibacterial activity.* J. Phys. Chem. C, 2006. **110**: p. 16248-16253.

17. Nowack, B. and T.D. Bucheli, *Occurrence, behavior and effects of nanoparticles in the environment.* Environ Pollut, 2007. **150**(1): p. 5-22.

18. Tolaymat, T.M., et al., *An evidence-based environmental perspective of manufactured silver nanoparticle in syntheses and applications: a systematic review and critical appraisal of peer-reviewed scientific papers.* Sci Total Environ, 2010. **408**(5): p. 999-1006.

19. Rai, M., A. Yadav, and A. Gade, *Silver nanoparticles as a new generation of antimicrobials.* Biotechnol Adv, 2009. **27**(1): p. 76-83.

20. Gao, J., et al., *Dispersion and toxicity of selected manufactured nanomaterials in natural river water samples: effects of water chemical composition.* Environ Sci Technol, 2009. **43**: p. 3322-3328.

21. Jin, X., et al., *High-through screening of silver nanoparticle stability and bacterial inactivation in aquatic media: Influence of specific ions.* Environ Sci Technol, 2010. **44**: p. 7321-7328.

22. Hoecke, K.V., et al., *Aggregation and ecotoxicity of CeO2 nanoparticles in synthetic and natural waters with variable pH, organic matter concentration and ionic strength.* Environmental Pollution, 2011. **159**: p. 970-976.

23. Bui, T.X. and H. Choi, *Influence of ionic strength, anions, cations, and natural organic matter on the adsorption of pharmaceuticals to silica.* Chemosphere, 2010. **80**(7): p. 681-686.

24. Liu, Y. and R. Guo, *The interaction between casein micelles and gold nanoparticles.* J Colloid Interface Sci, 2009. **332**(1): p. 265-269.

25. Fabrega, J., et al., *Silver nanoparticle impact on bacterial growth: effect of pH, concentration, and organic matter.* Environ Sci Technol, 2009. **43**: p. 7285-7290.

26. Oyanedel-Craver, V.A. and J.A. Smith, *Sustainable colloidal-silver-impregnated ceramic filter for point-of-use water treatment.* Environ. Sci. Technol., 2008. **42**: p. 927-933.

27. Vigeant, M.A., et al., *Reversible and irreversible adhesion of motile Escherichia coli cells analyzed by total internal reflection aqueous fluorescence microscopy.* Appl. Environ. Microbiol., 2002. **68**: p. 2794-2801.

28. Tzoris, A., V. Fernandez-Perez, and E.A.H. Hall, *Direct toxicity assessment with a mini portable respirometer.* Sensors and Actuators B: Chemical, 2005. **105**(1): p. 39-49.

29. Morones, J.R., et al., *The bactericidal effect of silver nanoparticles.* Nanotechnology, 2005. **16**(10): p. 2346-2353.

30. Elimelech, M., et al., *Particle Deposition and Aggregation: Measurement, Modelling and Simulation*. 1995, Oxford, England: Butterworth-Heinemann.

31. Suresh, A.K., et al., *Silver nanocrystallites: Biofabrication using Shewanella oneidensis, and an evaluation of their comparative toxcity on Gram-negative and Gram-positive bacteria.* Environ Sci Technol, 2010. **44**: p. 5210-5215.

32. Dror-Ehre, A., et al., *Silver nanoparticle-E. coli colloidal interaction in water and effect on E. coli survival.* J Colloid Interface Sci, 2009. **339**(2): p. 521-526.

33. Zook, J.M., et al., *Stable nanoparticle aggregates/agglomerates of different sizes and the effect of their size on hemolytic cytotoxicity.* Nanotoxicology, 2011. **5**: p. 517-530.

34. Sharma, V.K., R.A. Yngard, and Y. Lin, *Silver nanoparticles: green synthesis and their antimicrobial activities.* Adv Colloid Interface Sci, 2009. **145**(1-2): p. 83-96.

35. Xu, X., et al., *Real-time probing of membrane transport in living microbial cells using single nanoparticle optics and living cell imaging.* Biochemistry, 2004. **43**: p. 10400-10413.

36. Kim, J.S., et al., *Antimicrobial effects of silver nanoparticles.* Nanomedicine, 2007. **3**(1): p. 95-101.

37. Choi, O. and Z. Hu, *Size dependent and reactive oxygen species related nanosilver toxicity to nitrifying bacteria.* Environ Sci Technol, 2008. **42**: p. 4583-4588.

38. Simon-Deckers, A., et al., *Size-, composition- and shape-dependent toxicological impact of metal oxide nanoparticles and carbon nanotubes toward bacteria.* Environ Sci Technol, 2009. **43**: p. 8423-8429.

CHAPTER 3

THE EFFECT OF NATURAL WATER CONDITIONS ON THE ANTI-BACTERIAL PERFORMANCE AND STABILITY OF SILVER NANOPARTICLES CAPPED WITH DIFFERENT POLYMERS

By

Hongyin Zhang[1], James Smith[2], and Vinka Oyanedel-Craver[1*]

is published in Water Research, 46, 691-699

[1]Department of Civil and Environmental Engineering, University of Rhode Island, Bliss Hall 213, Kingston, RI 02881

[2]Department of Civil and Environmental Engineering, University of Virginia, Thornton Hall, Charlottesville, VA 22904

1 Abstract

This study evaluated the effect of natural water composition onto the bactericidal and physicochemical properties of silver nanoparticles (AgNP) stabilized with three different polymeric compounds.

All the nanoparticles behaved similarly in the water conditions tested. Compared to solutions with low organic matter content and monovalent ions, lower disinfection performances of AgNP suspensions were obtained in the following order seawater ≤ high organic matter content water ≤ high divalent cations content synthetic water. Suspension of AgNP in seawater and water with divalent cations (Ca^{2+} and Mg^{2+}) formed larger AgNP aggregates (less than 1400 nm) compared to other solutions tested (up to approximately 38 nm). The critical coagulation concentration (CCC) of AgNP was determined to quantitatively evaluate the stability of the nanoparticle suspension in different water conditions. When the concentration of dissolved organic matter was increased from 0 mg/L to 5 mg/L, the CCC increased by a factor in the range of 2.19 ± 0.25 for all AgNP in divalent solutions, but a smaller increase occurred, in the range of 1.54 ± 0.21 fold, when monovalent solutions were used.

The concentration of ionic silver released indicated that the dissolved Ag^{+} (3.6 - 48.2 ppb) was less than 0.5% of the total mass of Ag^{0} added. At all the conditions tested, the concentration of silver ions in solution had a negligible contribution to the overall anti-bacterial performance of AgNP.

This study demonstrated that the anti-bacterial performance of AgNP at selected natural water conditions decreases in the presence of dissolved natural organic matter or divalent ions, such as humic acid and calcium carbonate. These results may be

helpful in understanding the toxicity of AgNP in various natural water conditions and in explaining the risk associated with discharging AgNP in natural aquatic systems.

2 Introduction

Nanotechnology is an emerging and fast-developing technology. There are more than 1,300 nanotechnology based consumer products according to the Woodrow Wilson center in 2011 [1]. Among these nanoproducts, silver nanoparticles (AgNP) accounted for more than 23% of total applications of nanomaterials.

AgNP are of great interest because of their chemical catalytic ability, stability and antimicrobial properties [2, 3]. AgNP are introduced into consumer products, it is unavoidable that AgNP will be released into the natural water bodies [4]. Therefore, the fate and reactivity of these nanoparticles at different water chemistry conditions is essential to elucidate their impacts in microorganism commonly found in different water ecosystems.

AgNP can be synthesized using physical or chemical methods. Sharma et al. introduced the Tollens method, which involves the reduction of $Ag(NH_3)_2^+$ in the aqueous phase by an aldehyde (usually saccharides). Different stabilizing agents, such as sodium citrate, some surfactant and polymers are used to create a stable dispersion of AgNP in liquid solutions [2].

Critical coagulation concentration (CCC) is defined as the minimum amount of electrolyte that is required to completely destabilize a suspension. This parameter is frequently used to measure the stability of nanosuspensions since it quantify the minimum amount of electrolyte solutions that is required to destabilize the nanoparticle suspension [5]. Compared to “naked” AgNP, AgNP coated with

polymers have shown higher stability [5, 6]. Huynh and Chen, [5] found that the CCC value of AgNP coated with PVP is more than two folds and four folds higher than the value obtained for AgNP coated with sodium citrate [5] and "naked" AgNP, respectively [6]. While many researchers have manufactured and used AgNP stabilized with different compounds, only few research studies have compared their disinfection performance and stability (in terms of particle size and ξ-potential) using natural water conditions [7, 8].

For the purposes of this work, we selected casein, dextrin, and PVP-stabilized AgNP. Commercially available AgNP coated with casein was selected because casein because of their extensive application in point-of-use ceramic water filters [9, 10], therefore their performance and stability at natural water conditions is of great interest. PVP coating was selected because they are considered to be environmentally-friendly stabilizers and because other researchers have used them to conduct AgNP characterization and anti-microbial activity tests [2, 11]. Few studies have synthesized silver nanoparticles using dextrin as a coating agent and studied the antibacterial activity and physicochemical properties of the coated nanoparticles [12]. In this study, AgNP coated with casein, PVP and dextrin were used to examine the influence of different natural water conditions on the physicochemical characteristics of the particles and their antibacterial performance. Synthetic water conditions were also studied to isolate the effects of different ions and organic compounds on the disinfectant performance of AgNP.

3 Materials and methods

A non-pathogenic, wild strain of *E. coli* provided by IDEXX laboratories was used for bacteria disinfection experiments. *E. coli* was selected because of its use as a specific indicator of fecal contamination in drinking water and because of its extensive use in several studies on AgNP [9, 13, 14]. Determination of the *E. coli* concentration was performed using the membrane filtration technique, applying m-FC with Rosolic Acid Broth (Millipore) and 24-h incubation at 44.5 ^{0}C. Details regarding growth and stock solutions preparation can be found in the Appendix B.

Commercial AgNP (70.37% w/w Ag^{0}) stabilized with casein (AgNP-casein) were obtained from Argenol laboratories. AgNP stabilized with dextrin (dextrin from maize starch, average molecular weight: 1,670 g/mol, Sigma Aldrich) (AgNP-dextrin) and polyvinylpyrrolidone, (PVP, average molecular weight: 29,000 g/mol, Sigma Aldrich) (AgNP-PVP) were prepared via the Tollens method described by Kvitek et al. [15] with minor modifications, i.e., 0.35 wt% for both dextrin and PVP were added as stabilizers, respectively [15].The resultant concentrations of AgNP in the cell were measured as total silver using ICP-MS (X series, Thermo Elemental). Transmission Electron Microscopy (TEM) observations of the AgNP were performed with a transmission electron microscope (JEM-2100 TEM). The surface charge and average size of the AgNP in different water conditions were determined in triplicate with dynamic light scattering (DLS) using a Zetasizer (Nano ZS, ZEN 3600, Malvern) at 25 ^{0}C.

Critical coagulation concentration (CCC) refers to the concentration of the counter ions in an electrolyte solution that could completely eliminate the surface charge of particles so that the energy barrier to aggregation is removed, resulting in

rapid aggregation. CCC values were determined to evaluate the aggregation of AgNP in the different electrolyte solutions. CCC was calculated according to Huynh and Chen, [5]. (For the detailed procedure, see the Appendix B)

Different water samples and synthetic water solutions with monovalent salts, divalent salts, and humic acid were prepared. Bacteria deactivation batch tests were performed in duplicate using manometric respirometric equipment (OxiTop control system, WTW Weilheim, Germany). An OxiTop control system includes a sample bottle sealed with a measuring head, a small container for CO_2 absorbent fixed at the neck of the bottle, and an OxiTop controller for data recording. The test was based on automated pressure measurements conducted via piezoresistive electronic pressure sensors in a closed bottle at constant temperature.

Silver ions released in each batch test concentration were measured after 20 h by passing a sample through the same ultrafiltration membrane used for the cleaning and concentration of the nanoparticle solutions. Concentrations of silver ions as total silver in the percolate were measured using ICP-MS (X series, Thermo Elemental). Silver nitrate (ACS reagent grade) was used to compare the anti-microbial activity between AgNP and silver ions.

Figure 3-1 shows the flowchart of the major technique procedures used in this study. The experimental data obtained in this study was analyzed using SPSS 18.0. Bivariate correlation matrix among different factors (i.e., silver ion release, Cl^- concentration, divalent cation concentration) was established using bivariate correlation function.

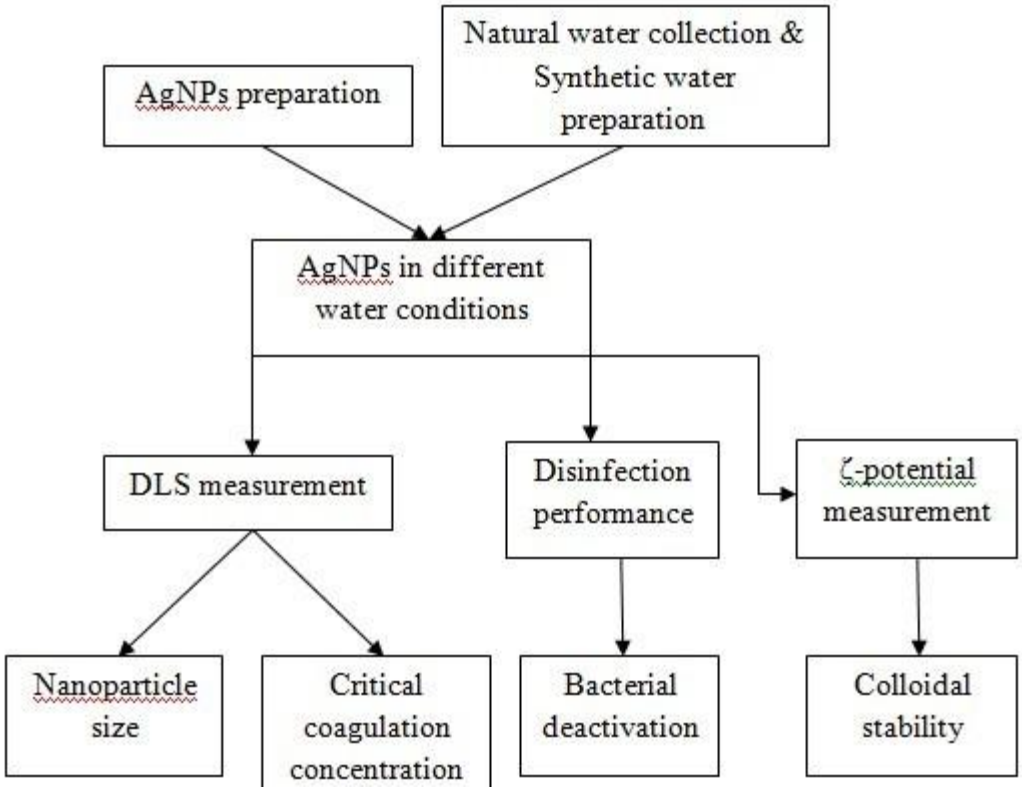

Figure 3-1 Flowchart of the major techniques used in this study.

4 Results and discussion

4.1 Characterization of AgNP

The shape and sizes of AgNP in DI water were determined by TEM. All three AgNP were spherical, which has been reported in other studies using the same manufacturing methods [15]. AgNP aggregates were observed in all TEM images. Average particle sizes of AgNP-casein, AgNP-dextrin, and AgNP-PVP measured using DLS were larger than those determined by TEM (Table B-2). The discrepancy is likely due to the formation of AgNP aggregates, as shown in the TEM images.In addition, DLS measurements are volume-squared weighted distributions. Compared to TEM size measurements, they can be influenced by nanoparticle aggregates in different water chemistries.

4.2 Effect of different water conditions on the characteristics of the AgNP

Figures 3-2 and 3-3 and Table B-3 (Appendix B) present the sizes and CCC values of AgNP for different water conditions. The largest aggregates were formed in the seawater, $CaCl_2$, and $MgCl_2$solutions which contain high concentration of divalent cations. Interestingly, sizes of AgNP in brackish water were smaller than those in ground water despite the higher concentration of divalent cations in the brackish water. This could be explained by the absorption of NOM, present in a relatively high concentration in brackish water, onto the surface of the nanoparticles, creating steric repulsion forces against aggregation and thus increasing the colloidal stability of the nanoparticles [8].

The data obtained from the CCC measurements (Figure 3-3) shows that (i) CCC values from divalent electrolyte solution were more than an order of magnitude higher than those in monovalent salt solution; (ii) the presence of NOM can increase the CCC values by up to 2.2 folds; (iii) AgNP-PVP shows the highest colloidal stability followed by AgNP-casein and AgNP-dextrin. The above-mentioned observations well supported the nanoparticle size measurements in Figure 3-2. Firstly, Shulze-Hardy rule indicates that the stability of a colloidal system is extremely sensitive to the valence of the counter-ions present in the solution. Therefore, the high concentrations of divalent cations (Table B-1) present in $CaCl_2$, $MgCl_2$ solutions and seawater can promote AgNP aggregation. Similar results were found for AgNP that were “naked” and coated with citrate or PVP [5, 6]. Figure 3-3 and Table A3 also provide evidence that CCC could be increased by the addition of humic acid, model NOM in this study. Similarly, previous studies showed that NOM could reduce aggregation and increase

CCC values of AgNP coated with citrate and PVP in different water chemistry conditions [5, 6]. However, Li et al. [6] using fulvic acid did not observe this trend. The discrepancy could be due to the fact that fulvic acid molecules are smaller than humic acid molecules [6].

Our study showed that the CCC values of AgNP with different coatings in all water conditions followed the same trend i.e., AgNP-PVP>AgNP-casein>AgNP-dextrin. It is proposed that the binding force of different atoms in the stabilizers on the surface of the AgNP plays an important role in the stability of AgNP [8]. Nitrogen atoms in PVP are more strongly bonded on the surface of AgNP in comparison with oxygen atoms in dextrin [8]. Casein includes both strong nitrogen atom bonds and weak oxygen atom bonds onto the nanoparticles [16]. Stronger binding forces could ensure a stronger attachment of the stabilizers on the surfaces of the AgNP, precluding substitution by other ions or polymers [15].

In addition, a steric repulsion effect can also influence the aggregation behavior. Long polymer chains may form complex steric configurations, thus increasing the repulsion force between nanoparticles [17, 18]. In our study, the length of the stabilizer chains were in the following order: PVP (MW polymer: 29,000; MW of monomer: 111) > dextrin (MW polymer: 1,670; MW monomer: 162). Therefore, the length of the stabilized chain could have an important effect on the stability of the AgNP for all of the natural and synthetic water conditions tested. Casein has a complicated molecular formula, and it is likely that the intricate steric configurations and the electrostatic effect of the casein proteins contributed to its stabilizing effect [19].

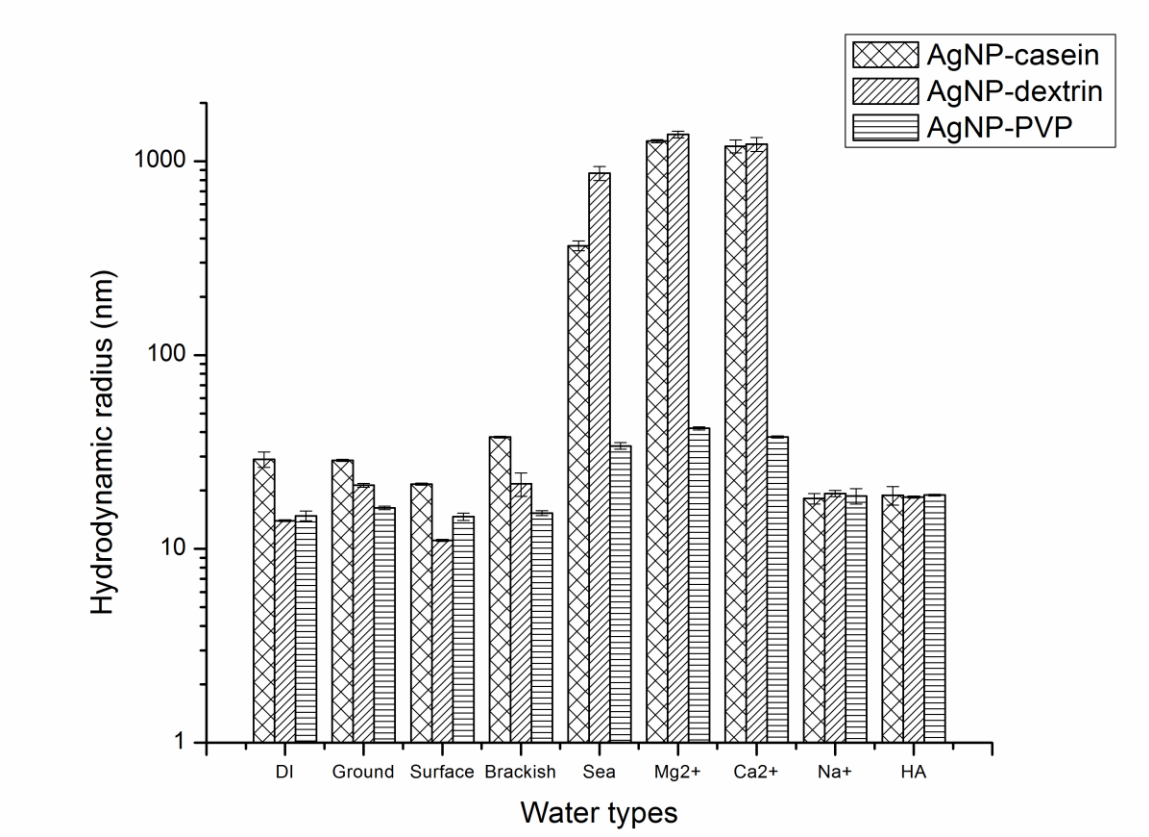

Figure 3-2 Plot of hydrodynamic particle sizes of all three AgNP in different water conditions. Incubation time: 20h, temperature: 25 ^{o}C, AgNP concentration in each sample: 11.5 mg/L. Labels on the x axis: DI (DI water), ground (ground water obtained in University of Rhode Island), surface (Thirty Acre pond water), Brackish (Brackish water in Card ponds), Sea (Seawater), Mg^{2+} (1,000 mg/L as Mg^{2+} in $MgCl_2$ solution), Ca^{2+} (1,000 mg/L as Ca^{2+} in $CaCl_2$ solution), Na^{+} (1,000 mg/L as Na^{+} in NaCl solution), HA (TOC=5 mg/L humic acid solution).

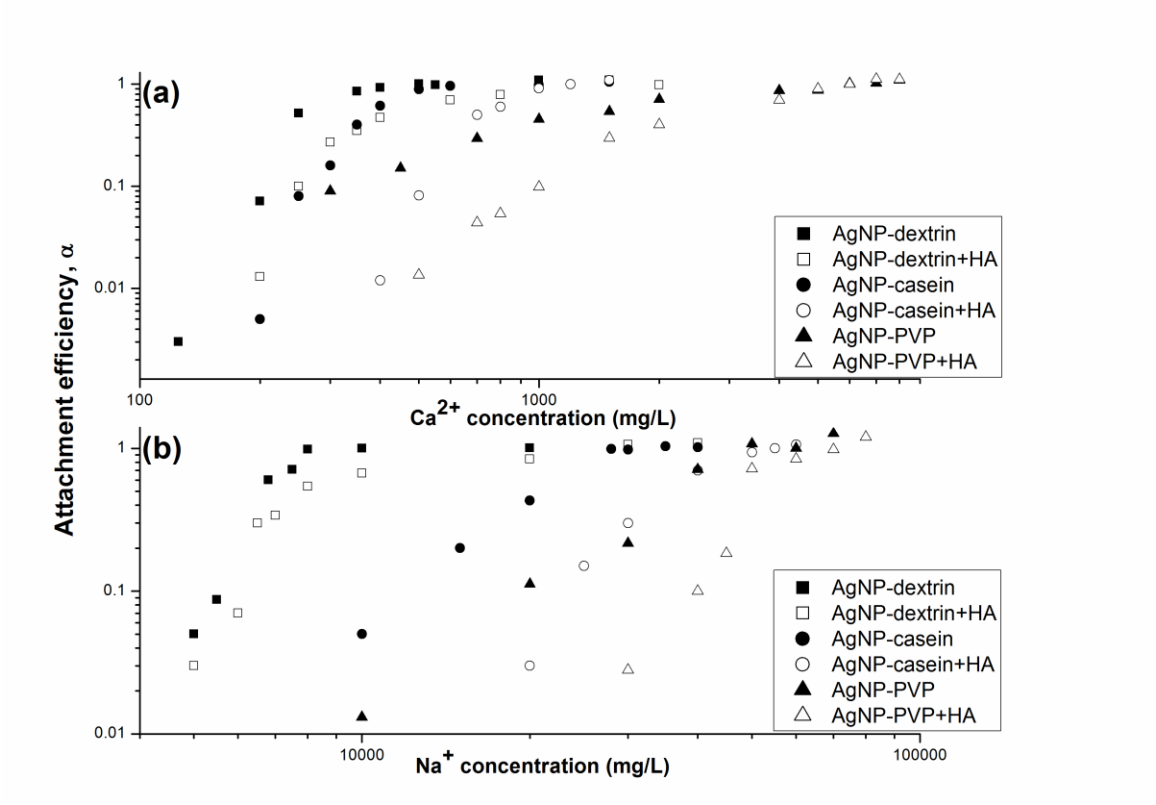

Figure 3-3 Attachment efficiencies of AgNP in different water conditions. (a) Attachment efficiencies of AgNP in different concentrations of $CaCl_2$ solutions in the absence and presence of HA. $CaCl_2$ concentrations: 100-8,000 mg/L; Humic acid concentration: 5 mg/L as TOC. (b) Attachment efficiencies of AgNP in different concentrations of NaCl solutions in the absence and presence of HA. Na^+ concentrations: 4,000-80,000 mg/L; Humic acid concentration: 5 mg/L as TOC. AgNP concentration in all water conditions: 11.5 mg/L.

4.3 ξ-potentials of AgNP and E. coli in different water conditions

ξ-potential relates to the stability of the colloidal systems. Its value (negative or positive) indicates the degree of repulsion between adjacent or charged particles in a colloidal system. As Figure 3-4 (a) shows, AgNP had negative ξ-potentials for all water conditions tested, which is attributed to the adsorption of various anions onto the

surfaces of the AgNP. Our values were smaller compared to those obtained by Jin et al. , who found that the ξ-potentials of AgNP at different fixed ionic strength solutions (5.6 mM) ranged from -10 mV to -60 mV and that, with the addition of divalent cations to the solutions, the range decreased to -10 mV to -40 mV. A different surface modification of the nanoparticles and, in our case, the higher concentration of electrolyte can explain the difference in the results. However, both studies showed that the attractive interaction between divalent cations and negatively charged AgNP led to more extensive aggregation and larger particles.

Figure 3-4 (b) shows that the absolute ξ-potential values for *E. coli* in different water conditionswere lower than those for AgNP solutions. Divalent cations were more likely to be adsorbed to the *E. coli* membrane, reducing the absolute ξ-potential values. Consequently, less electrostatic repulsion was produced when AgNP were mixed with the bacteria in solutions containing divalent cations, facilitating the interaction of the AgNP and the bacteria, thereby decreasing the survival rate of the *E. coli*.

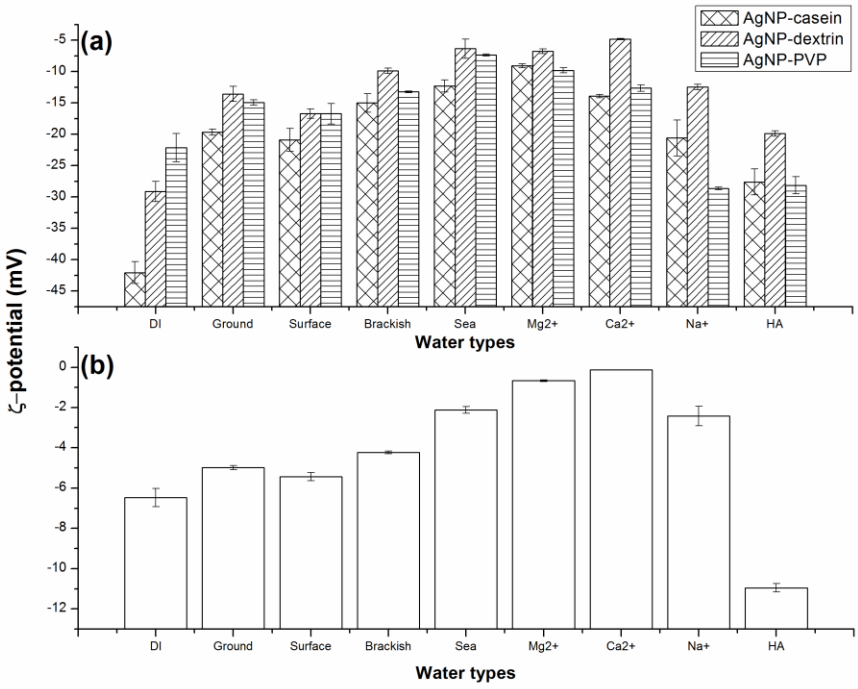

Figure 3-4 Plot of ξ-potential of AgNP (a) and *E. coli* (b) in the different water conditions. Incubation time: 20h, temperature: 25 ^{o}C, AgNP concentration in (a): 11.5 mg/L. *E. coli* concentration in (b): 10^{10} CFU/ml. The concentrations of the ions are listed in Table S1. Labels on the x axis: DI (DI water), ground (ground water obtained in University of Rhode Island), surface (Thirty Acre pond water), Brackish (Brackish water in Card ponds), Sea (Seawater), Mg^{2+} (1,000 mg/L as Mg^{2+} in $MgCl_2$ solution), Ca^{2+} (1,000 mg/L as Ca^{2+} in $CaCl_2$ solution), Na^{+} (1,000 mg/L as Na^{+} in NaCl solution), HA (TOC=5 mg/L humic acid solution).

4.4 Silver ion release in different water conditions

The release of silver ions (Figure 3-5) measured during the tests was less than 0.5% of the total mass of the silver added as AgNP (3.6 - 48.2 ppb). Discrepancies in the silver ion release have been found in previous studies. Liu and Hurt, [20] reported that the silver ion release of AgNP (initial concentration of 0.05 mg/L) in seawater

(ionic strength: 0.7 M) and deionized (DI) water after 24 h was 20 wt% and 50 wt%, respectively [20]. However, percentages below 1% also have been obtained under conditions similar to those used in this study [7, 21]. In this study, the silver ion release was sensitive to different water chemistries. It was previously reported that Cl^- may co-precipitate Ag^+ by forming AgCl, and NOM could coat the AgNP surface rapidly and inhibit AgNP dissociation [7, 21]. This could explain why silver ion release in water conditions with high Cl^- and NOM content is small. The lowest silver ion release was found in the humic acid solution. Since the TOC concentration in the humic acid solution was similar to the TOC concentrations found in natural water, the low ion release in humic acid solution may be attributed to the difference between humic acid and other NOM species in natural waters. To determine the contribution of the released silver ions to the overall disinfection performance of the AgNP, several $AgNO_3$ solutions were prepared, ranging from 1 to 50 ppb (as Ag^+). The survival rate of *E coli* was determined by the manometric respirometric method mentioned earlier. At all the concentrations tested, no significant disinfection efficacy was observed (Figure A2). Similarly, Suresh et al. [21] indicated that a concentration of 0.48 mg Ag^+/L released from AgNP (initial concentration: 100 mg/L) had no significant effect on *E. coli* when he used an initial concentration of 10^5 CFU/mL [21]. Fabraga et al. [22] indicated that 2-20 ppb of silver ion showed negligible antimicrobial property. The results we obtained likely can be attributed to the low silver ion concentrations at these water conditions and the high *E. coli* concentration used (10^{10} CFU/mL) [22]. The fact that silver ion concentrations were low and that they made a negligible contribution to the overall anti-microbial effect do not imply that silver release did not

occur. Most likely, due to the high concentration of Cl^-, silver released from the nanoparticles formed AgCl, which was precipitated. Additionally, although some previous studies reported high bactericidal properties for silver ions [13, 15], however, microbial growth-based methods were use the antibacterial properties of the AgNP. The growth-based methods measure the bacteriostatic effect of the nanoparticles, while the respirometric respiration method (used in this study) measures the total deactivation of bacteria. Therefore, it is likely that at similar concentration of AgNP, respirometry based methods will show a lower activity than growth-based methods since the bacteria could have lost their capacity to replicate, while maintaining some (or full) metabolic activity.

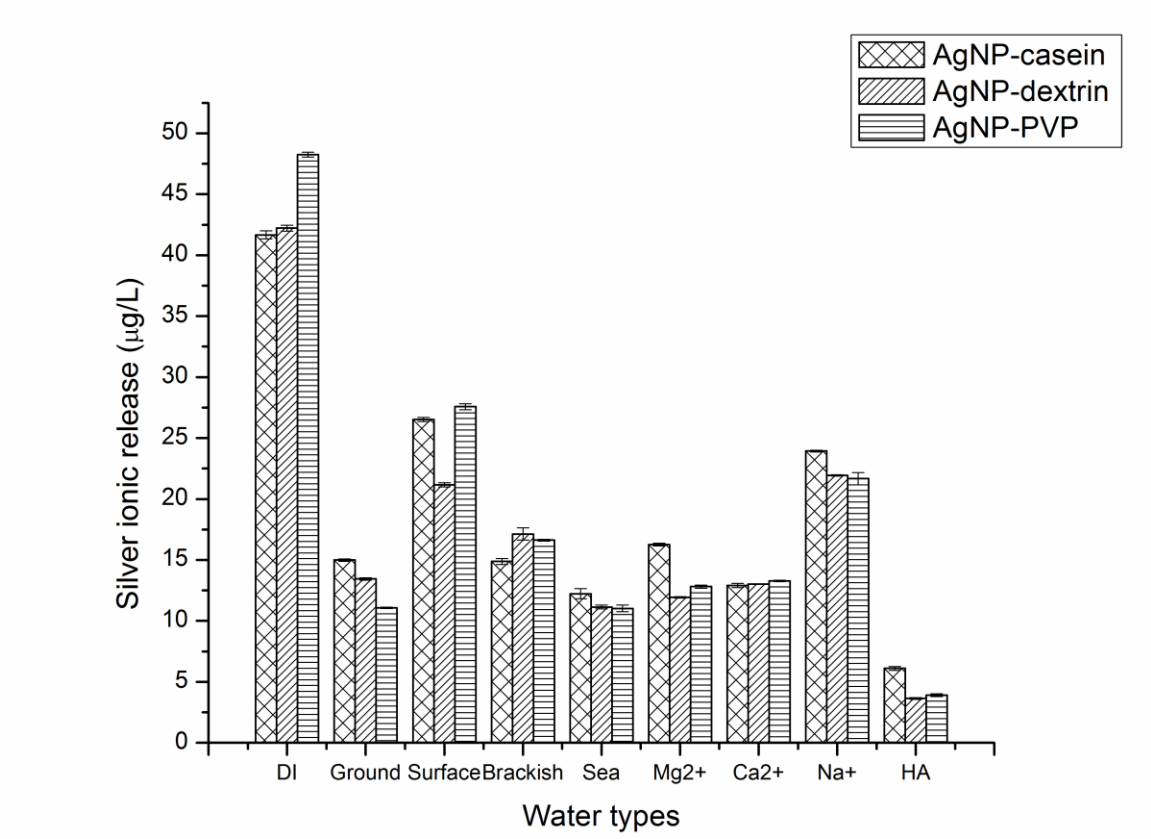

Figure 3-5 Silver ionic release in different water conditions. Incubation time: 20h, temperature: 25 ^{o}C, AgNP concentration in each sample: 11.5 mg/L. Labels on the x axis: DI (DI water), ground (ground water obtained in University of Rhode Island), surface (Thirty Acre pond water), Brackish (Brackish water in Card ponds), Sea (Seawater), Mg^{2+} (1,000 mg/L as Mg^{2+} in $MgCl_2$ solution), Ca^{2+} (1,000 mg/L as Ca^{2+} in $CaCl_2$ solution), Na^{+} (1,000 mg/L as Na^{+} in NaCl solution), HA (TOC=5 mg/L humic acid solution).

4.5 Effect of different water conditions on the disinfection performance of AgNP

Prior to assessing the disinfection performance of AgNP, the toxicities of the three stabilizers were measured using the same respirometric method. The results indicated that no toxicity was associated with the three stabilizers (data not shown).

Figure 3-6 shows the disinfection performance of the three AgNP in different water conditions. For natural water conditions, we found a similar disinfection behavior of AgNP in surface and brackish water. This likely occurred because of the presence of NOM that could be adsorbed on the surface of AgNP, reducing their toxicity by creating physical barriers between the nanoparticles and *E. coli* [8]. Anionic ligands, such as Cl^-, also could impair the toxicity of the AgNP by reacting with their surfaces to form AgCl, thus reducing their toxicity. Different from surface and brackish water, AgNP in ground water had greater disinfection performance, which likely was due to the lower NOM content. It is noteworthy that the disinfection performance of AgNP in seawater was the lowest among all the water conditions. In addition to the above-mentioned factors that reduce the toxicity of AgNP, the formation of the large aggregates that were observed in seawater (Figure 3-2) may impair their toxicity.

In synthetic electrolyte solutions, the order of the Cl^- content in NaCl, $CaCl_2$, and $MgCl_2$ solution was $MgCl_2$>$CaCl_2$>NaCl. The toxicity of AgNP should follow the order of $MgCl_2$<$CaCl_2$<NaCl since Cl^- content could plays a role in reducing the toxicity (due to silver precipitation). However, the order of measured toxicity of AgNP in the electrolyte solutions was NaCl>$CaCl_2$≈ $MgCl_2$. This is likely because the bactericidal property of the AgNP could be size-dependent (Figure B-3). It is noteworthy that the sizes of the AgNP aggregates in the $CaCl_2$ and $MgCl_2$ solutions were much larger than that in the NaCl solution (Figure 3-2). This result agrees with previously published data, suggesting that the toxicity of AgNP is size-dependent [14, 23, 24]. Smaller particles can attach to and penetrate cell membranes more easily than

larger particles and therefore damage the cell membrane by impairing its permeability and interfering the respiration process [14, 23, 24]. In this study, HA solution exhibited lower toxicity than other synthetic electrolyte solutions despite the fact that the sizes of the AgNP in the HA solution were similar to those in the NaCl solution. Previous studies have proposed that the low toxicity is due to the rapid coating of the surface of AgNP by humic acid, which creates a physical barrier that impedes AgNP-bacteria interactions and thus reduces their toxicity [8, 22].

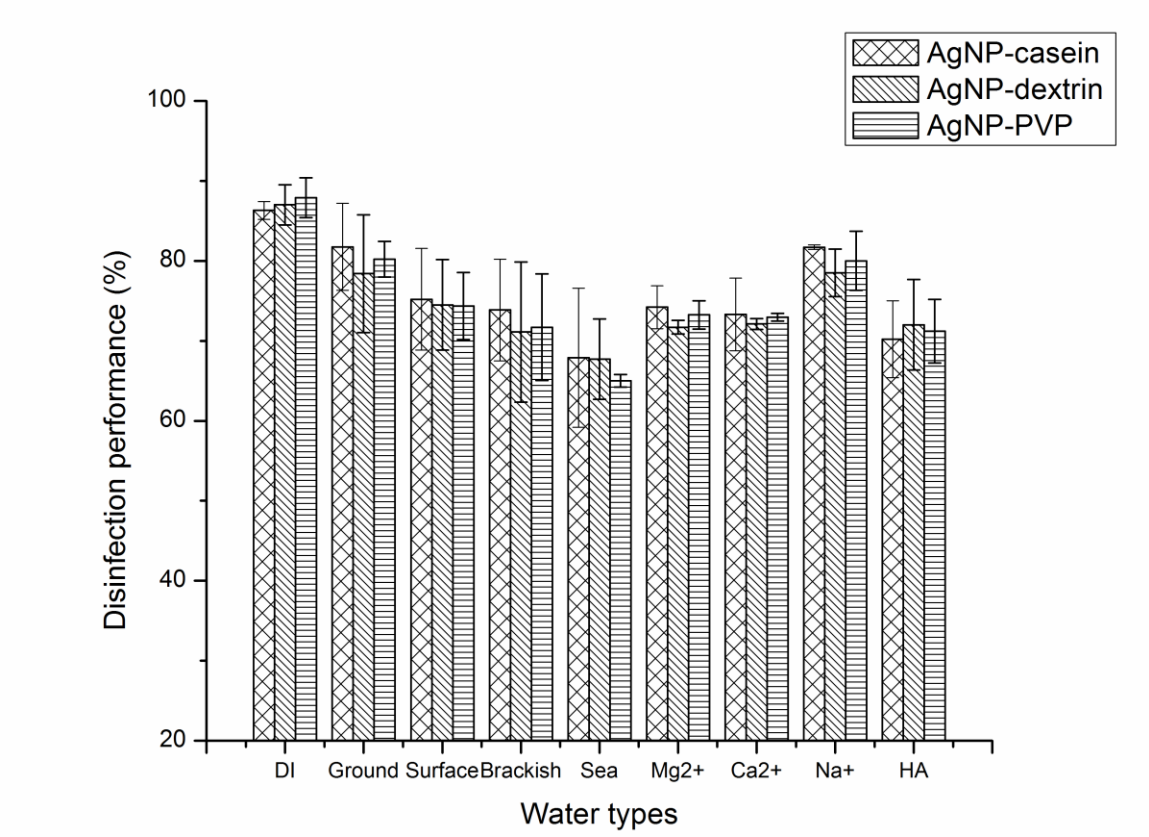

Figure 3-6 Plot of disinfection performance of AgNP stabilized with casein, dextrin and PVP in collected water samples and synthetic waters. Incubation time: 20h, temperature: 25 ^{o}C, AgNP concentration in each sample: 11.5 mg/L. Labels on the x axis: DI (DI water), ground (ground water obtained in University of Rhode Island), surface (Thirty Acre pond water), Brackish (Brackish water in Card ponds), Sea (Seawater), Mg^{2+} (1,000 mg/L as Mg^{2+} in $MgCl_2$ solution), Ca^{2+} (1,000 mg/L as Ca^{2+} in $CaCl_2$ solution), Na^{+} (1,000 mg/L as Na^{+} in NaCl solution), HA (TOC=5 mg/L humic acid solution).

The statistical analysis showed that Cl^{-} concentration, divalent cation concentration, NOM concentration and silver ion release are significantly correlated

with the antibacterial activity of AgNP (Table B-4). We propose that a combination of the above-mentioned factors is responsible for the disinfection performance of AgNP.

Table B-4 and Table B-5 show the correlation analysis for all the conditions tested and water conditions without NOM, respectively. When NOM is included in the analysis no correlation between size and antibacterial activity was obtained. However, when NOM-containing water conditions were removed from the analysis, the bactericidal effect of AgNP is significantly correlated with particle size (Table B-5).

5 Conclusions

Several conclusions can be drawn from the results of this study, i.e., (i) the anti-microbial performance of AgNP is mainly particle size-dependent in absence of NOM, and NOM can mitigate the toxicity of AgNP; (ii) the aggregation of AgNP depends on the ions and NOM at different water conditions; divalent cations can significantly enhance the aggregation; and (iii) the silver ion release level that was detected made a negligible contribution to the anti-microbial activity of AgNP at the experimental conditions we evaluated. The results showed that AgNP are very active at all the water chemistry conditions tested but their bactericidal property could be impaired by the HA content of such waters. Water that contains high divalent cation concentrations also could reduce the bactericidal properties of AgNP due to the formation of large AgNP aggregates and consequently precipitation. Finally, this study clearly demonstrated the complexity of the interactions of AgNP with different dissolved and particulate species that commonly are found in natural waters and the need for

standardized methodologies to evaluate the performance and impacts of these nanomaterials.

REFERENCE

1. *Woodrow Wilson Center*. 2011; Available from: http://www.nanotechproject.org/inventories/consumer/analysis_draft/.
2. Sharma, V.K., R.A. Yngard, and Y. Lin, *Silver nanoparticles: green synthesis and their antimicrobial activities.* Adv Colloid Interface Sci, 2009. **145**(1-2): p. 83-96.
3. Tolaymat, T.M., et al., *An evidence-based environmental perspective of manufactured silver nanoparticle in syntheses and applications: a systematic review and critical appraisal of peer-reviewed scientific papers.* Sci Total Environ, 2010. **408**(5): p. 999-1006.
4. Colvin, V.L., *The potential environmental impact of engineered nanomaterials.* Nature Biotechnol., 2003. **21**: p. 1166-1170.
5. Huynh, K.A. and K.L. Chen, *Aggregation kinetics of citrate and polyvinylpyrrolidone coated silver nanoparticles in monovalent and divalent electrolyte solutions.* Environ Sci Technol, 2011. **45**(13): p. 5564-5571.
6. Li, X., J.J. Lenhart, and H.W. Walker, *Dissolution-accompanied aggregation kinetics of silver nanoparticles.* Langmuir, 2010. **26**(22): p. 16690-16698.
7. Jin, X., et al., *High-through screening of silver nanoparticle stability and bacterial inactivation in aquatic media: Influence of specific ions.* Environ Sci Technol, 2010. **44**: p. 7321-7328.
8. Gao, J., et al., *Dispersion and toxicity of selected manufactured nanomaterials in natural river water samples: effects of water chemical composition.* Environ Sci Technol, 2009. **43**: p. 3322-3328.

9. Oyanedel-Craver, V.A. and J.A. Smith, *Sustainable colloidal-silver-impregnated ceramic filter for point-of-use water treatment.* Environ. Sci. Technol., 2008. **42**: p. 927-933.

10. Kallman, E., V. Oyanedel-Craver, and J. Smith, *Ceramic Filters Impregnated with Silver Nanoparticles for Point-of-Use Water Treatment in Rural Guatemala.* Journal of Environmental Engineering, 2011. **137**: p. 407-415.

11. Rai, M., A. Yadav, and A. Gade, *Silver nanoparticles as a new generation of antimicrobials.* Biotechnol Adv, 2009. **27**(1): p. 76-83.

12. Patakfalvi, R., et al., *Synthesis and direct interactions of silver colloidal nanoparticles with pollutant gases.* Colloid and Polymer Science, 2008. **286**: p. 67-77.

13. Choi, O., et al., *The inhibitory effects of silver nanoparticles, silver ions, and silver chloride colloids on microbial growth.* Water Res, 2008. **42**(12): p. 3066-3074.

14. Morones, J.R., et al., *The bactericidal effect of silver nanoparticles.* Nanotechnology, 2005. **16**(10): p. 2346-2353.

15. Kvitek, L., et al., *Effect of surfactants and polymers on stability and antibacterial activity of silver nanoparticles (NPs).* J. Phys. Chem. C, 2008. **112**: p. 5825-5834.

16. Manno, D., et al., *Synthesis and characterization of starch-stabilized Ag nanostructures for sensors applications.* Journal of Non-Crystalline Solids, 2008. **354**(52-54): p. 5515-5520.

17. Chen, K.L., et al., *Assessing the colloidal properties of engineered nanoparticles in water: case studies from fullerene C60 nanoparticles and carbon nanotubes.* Environmental Chemistry, 2010.

18. Elimelech, M., et al., *Particle Deposition and Aggregation: Measurement, Modelling and Simulation*. 1995, Oxford, England: Butterworth-Heinemann.

19. Liu, Y. and R. Guo, *The interaction between casein micelles and gold nanoparticles.* J Colloid Interface Sci, 2009. **332**(1): p. 265-269.

20. Liu, J. and R.H. Hurt, *Ion release kinetics and particle persistence in aqueous nano-silver colloids.* Environ. Sci. Technol., 2010(44): p. 2169-2175.

21. Suresh, A.K., et al., *Silver nanocrystallites: Biofabrication using Shewanella oneidensis, and an evaluation of their comparative toxcity on Gram-negative and Gram-positive bacteria.* Environ Sci Technol, 2010. **44**: p. 5210-5215.

22. Fabrega, J., et al., *Silver nanoparticle impact on bacterial growth: effect of pH, concentration, and organic matter.* Environ Sci Technol, 2009. **43**: p. 7285-7290.

23. Zook, J.M., et al., *Stable nanoparticle aggregates/agglomerates of different sizes and the effect of their size on hemolytic cytotoxicity.* Nanotoxicology, 2011. **5**: p. 517-530.

24. Sondi, I. and B. Salopek-Sondi, *Silver nanoparticles as antimicrobial agent: a case study on E. coli as a model for Gram-negative bacteria.* J. Colloid Interface Sci., 2004. **275**(1): p. 177-182.

CHAPTER 4

ANTIVIRAL EFFECT OF SILVER NANOPARTICLES IN DIFFERENT WATER CHEMISTRY CONDITIONS

By

Hongyin Zhang and Vinka Oyanedel-Craver*

is in preparation to submit to Water Research

Department of Civil and Environmental Engineering, University of Rhode Island, Bliss Hall 213, Kingston, RI 02881

1 Abstract

In this study, the effect of different water chemistry conditions on the antiviral performance of silver nanoparticles (AgNP) stabilized with commonly used compounds sodium citrate (cit) and polyvinylpyrrolidone (PVP) has been evaluated. Particle size, aggregation kinetics, and zeta potentials of both silver nanoparticles and MS2 bacteriophage were measured. It was found that both nanoparticles and MS2 virus behaved similarly in the water conditions tested. The antiviral experiment was conducted using a double agar layer technique. The result shows that a 2-h exposure of MS2 bacteriophage to silver nanoparticles (1 mg/L) did not affect the survival (>88.9%) of the MS2 bacteriophage. However, a slight decrease in the virus survival was found in aqueous solutions containing high concentration of Ca^{2+}. This study may be helpful in understanding the antiviral property of AgNP in various water chemistry conditions and in explaining the environmental risk associated with AgNP discharge in natural aquatic systems.

2 Introduction

Silver nanoparticles (AgNP) have a wide range of applications especially as an antimicrobial agent. It is estimated that AgNP based consumer products account for more than 23% of the total nanomaterials impregnated products. Due to their extensive application in industry and households, it is inevitable that AgNP will be released into the natural aquatic systems and interact with the local microorganisms [1].

Previous studies have evaluated the toxicity of AgNP towards different microorganisms in aquatic system. Gao et al. [2] have reported that the LC_{50} (μg/L) of AgNP against *Escherichia coli* (*E. coli*) and *Ceriodaphnia dubia* (*C. dubia*) are less

than 112.14 and 6.18 μg/L, respectively. Zhang et al. [3] showed that the antibacterial performance of AgNP (11.2 mg/L) ranges from 67.9-81.8% *E. coli* inhibition in surface, ground, brackish, and sea water. Studies on toxicity of AgNP against other microorganisms such as *Staphylococcus aureus* [4], *Leuconostoc mesenteroides* [5], *Bacillus subtilis* [6], *Pseudomonas aeruginosa* [7] were also reported. However, little is known about the antiviral effect of AgNP. A recent study reported that AgNP (particle size: 21 nm) could not inactivate MS2 bacteriophage in phosphate buffer solution (PBS) even at their highest concentration (5 mg/L). Another study shows that IC_{50} of AgNP on different strains of HIV-1 virus ranged from 0.19-0.91 mg/mL [8].

Three possible mechanism of antiviral effect have been proposed. Studies have reported that the silver ion dissolved from AgNP can cause toxicity by interacting with viral DNA or RNA and the thiol groups in capsule proteins [9] [10]. Lara et al. [9] proposed that AgNP can inhibit the virus binding onto host cells by direct interacting with viral particles with similar sizes. Liga et al. [10] showed virus can be inactivated photocatalytically by AgNP doped TiO_2 nanoparticles due to the generation of reactive oxygen species (ROS).

The mechanisms proposed have associated the antiviral property of AgNP with their physicochemical properties such as particle size and dissolution of AgNP. These physicochemical properties vary in different water chemistry conditions. For example, it has been widely reported that AgNP tend to aggregate in aqueous solutions containing high concentration of divalent cations such as Ca^{2+} and Mg^{2+}[11-15]. Ionic strength and the natural organic matter content in water can also alter the dissolution behavior of AgNP [3, 11, 16, 17].

As viruses are responsible for a wide spectrum of diseases in bacteria, plants, and animals and they play important role in aquatic food webs as active constituents of the microbial loop [18], it is important to investigate the antiviral effect of discharged AgNP in different water conditions to elucidate their environmental risks. However, to the author's knowledge, few studies have focused on this issue [8].

In this study, we selected sodium citrate and PVP stabilized AgNP because these two stabilizers are environmentally friendly and have been used in previous research [3, 13, 14, 16, 19-21]. These AgNP were used to examine the influence of different natural water conditions on the physicochemical characteristics of the nanoparticles and their antiviral property. Synthetic water conditions were studied to isolate the effects of different ions and organic compounds on the antiviral performance of AgNP.

3 Materials and methods

3.1 MS2 bacteriophage preparation

MS2 bacteriophage was selected as a model virus in this study because they have been widely studied and allow us to compare the results. The ATCC 15597-B1 MS2 bacteriophage was cultured following the ATCC procedure. A tryptic soy broth solution (TSB) containing 10 g/L Tryptone, 1 g/L yeast extract, 8 g/L NaCl was prepared and autoclaved. Then, filter-sterilized 10 ml glucose solution (10 w/w%), 2.0 ml $CaCl_2$ solution (1 M), and 1.0 ml Thiamine (10 g/L) was added in TSB. *E. coli* (ATCC 15597) cells were grown in this Luria-Bertani medium for approximately 12 h under incubation conditions (37 ^{o}C). The bacterial stock has a typical concentration of 10^8 CFU/ml. MS2 bacteriophage was propagated using a double agar layer (DAL)

technique. Approximately 100 µL of bacteriophage, 200 µL of host bacteria, and 5 ml LB containing 5 g/L agar, 0.1% glucose, 2 mM $CaCl_2$ and 0.1 mg/ml Thiamine) were poured into plates containing 15 g/L agar. The plates were incubated at 37 ^oC overnight and harvested by adding 1.0 mM NaCl solution to the surface of the plate. The liquid was collected and centrifuged at 2000 rpm for 20 min at room temperature and the supernatant was collected and filtered with 0.2 µm low-protein binding membrane (Whatman) to remove materials larger than 200 nm. Further filtration was conducted using a 0.05 µm low-protein binding membrane (Whatman). Finally, ultrafiltration was applied using a 10 kDa ultrafiltration membrane to remove nutrients and small debris. The obtained MS2 bacteriophage was enumerated by the abovementioned DAL technique (typical concentration: 10^6 PFU/ml).

3.2 Synthetic water solutions preparation

Synthetic water solutions were prepared using NaCl, $CaCl_2$, and HA with cations concentrations ranging from 10-10,000 mg/L (ionic strength for NaCl: 0.44-440 mM; ionic strength for $CaCl_2$: 0.75-750 mM) and humic acid ranging from 1-10 mg/L as total organic carbon (TOC). Natural water samples were collected from in Rhode Island from Thirty Acre Pond (surface water) and Narragansett Bay (seawater). Ground water was collected in Kingston campus, University of Rhode Island.

3.3 AgNP preparation and characterization

AgNP stabilized with sodium citrate (Sigma Aldrich) (AgNP-Cit) and PVP (average molecular weight: 29,000 g/mol, Sigma Aldrich) (AgNP-PVP) were prepared via the Tollens method described by Kvitek et al. [20] with minor modifications. 0.035 w/w% for both sodium citrate and PVP were added respectively. The obtained AgNP

suspensions were cleaned using DI water by ultrafiltration using a 10k kDa membrane (Whatman) in an ultrafiltration cell (Millipore). Concentrations of the AgNP were measured as total silver using ICP-AES (Thermo Elemental).

3.4 Bacteriophage inactivation by AgNP

AgNP were added into the synthetic solutions and natural water samples. Then, 100 µl of MS2 stock solution was added into the suspension to obtain the final silver concentration of 1 mg/L. After 2-h exposure to AgNP in dark condition at room temperature, the AgNP were exposed to 400 mg/L of sodium thiosulfate for 2 min to neutralize any AgNP or silver ions remaining in solution. MS2 in these water samples was served as the controls. The phage samples were serially diluted in 1 mM NaCl solution during DAL assay. The plates were incubated at 37 ^{o}C overnight and only samples with the number of PFU from 0 to 300 were enumerated. Silver nitrate was used to compare the antiviral activity between AgNP and silver ions.

3.5 Particle size, aggregation kinetics, and zeta potential measurement

Particle size, aggregation kinetics, and zeta potential were measured for both AgNP and MS2 phages using the same concentration of AgNP or virus as used in the antiviral assay was applied (1 mg/L). AgNP or MS2 phages were suspended in the same aqueous solutions used in the antiviral assay for 2 h. The average size and zeta potential of the AgNP and viral particles were then determined in duplicate using a Zetasizer (Nano ZS, ZEN 3600, Malvern) at 25 ^{o}C. For all the aggregation kinetics experiments, DLS measurements recorded the hydrodynamic diameter of AgNP and viral particles as a function of time at 100 s time intervals. The initial aggregation rate

of AgNP was calculated by conducting a linear least-squares regression analysis of hydrodynamic radius over time.

3.6 Silver ion release experiment

Ion release from AgNP samples was quantified by ultrafiltration using a 3 kDa molecular weight cut-off membrane as described previously [22]. Nitric acid was added to the percolate (HNO_3 concentration: 2%). ICP-AES was used to quantify the total silver concentration.

4 Results and discussion

4.1 Effect of different water chemistry conditions on the physicochemical characteristics of the AgNP and MS2 phage

Figure 4-1 and 4-2 present the sizes and aggregation kinetics of AgNP and MS2 particles in different water conditions. The average size of AgNP increased with increasing cations concentration. In synthetic aqueous solutions, larger aggregates were formed in the NaCl and $CaCl_2$ solutions contain high concentration of cations. This figure also shows that Ca^{2+} can produce large aggregates more effectively. In HA solutions, particle sizes of AgNP and MS2 are quite stable. The aggregation kinetics measured in Figure 2 well supported the nanoparticle size measurement. In natural water conditions, AgNP and MS2 in seawater formed the largest aggregates. Ca^{2+} ions appear to have a substantial effect on destabilization of the AgNP and MS2 particles compared to monovalent cations. Effect of divalent cations on the aggregation behavior of AgNP and viral particles has been previously reported [12-14, 23, 24]. These observations agree well with Shulze-Hardy rule, which indicates that the stability of a colloidal system is extremely sensitive to the valence of the counterions

present in the system. In our case, cations in aqueous solutions can adsorb on the surface of the particles, neutralize the negative surface charges, and remove the energy barrier between particles, which allows particles to aggregate easily. AgNP and MS2 in HA solution are very stable. Previous studies proposed that HA molecules can rapidly adsorb on the surface of nanoparticles and create steric repulsion [3, 13, 25]. Therefore, HA have a stabilizing effect on nanoparticles. Compared with citrate coated AgNP, AgNP-PVP is more stable due to the combining effects of electrostatic repulsion and steric repulsion. The nitrogen atom in PVP can bind with AgNP strongly. The strong attachment of the PVP molecules on nanoparticle surface preclude substitution by other ions or polymers and create steric repulsion between nanoparticles [20]. Weak aggregation behavior of MS2 virus was also found. Previous studies suggested that steric repulsion from the capsule protein hinders their aggregation [23, 24, 26]. In addition, steric interaction energy contributed by osmotic and elastic repulsive force from the virus's fiber also increases stability of viral particles [23, 26].

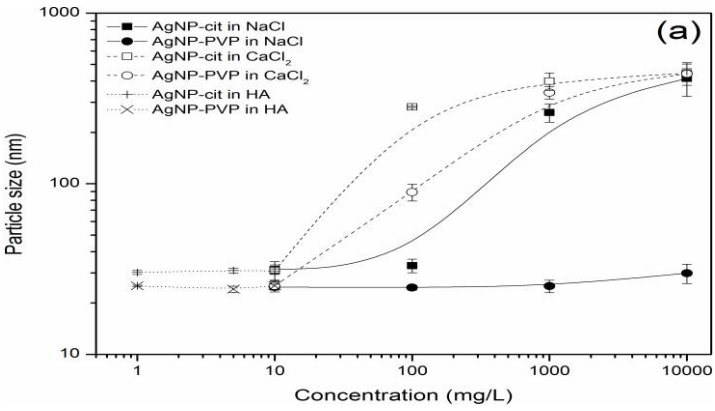
(a)
AgNP-cit in NaCl
AgNP-PVP in NaCl
AgNP-cit in CaCl2
AgNP-PVP in CaCl2
AgNP-cit in HA
AgNP-PVP in HA
Particle size (nm)
Concentration (mg/L)

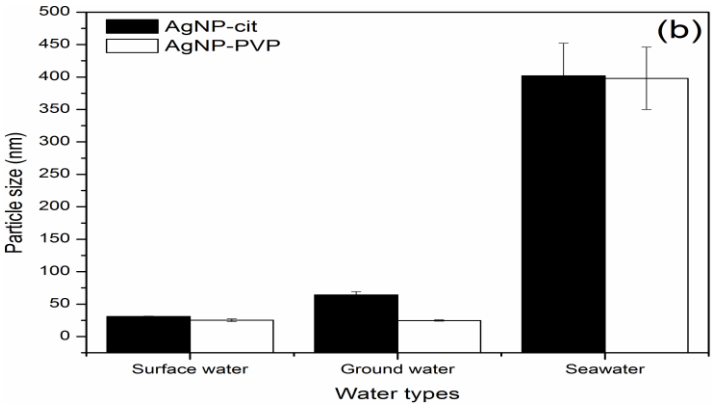
(b)
AgNP-cit
AgNP-PVP
Particle size (nm)
Surface water
Ground water
Seawater
Water types

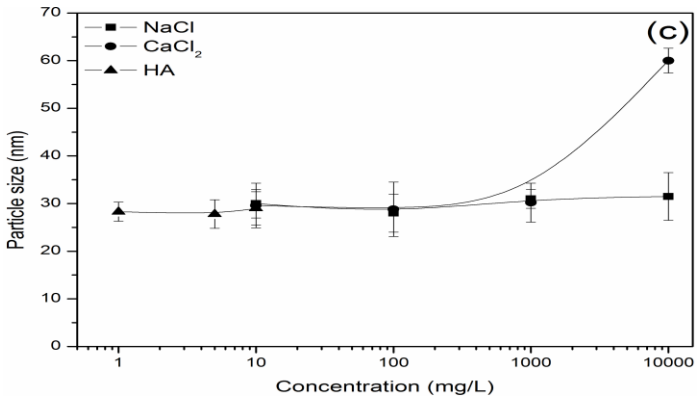
(c)
NaCl
CaCl2
HA
Particle size (nm)
Concentration (mg/L)

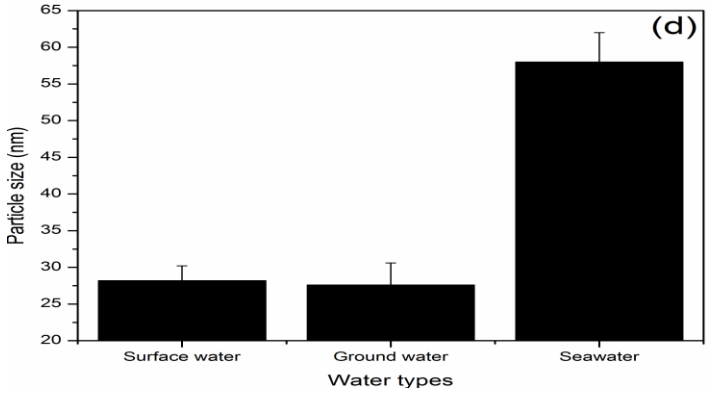
(d)
Particle size (nm)
Surface water
Ground water
Seawater
Water types

Figure 4-1 Particle size of AgNP and MS2 bacteriophage in different water conditions: (a) AgNP in synthetic aqueous solutions; (b) AgNP in natural water conditions; (c) MS2 bacteriophage in synthetic aqueous solutions; (d) MS2 bacteriophage in natural water conditions

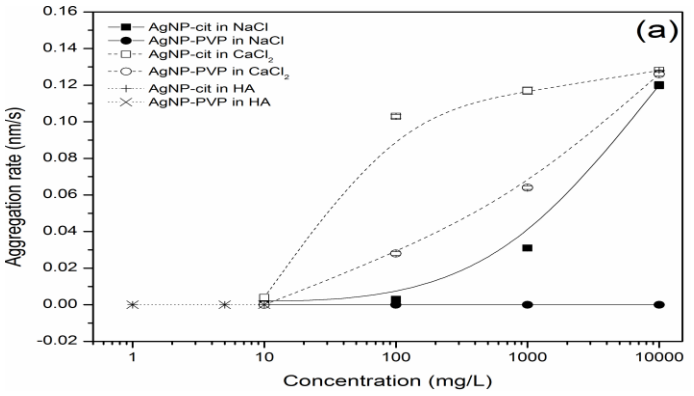
(a)
AgNP-cit in NaCl
AgNP-PVP in NaCl
AgNP-cit in CaCl2
AgNP-PVP in CaCl2
AgNP-cit in HA
AgNP-PVP in HA
Aggregation rate (nm/s)
Concentration (mg/L)

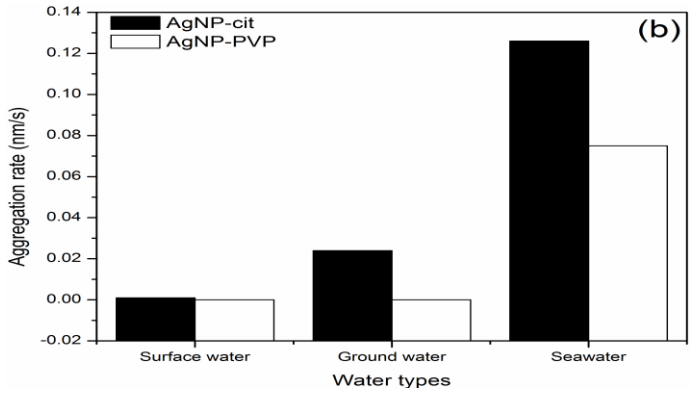
(b)
AgNP-cit
AgNP-PVP
Aggregation rate (nm/s)
Surface water
Ground water
Seawater
Water types

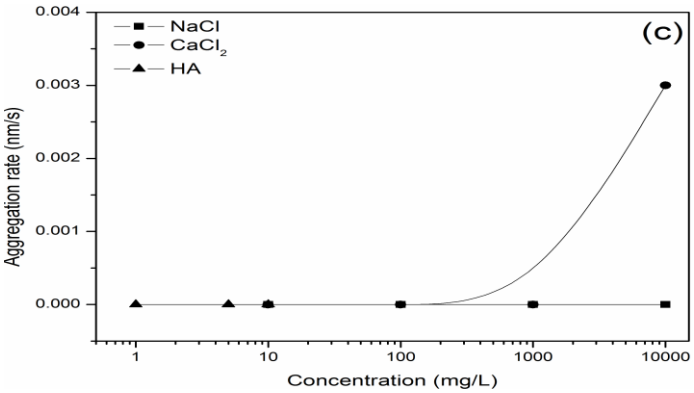
(c)
NaCl
CaCl2
HA
Aggregation rate (nm/s)
Concentration (mg/L)

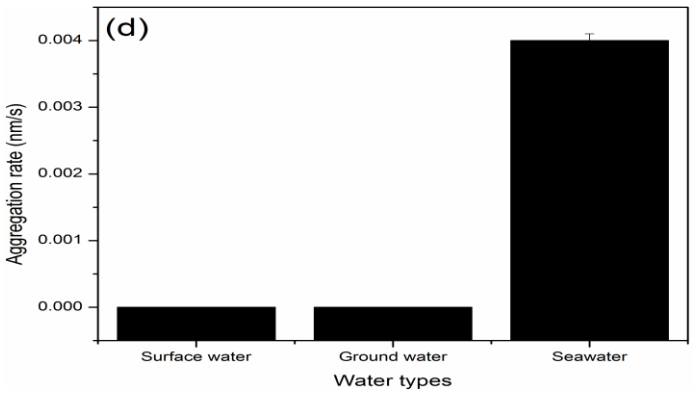
(d)
Aggregation rate (nm/s)
Surface water
Ground water
Seawater
Water types

Figure 4-2 Aggregation rates of AgNP and MS2 bacteriophage in different water conditions: (a) AgNP in synthetic aqueous solutions; (b) AgNP in natural water conditions; (c) MS2 bacteriophage in synthetic aqueous solutions; (d) MS2 bacteriophage in natural water conditions

Zeta potential is related to the stability of a colloidal system. Results from zeta potential measurements (Figure 4-3) showed that zeta potentials of AgNP and MS2 are negative across all water chemistry conditions, indicating the surface charge of the particles is negative. Zeta potentials became less negative with increasing electrolyte concentrations due to the surface charge screening by the cations. Consistent with the particle size measurement, zeta potential measurements agree with the Shulze-Hardy rule, showing that Ca^{2+} is more effective to neutralize the surface charges than Na^{+}.

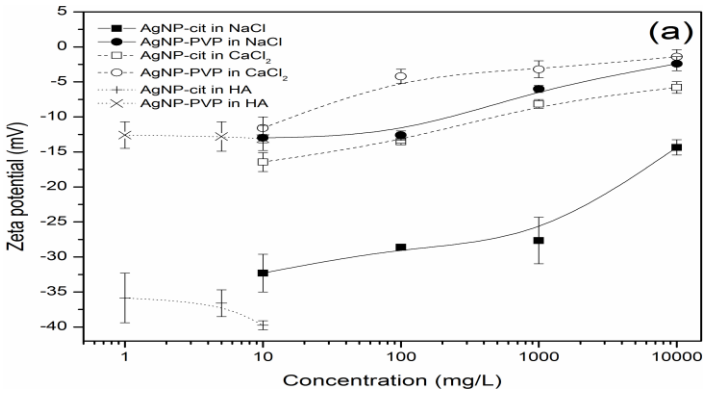
(a)
AgNP-cit in NaCl
AgNP-PVP in NaCl
AgNP-cit in CaCl2
AgNP-PVP in CaCl2
AgNP-cit in HA
AgNP-PVP in HA
Zeta potential (mV)
Concentration (mg/L)

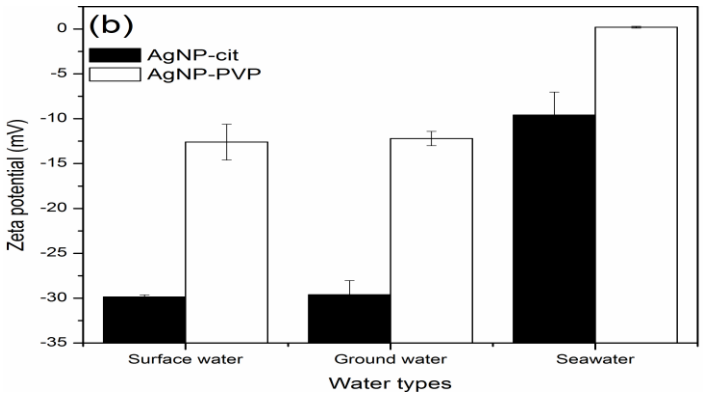
(b)
AgNP-cit
AgNP-PVP
Zeta potential (mV)
Surface water
Ground water
Seawater
Water types

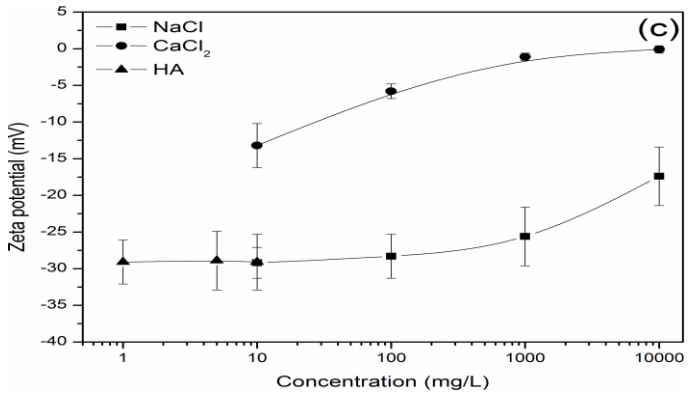
(c)
NaCl
CaCl2
HA
Zeta potential (mV)
Concentration (mg/L)

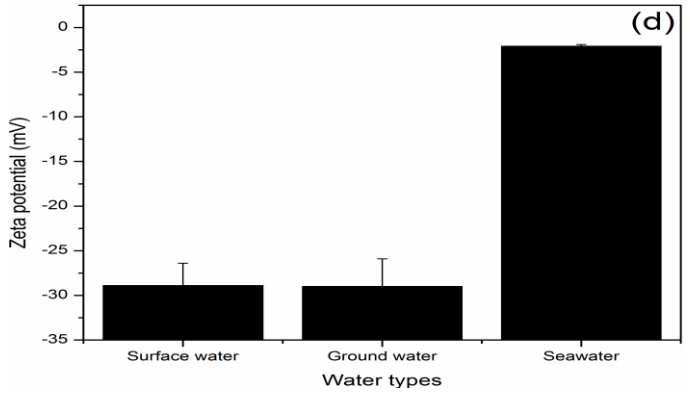
(d)
Zeta potential (mV)
Surface water
Ground water
Seawater
Water types

Figure 4-3 Zeta potential of AgNP and MS2 bacteriophage in different water conditions: (a) AgNP in synthetic aqueous solutions; (b) AgNP in natural water conditions; (c) MS2 bacteriophage in synthetic aqueous solutions; (d) MS2 bacteriophage in natural water conditions.

4.2 Dissolution of AgNP in different water conditions

Table 4-1 shows the dissolved concentration of Ag^+ released from AgNP in various water conditions.

Table 4-1 Dissolution of AgNP in different water chemistry conditions (water chemistry conditions include concentrations of cations (in mg/L) in synthetic electrolyte solutions and the natural water samples)

Silver nanoparticles	Water chemistries		Dissolved Ag (ppb)
AgNP-cit	Na^+ (mg/L)	10	ND
		10^2	3.0 ±1.5
		10^3	16.0 ±4.0
		10^4	319.0 ±3.0
	Ca^{2+} (mg/L)	10	ND
		10^2	ND
		10^3	ND
		10^4	18.6 ±2.6
	HA (mg/L as TOC)	1	ND
		5	ND
		10	ND
	Surface water		4.4 ±4.4
	Ground water		5.9 ±1.0
	Seawater		2.8 ±1.0
AgNP-PVP	Na^+ (mg/L)	10	ND
		10^2	2.7 ±0.4
		10^3	5.4 ±1.0
		10^4	162.0 ±36.0
	Ca^{2+} (mg/L)	10	ND
		10^2	ND
		10^3	ND
		10^4	17.0 ±2.4
	HA (mg/L as TOC)	1	ND
		5	ND
		10	ND
	Surface water		4.5 ±4.5
	Ground water		4.6 ±0.5
	Seawater		3.0 ±2.5

ND: not detected

It is noteworthy that dissolution of AgNP increases with increasing NaCl concentration. This phenomenon could be caused by the reaction between released

Ag^+ with Cl^-. It is well known that Ag^+ and Cl^- can form AgCl precipitate. Further increase in Cl^- concentration can react with AgCl to form soluble silver chloride complexes $AgCl_2^-$ and $AgCl_3^{2-}$, which is responsible for the increased dissolved silver concentration. Our results agree with previous literatures. Ken and Vikesland. [1] reported the dissolved silver concentration increased with increasing NaCl concentration (10-550 mM) for after approximately 2 weeks experiment. However, dissolved silver was only detected in $CaCl_2$ solution at the highest electrolyte concentration (10^4 mg/L Ca^{2+}). It is proposed that the AgNP dissolution in $CaCl_2$ could be inhibited due to the formation of AgNP aggregates, which could diminish the exposed surface area of AgNP and hinder the mass transport of reactants to active sites. Soluble silver chloride complex can still be formed in the presence of excessive Cl^-.

No dissolved silver was observed in presence of HA. Previous studies suggested that natural organic compound such as HA could inhibit AgNP dissolution by several mechanisms including surface adsorption to block AgNP oxidation sites, reversible reaction of released Ag^+ to Ag^0 with HA as a reductant [2-5]. In natural water samples, less AgNP dissolution was found in seawater compared with surface and ground water. This could be due to the combining effects of the two abovementioned dissolution inhibition mechanisms: aggregation and presence of natural organic compounds. Similarly, Liu and Hurt. [2] compared the dissolution kinetics of AgNP in DI, low salt seawater buffer, and seawater. It was found that the silver release is much slower in seawater than in DI water.

4.3 Antiviral effect of AgNP in various water conditions

Figure 4-4 shows the survival of virus after treatment with AgNP for 2 h. Overall, over 90% MS2 phages survived after treatment with AgNP in all water chemistry conditions tested. Environmental factors such as ionic strength, specific ions, and presence of natural organic compounds that influence toxicity of AgNP have been reported [3, 6-11]. Previous published work suggested that these environmental factors affect the physicochemical properties of AgNP which is closely associated to their toxicity [9]. Ionic strength and presence of divalent or multivalent cations result in aggregation of AgNP. Large aggregates exhibited lower toxicity compared with monodispersed nanoparticles [3, 11-13]. Specific ions such as Cl^- and SO_4^{2-} presence in water can form complexes with released silver ions. The complexes are usually less toxic than Ag^+ [7, 8]. Natural organic compounds can also reduce toxicity of AgNP by inhibiting AgNP dissolution and adsorbing on the nanoparticle surface to create physical barriers between nanoparticles and microorganism [2, 6]. The combination of these environmental factors diminishes the antiviral performance of AgNP. In addition, compared to other microorganisms such as bacteria, MS2 bacteriophage is more resistant to AgNP [14]. Our result is consistent with previous studies. You et al. [14] reported that AgNP (coated with polyvinyl alcohol) failed to inactivate MS2 bacteriophage at the highest concentration (5 mg/L Ag) tested, which is related to the availability of dissolved Ag^+ and their preferable binding to virus structures. Other study found that 5 mg/L uncoated and polysaccharide coated AgNP (particle size 10 nm) had no effect on virus propagation [15]. Interestingly, it is also noteworthy that a slight decrease in virus survival was observed in aqueous solutions containing high concentration of Ca^{2+}. As zeta potential deceases with increasing ionic strength,

divalent cations enhanced the interaction between nanoparticles and MS2 phages by forming aggregates, which may result in a slight increase in the antiviral activity of AgNP [10]. Previous studies have reported similar effect on bacteria [10, 16]. In addition, AgNP can facilitate MS2 phage to infect the bacteria host by changing bacteria cell membrane structures and permeability [14]. However, aggregation of AgNP can reduce the membrane disruption effect [3], which may consequently interfere with the ability of the virus to infect the *E. coli* bacteria resulting in less plaque forming units found in the agar plates.

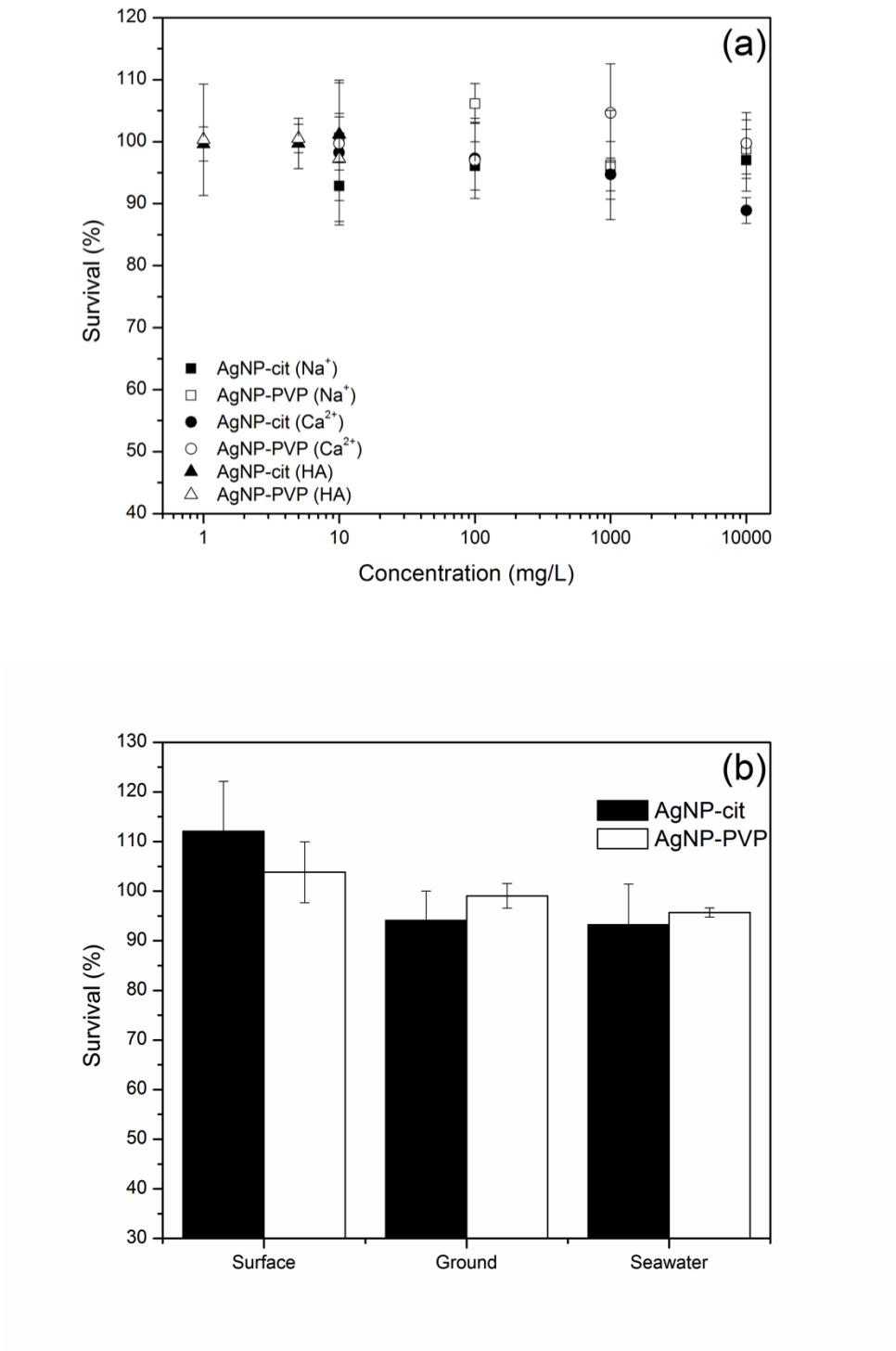

Figure 4-4 Survival of MS2 bacteriophage in various water conditions after treatment with AgNP for 2-h. (AgNP concentration: 1 mg/L)

5 Conclusion

Conclusively, this study has demonstrated that presence of divalent cations in aqueous solutions destabilize AgNP and MS2 phages. Presence of Cl^- enhances dissolution of AgNP by forming soluble $AgCl_2^-$ and $AgCl_3^{2-}$ complexes. Antiviral experiments showed that AgNP have negligible antiviral effect on MS2 bacteriophage regardless of the various water chemistry conditions due to the environmental factors (such as ionic strength and presence of specific ions such as Cl^-) that can reduce AgNP toxicity. Finally, this study shows that the complexity of the interactions of AgNP with different dissolved and particulate species that are commonly found in synthetic aqueous solution and natural waters. The results of this study provides insights into the potential environmental impact of discharged AgNP on the naturally occurring virus community.

REFERENCE

1. Colvin, V.L., *The potential environmental impact of engineered nanomaterials.* Nature Biotechnol., 2003. **21**: p. 1166-1170.
2. Gao, J., et al., *Dispersion and toxicity of selected manufactured nanomaterials in natural river water samples: effects of water chemical composition.* Environ Sci Technol, 2009. **43**: p. 3322-3328.
3. Zhang, H., J.A. Smith, and V. Oyanedel-Craver, *The effect of natural water conditions on the anti-bacterial performance and stability of silver nanoparticles capped with different polymers.* Water Res., 2012. **46**(3): p. 691-699.
4. Kim, J., *Antibacterial activity of Ag+ ion-containing silver nanoparticles prepared using the alcohol reduction method.* J. Ind. Eng. Chem., 2007. **13**: p. 718-722.
5. Vertelov, G., et al., *A versatile synthesis of highly bactericidal myramistin stabilized silver nanoparticles.* nanotechnology, 2008. **19**(355707-355708).
6. Yoon, K., et al., *Antimicrobial effect of silver particles on bacterial contamination of activated carbon fibers.* Environ. Sci. Technol., 2008. **42**: p. 1251-1255.
7. Balogh, L., et al., *Dendrimer-silver complexes and nanocomposites as antimicrobial agents.* Nano. Lett., 2001. **1**: p. 18-21.
8. You, J., Y. Zhang, and Z. Hu, *Bacteria and bacteriophage inactivation by silver and zinc oxide nanoparticles.* Colloids Surf B Biointerfaces, 2011. **85**(2): p. 161-167.

9. Lara, H.H., et al., *Mode of antiviral action of silver nanoparticles against HIV-1.* J Nanobiotechnology, 2010. **8**: p. 1.

10. Liga, M.V., et al., *Virus inactivation by silver doped titanium dioxide nanoparticles for drinking water treatment.* Water Res, 2011. **45**(2): p. 535-544.

11. Zhang, H. and V. Oyanedel-Craver, *Evaluation of the disinfectant performance of silver nanoparticles in different water chemistry conditions.* J. Environ. Eng., 2012. **138**: p. 58-66.

12. Li, X., J.J. Lenhart, and H.W. Walker, *Dissolution-accompanied aggregation kinetics of silver nanoparticles.* Langmuir, 2010. **26**(22): p. 16690-16698.

13. Li, X., J.J. Lenhart, and H.W. Walker, *Aggregation kinetics and dissolution of coated silver nanoparticles.* Langmuir, 2012. **28**(2): p. 1095-1104.

14. Huynh, K.A. and K.L. Chen, *Aggregation kinetics of citrate and polyvinylpyrrolidone coated silver nanoparticles in monovalent and divalent electrolyte solutions.* Environ Sci Technol, 2011. **45**(13): p. 5564-5571.

15. Thio, B.J., et al., *Mobility of capped silver nanoparticles under environmentally relevant conditions.* Environ Sci Technol, 2012. **46**(13): p. 6985-6991.

16. Liu, J. and R.H. Hurt, *Ion release kinetics and particle persistence in aqueous nano-silver colloids.* Environ. Sci. Technol., 2010(44): p. 2169-2175.

17. Liu, J., Sonshine, D. A., Shervani, S., Hurt, R, *Controlled Release of Biologically Active Silver from Nanosilver Surfaces.* ACS Nano, 2010. **4**: p. 6903-6913.

18. Hewson, I., C. Chow, and J. Fuhrman, *Ecological role of viruses in aquatic ecosystems*. 2010, Chichester: eLS. John Wiley & Sons Ltd.

19. Panacek, A., et al., *Silver colloid nanoparticles: synthesis, characterization and their antibacterial activity.* J. Phys. Chem. C, 2006. **110**: p. 16248-16253.

20. Kvitek, L., et al., *Effect of surfactants and polymers on stability and antibacterial activity of silver nanoparticles (NPs).* J. Phys. Chem. C, 2008. **112**: p. 5825-5834.

21. Li, X. and J.J. Lenhart, *Aggregation and dissolution of silver nanoparticles in natural surface water.* Environ Sci Technol, 2012. **46**(10): p. 5378-5386.

22. Jin, X., et al., *High-through screening of silver nanoparticle stability and bacterial inactivation in aquatic media: Influence of specific ions.* Environ Sci Technol, 2010. **44**: p. 7321-7328.

23. Gutierrez, L. and T.H. Nguyen, *Interactions between rotavirus and Suwannee River organic matter: aggregation, deposition, and adhesion force measurement.* Environ Sci Technol, 2012. **46**(16): p. 8705-8713.

24. Mylon, S., et al., *Influence of salts and natural organic matter on the stability of bacteriophage MS2.* Langmuir, 2010. **26**: p. 1035-1042.

25. Fabrega, J., et al., *Silver nanoparticle impact on bacterial growth: effect of pH, concentration, and organic matter.* Environ Sci Technol, 2009. **43**: p. 7285-7290.

26. Wong, K., et al., *Influence of inorganic ions on aggregation and adsorption behaviors of human adenovirus.* Environ Sci Technol, 2012. **46**(20): p. 11145-11153.

CHAPTER 5

EFFECT OF SILVER ON THE BACTERIAL REMOVAL EFFICACY OF LOCALLY-PRODUCED CERAMIC WATER FILTERS

By

Justine Rayner[1], Hongyin Zhang[2], Jesse Schubert[3], Pat Lennon[3], Daniele Lantagne[1] and Vinka Oyanedel-Craver[2*]

is accepted in ACS Sustainable Chemistry & Engineering

[1]Department of Civil and Environmental Engineering, Tufts University, Anderson Hall 207, 200 College Avenue, Medford MA 02155

[2]Department of Civil and Environmental Engineering, University of Rhode Island, 1 Lippitt Road, Kingston, RI 02881

[3]PATH, 2201 Westlake Ave, Seattle, WA 98121

1 Abstract

Locally produced ceramic water filters (CWF) are an effective technology to treat pathogen-contaminated drinking water at the household level. CWF manufacturers apply silver to filters during production; although the silver type and concentration vary and evidence-based silver application guidelines have not been established. We evaluated the effects of three concentrations of two silver species on effluent silver concentration, *E. coli* removal, and biofilm formation inside ceramic disks manufactured with clay imported from three CWF factories using sawdust as the burn-out material. Additionally, we evaluated performance using water with three chemistry characteristics on disks made from the clays using either sawdust or rice husk as burn-out material. Results showed: 1) desorption of silver nitrate (Ag^{+}) was higher than desorption of silver nanoparticle (AgNP) for all disks; 2) effluent concentration, *E. coli* removal, and biofilm formation inside the disks were dose-dependent on the amount of silver applied; and, 3) neither water chemistry conditions nor burn-out material showed an effect on any of the parameters evaluated at the silver concentration tested. Recommendations for filter manufacturers to use only silver nanoparticles at a higher concentration than currently recommended are discussed.

2 Introduction

Worldwide, an estimated 783 million people do not have access to an improved water source [1] and hundreds of millions more drink water that is contaminated at the source or during collection, transport or storage [2]. Drinking water contaminated by pathogenic microorganisms causes gastrointestinal infections, which account for 1.87 million childhood deaths each year, mostly in developing countries [3]. Potters for

Peace (PfP) style ceramic water filters (CWF) are a low-cost technology produced locally in developing countries by pressing a mixture of clay and an organic (burn-out) material into the filter shape and then firing it to a ceramic state. Combustion of the burn-out material during the firing process creates the filter structure. CWFs remove pathogens from water by retaining them on the surface or trapping them within the filters pores.

CWFs are effective at removing more than 99% of protozoan[4, 5]and 90-99.99% of bacterial organisms from drinking water [6],however, the removal of viruses remains a challenge. In the field, water treated by CWFs is often improved to the World Health Organization's (WHO) low-risk standard [7] of fewer than 10 CFU (colony forming unit) *E. coli* /100 mL [6], and filter use has been associated with a reduction in diarrheal disease among users [8].

Silver nanoparticles (AgNP) and silver nitrate ($AgNO_3$, Ag^+) are known anti-microbial agents, and are added to filters, mostly after the firing process [9]. Reported log reduction values (LRVs) of *E. coli* by CWFs coated with AgNP range from 2.5 to 4.56 [9, 10]. LRVs of 2.1 to 2.4 of *E. coli* have been measured using filters coated with Ag^+ [6]; however, in the same study similar LRVs were also measured in CWFs without Ag^+ application [6]. In production, 83% of factories use AgNP and 17% use Ag^+ [11]. Factories use Ag^+ because it is cheaper than AgNP and/or it is locally available. The concentration of silver applied at each factory varies. Reported AgNP concentrations range from 107 to 288 ppm [11], excluding probable outliers. The silver solution is applied to fired filters by brushing or dipping. When silver solution is applied by brushing, factories reported applying from 32 to 96 mg of AgNP per filter.

The current guideline, which is experiential rather than evidence based, is 64 mg of AgNP per filter [12].

A variety of water sources are used at factories to prepare silver solutions, from untreated surface water to treated water [11].Water characteristics at the filter user's home also vary with location. Previous studies have reported a reduction in antibacterial properties of AgNP with increased size of the nanoparticle clusters due to aggregation in the presence of divalent ions such as Ca^{2+} and Mg^{2+} [13, 14]. In addition, water can contain organic compounds, such as humic acids (HA). These can rapidly coat the nanoparticle surfaces, creating a physical barrier that prevents interaction between nanoparticles and bacteria [13-15].While previous studies have reported that different water chemistry conditions can impact the disinfection performance of AgNP in the aqueous phase, these parameters have not been evaluated on CWFs either in the field or in laboratory tests.

Desorption of silver from coated CWFs has been reported during the first flushes of water [9]. A study using phosphate buffer as influent solution reported a decrease in silver concentration (as total silver) in effluent from AgNP-impregnated CWFs to below the United States Environmental Protection Agency (USEPA) maximum contaminant level (MCL) for silver [16] in drinking water (0.1 mg/L or 100 ppb) within few flushes [9]. To our knowledge, no comprehensive study has evaluated the desorption of either AgNP or Ag^{+} from CWFs using different pottery clays and water chemistry conditions.

In this study, we evaluated the performance of ceramic disks manufactured with clays from three different factories and two types of burn-out material, sawdust and

rice husks. In Phase I, disks manufactured with the different clays and sawdust were coated with three different concentrations of either AgNP or Ag^+ and evaluated for: 1) effluent silver concentration and silver retention; 2) *E. coli* removal; and, 3) biofilm formation. In Phase II, the influence of three water chemistries (Na^+-NaCl, Ca^{2+}-$CaCl_2$, and humic acid as natural organic matter) on AgNP and Ag^+ were evaluated on disks manufactured with each of the clays and each of the burn-out materials against the same outcome parameters.

3 Experimental

3.1 Disk manufacturing and pretreatment

While PFP-style filters are a 10-liter capacity filter pot, in this study 10-cm diameter disks were manufactured to simplify transport and testing. Disks were manufactured at Advanced Ceramics Manufacturing (Tucson, AZ) with clay imported from filter factories in Indonesia (Indo), Tanzania (Tanz) and Nicaragua (Nica). The burn-out material, processed between U.S. sieve numbers 16 and 30 (1.19-mm and 0.595-mm openings, respectively), comprised 15% (burn-out:clay ratio by weight) of the filter mixture. Disks were pressed at 3.58 PSI and air-dried. The different clays required different firing temperatures in order to achieve sufficient strength for testing. Fired disk thickness was approximately 1.5 cm. At the manufacturing facility, disks were boiled in water for one hour and the percent porosity of each disk was calculated by dividing the difference between saturated weight and dry weight by the geometric disk volume.

Disks were then shipped to the University of Rhode Island (URI) where they were cut to 3.8 cm diameter to fit existing filter holders. To eliminate any possible

microbiological contamination, disks were heat treated to 550 ℃ for 30 min, then allowed to cool at room temperature. The sides of the disks were sealed with silicone, allowed to dry, and then sealed in the filter holders with silicone.

3.2 Disk characterization

Tracer experiments were conducted to determine the intrinsic characteristics of the disks and to identify possible anomalies such as preferential channels in the porous matrix. Tracer tests and the subsequent determination of the advection and dispersion coefficients were performed using the procedure described in Oyanedel-Craver et al. [9] but with NaCl instead of tritiated water.

3.3 Silver release and retention

Suspended silver nanoparticles (AgNP) (coated with casein; 70 w/w% AgNP) was purchased from Laboratorios Argenol and dissolved silver (Ag^+) from Sigma Aldrich. Silver was applied by brushing each disk with a specific concentration of either Ag^+ or AgNP in the appropriate electrolyte solution according to the procedure described in Oyanedel-Craver et al. [9]. Disks were then flushed with a bacteria-free solution for 24 hours. Effluent silver concentration was measured after preserving samples by adding 2% nitric acid, using inductively coupled plasma atomic emission spectroscopy (ICP-AES) after 100 minutes, 200 minutes, 300 minutes, and at 24 hours. Percent retention of silver (R) was calculated by dividing the difference between the initial mass of silver added (m_0) and the total mass of silver released over the 24 hours period (m_t), by the initial amount of silver added to the disk:

$$R = \frac{m_0 - m_t}{m_0}$$

3.4 Bacterial removal performance

The two phases of microbiological removal testing included: 1) the determination of the optimal amount of silver required to achieve maximum bacterial deactivation (only on sawdust disks); and, 2) evaluation of the bacterial removal efficacy under different influent water chemistry conditions (using both sawdust and rice-husk disks) using current recommended silver concentration [12] (Table 5-1). Phase I and Phase II tests were conducted in duplicate, using two disks of each clay. In Phase I, only disks manufactured with sawdust were tested due to not having sufficient disks with rice husks for both phases of the study. In Phase II, disks manufactured with sawdust or rice husk and each of the clays were tested.

Table 5-1 Experimental conditions

Study Phase & Burn-out	Silver (AgNP or Ag^+) concentration (mg/g)	Water characteristics
I Sawdust	0.003	10% phosphate buffer solution
	0.03	
	0.3	
II Sawdust or rice husk	0.003	150 mg/L Na^+-NaCl
	0.003	150 mg/L Ca^{2+}-NaCl
	0.003	5 mg/L humic acid as total organic

After 24 hours of flushing with a bacteria free solution, a concentration of 10^6 CFU/mL *E. coli* in water of the same chemical composition as used during the flushing stage (i.e., deionized water with a buffer solution, electrolytes, or humic acid) was prepared and continuously fed to the disks at a flow rate of 0.5 mL/min using a peristaltic pump. The concentration of bacteria in the influent and effluent were

measured using the method described by Vigeant et al. [17]. Samples (10 mL) were taken daily for 10 days, and LRVs were calculated. For Phase I testing, a phosphate buffer solution was selected to minimize natural decay of bacteria during the test period. A fresh solution of bacteria was prepared daily for Phase I and Phase II testing.

At a feed of 0.5 mL/min for 10 days, the total throughput for each disk over the study period was ~7.2 L, which equates to ~1300 L through a full-sized filter. This was calculated by multiplying the flow rate per cm^2 of the filter disk by the area of a full-sized Nicaraguan filter using filter dimensions presented in van Halem. [5] Using this calculation, the test period simulated approximately four months of a filter treating 10 L of water per day.

3.5 Bacteria retention

After completing the bacterial removal tests, the concentration of biofilm (viable bacteria) contained in the pores of the disks was determined. The disks were ground and 10 grams were transferred to a 50-ml flask. The bacteria were dispersed in the buffer solution by gentle sonication (20% amplitude) for 15 minutes to detach the bacteria from the ceramic material. The concentration of bacteria was determined using Vigeant et al. [17] as above.

4 Results

4.1 Disks characterization

A total of 144 disks were tested, including 30 each of Indo-sawdust, Tanz-sawdust, and Nica-sawdust and 18 each of Indo-rice husk, Tanz-rice husk, and Nica-rice husk. The average advection (v) (directly proportional to the fluid velocity) and

dispersion (D) (directly proportional to the effective porosity) coefficients and geometric porosity values for the ceramic disks manufactured from the same recipe were similar. Results from disks manufactured with Indonesian and Tanzanian clays were also similar; however, disks manufactured with the Nicaraguan clay had higher advection and dispersion coefficients, indicating that the solute spread fastest through the Nicaraguan disks. For each of the clay groups, disks manufactured with rice husk had slightly lower porosities than disks manufactured with sawdust. Values are presented in Table B-1.

4.2 Phase I

Silver release and retention

For both types of silver and regardless of clay type, a higher concentration of silver was measured in effluent from disks coated with higher concentrations of silver (Figure 5-1).

With the exception of 0.003 mg/g Ag^{+}, for each silver concentration Ag^{+} resulted in a higher effluent silver concentration in comparison with AgNP. Silver concentration in the effluent reduced with solution throughput regardless of silver type. Effluent silver concentration from AgNP-coated disks was below the USEPA MCL after 24 hours in all but one case (disks made with Nicaraguan clay and impregnated with 0.3 mg/g AgNP) (Table C-2). Effluent concentration from disks impregnated with 0.3 mg/g Ag^{+} exceeded the USEPA's MCL in all cases and ranged from 797 ppb to 2,697 ppb after 24 hours.

An increased concentration of silver resulted in increased silver retention in disks coated with AgNP regardless of clay type (Figure 5-2). AgNP retention did not vary

widely between disks made with different clays. A greater percentage of AgNP was retained in disks in comparison with Ag^+, most notably in disks made with Nicaraguan clay. An increase in Ag^+ concentration from 0.003 mg/g to 0.03 mg/g resulted in increased retention; however, the highest concentration of Ag^+ 0.3 mg/g resulted in the lowest percent retention.

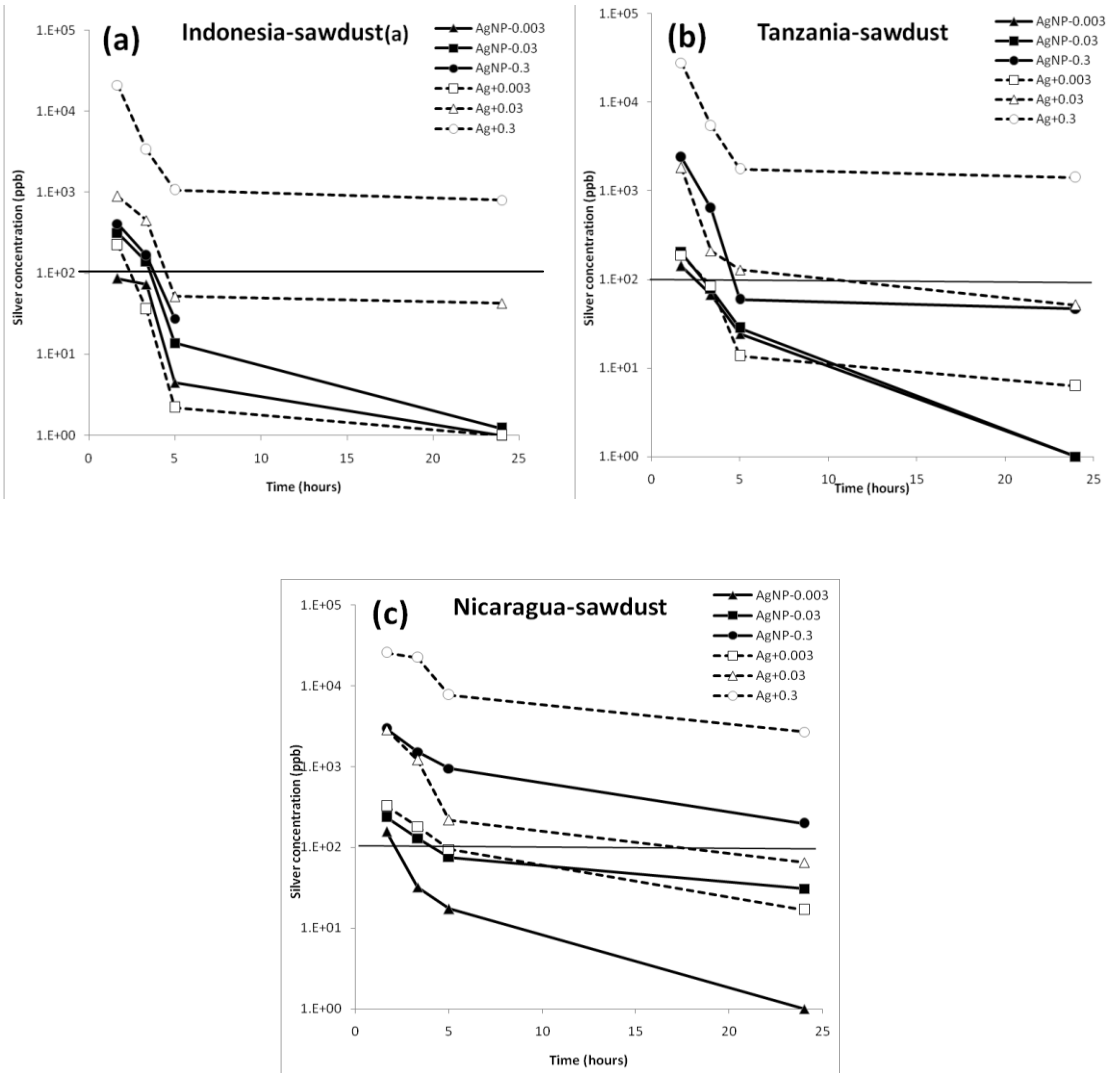

Figure 5-1 Concentration of silver (as total silver) in effluent from disks manufactured with Indonesian (a), Tanzanian (b), or Nicaraguan (c) clay and sawdust, coated with different concentrations (mg/g) of either AgNP or Ag^{+} (horizontal line at 1.E+02 represents USEPA MCL for silver)

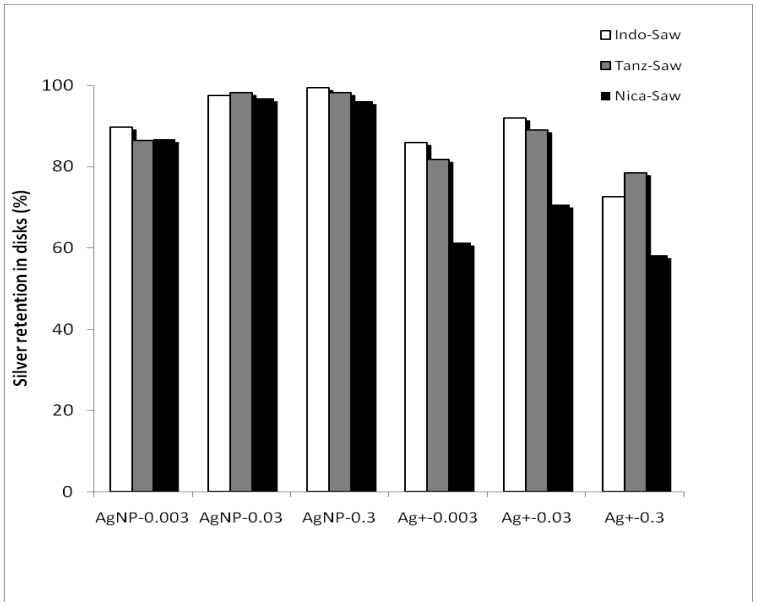

Figure 5-2 Percent silver retention in disks manufactured with different clays and sawdust coated with different species of silver of varying concentrations (mg/g).

Bacterial Removal Performance

In all samples, a sharp reduction in LRV was observed from day one to five (Figure 5-3); however, the LRV leveled off from day five to ten. Thus, the LRV performance comparison is based on the average of the results from the last five days of testing.

Disks made with Indonesian and Tanzanian clay resulted in an increased LRV with increased silver concentration, regardless of species applied (Figure 5-3). No change in terms of LRV was measured from Nicaraguan disks regardless of silver species or concentration applied. LRV was comparable between disks coated with AgNP and Ag^{+}, with the exception of Ag^{+} applied at 0.3 mg/g which achieved the highest LRV in both Tanzanian and Indonesian disks.

Disks made with either Indonesian or Tanzanian clay and coated with 0.3 mg/g AgNP achieved >4 LRV on the 10th day of testing (1-1.7 LRV improvement over control disks without silver). A small improvement in LRV over the control disks was measured with 0.03 mg/g of either silver (<1 LRV) but disks coated with 0.003 mg/g of silver showed little or no improvement in LRV in comparison with the control disks.

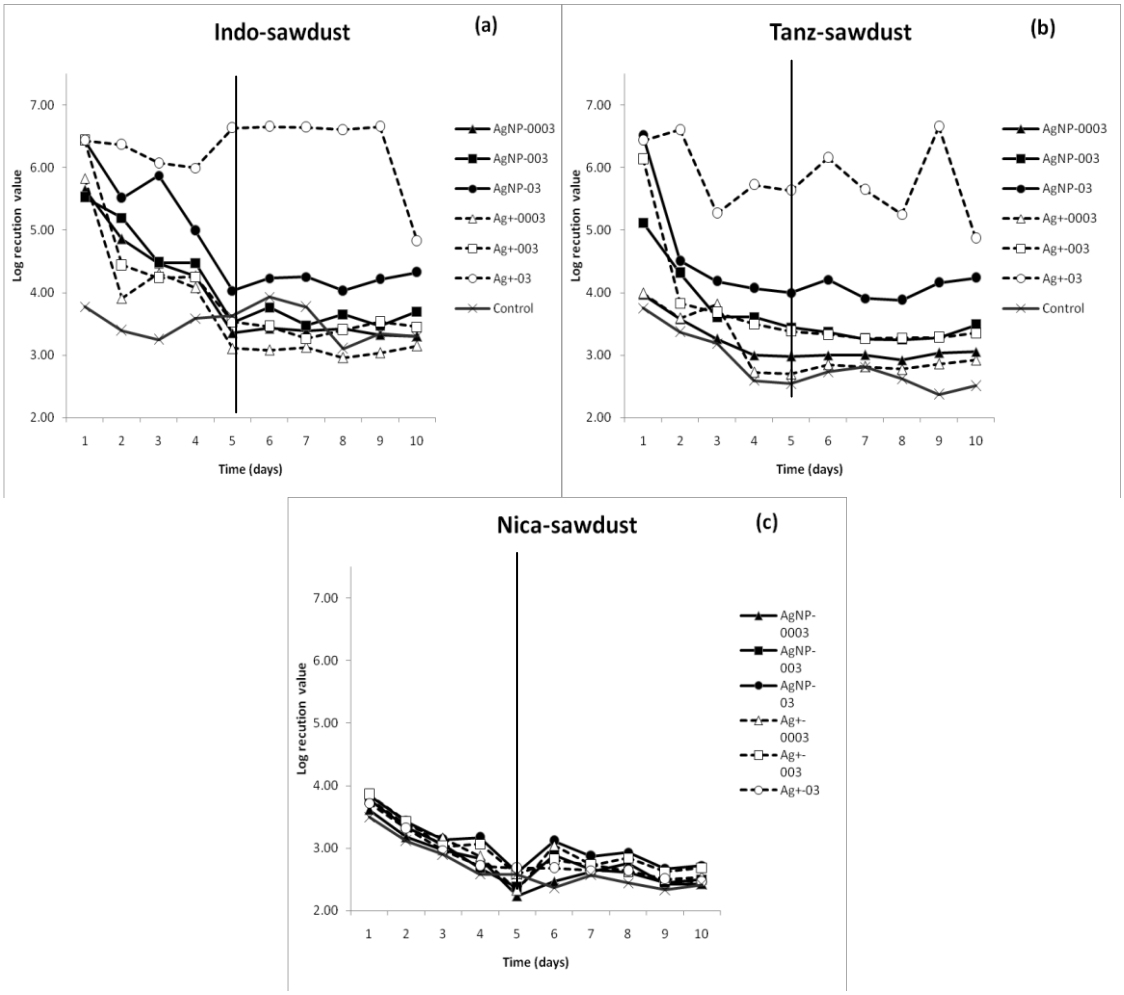

Figure 5-3 Bacterial log reduction values (LRV) of disks manufactured from Indonesian (a), Tanzanian (b), and Nicaraguan (c) clay and sawdust coated with varying amounts (mg/g) of either AgNP or Ag^{+}. Vertical lines indicate the 5th day of operation.

Viable Bacteria Retention Inside the Disks

The concentration of viable bacteria inside disks decreased with increased silver concentration of either AgNP or Ag^{+}, with the exception of disks made with Nicaraguan clay which showed little difference in viable bacteria regardless of silver concentration (Figure 5-4). Results between AgNP and Ag+ were comparable, although disks coated with 0.3 mg/g of AgNP had fewer viable bacteria than Ag^{+}. Small changes were detected in the amount of viable bacteria remaining in disks coated with 0.003 mg/g of either silver species and the control groups (without silver application), regardless of clay type.

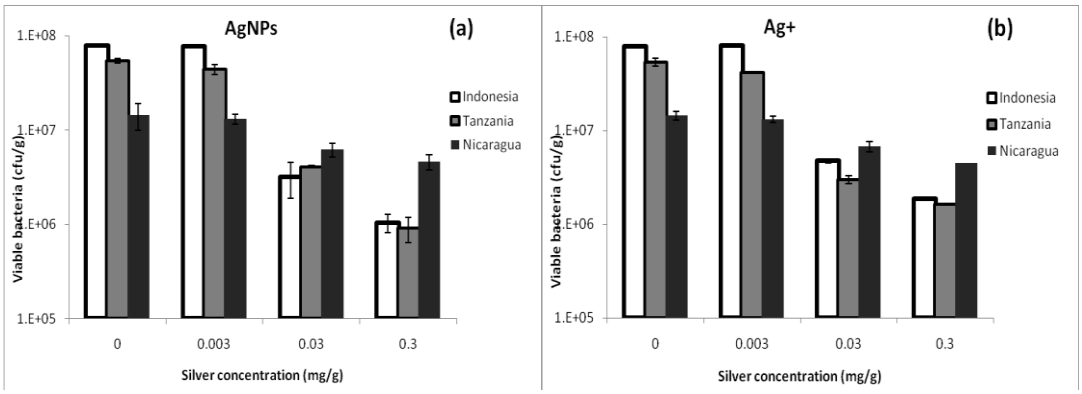

Figure 5-4 Viable bacteria detected in disks manufactured with sawdust coated with varying amounts of AgNP (a) or Ag^{+} (b).

4.3 Phase II

Effect of Influent Chemical Composition and Burn-out Material on Silver

Effluent concentration of silver from disks manufactured with rice husk or sawdust with 0.003 mg/g of either silver was below the MCL value of 100 µg/L after two hours of influent throughput with each water chemistry used (Figure B-1). Variation in influent water characteristics resulted in little difference in silver retention

among disks treated with AgNP (Figure B-2). In disks coated with Ag^+, there was some variability in silver retention in disks manufactured with Tanzanian and Nicaraguan clays when HA was used as the influent solution. A difference in silver retention was not observed between disks manufactured with the same clay but different burn-out materials.

For each clay, LRVs were similar regardless of influent water chemistry applied, the silver type or the burn-out material used (Figure B-3). The amount of viable bacteria retained in disks coated with AgNP or Ag^+ was similar regardless of the influent water chemistry conditions or burn-out material (Figure B-3). Fewer viable bacteria were retained in disks manufactured with clay from Nicaragua than disks made with either Indonesian or Tanzanian clays regardless of silver type or influent water chemistry.

5 Discussion and Recommendations

In this study, we evaluated AgNP and Ag^+ performance at varying concentrations in disks manufactured with filter material manufactured from clays from different countries. Additionally, silver was evaluated under water chemistries in disks manufactured with different clays and different burn-out materials. Disks were used as a model for full-sized filters due to space, time and laboratory constraints. The main difference between our methods and full-sized filters is the manufactured procedure. At CWF manufacturing facilities, filter mixture recipes are established by selecting a ratio and firing temperature that, using the locally available materials, result in filters that meet specific quality criteria such as flow rate, LRV and strength. In this study, rather than manufacture filter disks that would have met factory quality criteria, the

ratio of clay to burn-out material was held constant regardless of the clay origin or burn-out type in order to keep all variables except silver application constant. Firing temperature was thus adjusted, depending on the clay, to achieve enough disk strength for testing. A variation in pore structure likely resulted from using the same amount of burn-out material regardless of burn-out material type or clay properties and also as a result of the variation in firing temperature.

Disks manufactured from Indonesian and Tanzanian clays had comparable advection and dispersion parameters and their porosity and mechanical strength were suitable for testing. The higher advection and dispersion coefficients in disks manufactured with Nicaraguan clay suggested the solute spread faster, possibly due to larger or more interconnected pores. The Nicaraguan clay was exceptionally challenging to work with during manufacturing and the firing temperature (1085 ℃) likely resulted in a level of vitrification (over-fired) not found in filters at the factory level. A separate particle size analysis carried out on the raw clays used in this research found a very low percentage of clay (<2 micron) in the material from Nicaragua in comparison with the Tanzanian and Indonesians clays (0.5%, 28.5% and 31%, respectively)[18]. Results from the Nicaraguan disks should therefore be interpreted with caution in this study. In future research, we recommend holding pore structure constant – as opposed to mix ratio and manufacturing variables – to account for differences in manufacturing needed for different raw materials.

The results of our study showed: 1) increased desorption of Ag^{+} compared with AgNP; 2) a difference between effectiveness of AgNP and Ag^{+} (Ag^{+} is more effective at high concentration) ; 3) variation in LRV of *E. coli* depending upon silver

concentration; 4) variation in biofilm formation depending upon silver concentration; and, 4) at the concentrations tested, no impact of water chemistry on the efficacy of silver. These results are discusssed in the following paragraphs.

Using phosphate buffer influent water, disks retained AgNP more efficiently that Ag^{+}. Desorption of AgNP ranged from 5% to 10% for all disks tested, while for Ag^{+}, 10% to 30% desorbed from Tanzanian and Indonesian clay disks and 30% to 40% from Nicaraguan clay disks. This effect has been reported by other authors who evaluated sorption of silver species on unfired clays [19]. Ag^{+} can be displaced by cations with higher valence or higher charge density, while AgNP are trapped in the nano- and micro- porous structure of the filter allowing a slow release of silver ions as the surface of the nanoparticles is oxidized by the dissolved oxygen in water [20].

In the Indonesian and Tanzanian clays, for both silver species, a dose-response relationship was observed: an increased concentration of silver resulted in increased LRV of *E. coli*.

Disks coated with 0.3 mg/g Ag^{+} resulted in the highest LRV; however, this was likely the effect of the high concentration of silver in the effluent (one order of magnitude above the EPA MCL) and therefore bacteria deactivation is achieved via a different mechanism of action than the contact of the silver sorbed/trapped in the porous structure of the disks. With lower concentrations of silver, comparable bacterial reduction was achieved between AgNP and Ag^{+}; however, less silver was measured in the effluent of disks coated with AgNP. The application of high concentrations of Ag^{+} in filters causes concern about: 1) the time that Ag^{+} remains in the filter material, thus having implications on long-term of silver efficacy; and, 2)

potential health consequences associated with ingestion of elevated concentrations of Ag^+ by filter users. The Nicaraguan disks showed little change in LRV regardless of the type or concentration of silver applied.

In disks manufactured with Indonesian and Tanzanian clays, an application of 0.03 mg/g of AgNP resulted in a 0.4 and 1.0 LRV improvement, and disks coated with 0.3 mg/g AgNP, resulted in a 1 and 1.7 LRV by the 10^{th} day of testing in comparison with the control group, respectively. The Tanzanian disks showed a greater change in LRV than the Indonesian disks, which may be due to differences in the clay or firing temperature. Disks made from Indonesian and Tanzanian clay coated with 0.3 mg/g achieved similar LRV (>4) on the 10th day of testing. With the exception of disks manufactured with Nicaraguan clay, after 24 hours the concentration of AgNP in filter effluent was below the EPA MCL for each concentration tested, therefore safer for users and compliant under the current drinking water recommendation.

The application of 0.003 mg/g of either silver did not demonstrate improved LRV over the control disks (without silver) after 10 days of testing (equivalent to 1300 L throughput in a full-sized filter). This data is consistent with another study that compared CWF performance with and without Ag^+ application [6].

The biofilm quantification inside the disks supports and expands upon the LRV results. An increase in silver concentration resulted in reduced biofilm formation in disks; and, disks with a higher concentration of AgNP had less biofilm formation than disks with a higher concentration of Ag^+. The results of this study demonstrated that a silver coating reduces the biofilm formation (up to two orders of magnitude) compared

with disks without silver. To our knowledge this is the first study providing quantitative information about the antibiofouling properties of silver in CWF.

Phase II of our study focused on evaluating the impact of: 1) inorganic and organic compounds present in natural water; and, 2) burn-out materials, on silver sorption, bacterial removal, and biofilm formation. The silver concentration (0.003 mg/g) used in this phase was selected to minimize the impact of residual silver from either AgNP or Ag^+ on bacteria deactivation. At the selected test conditions, a difference was not observed between the clays, burn-out material, or the silver species with the water chemistries evaluated in terms of silver retention, LRV or concentration of viable bacteria remaining in the disks. This could be due to the low concentration of silver used, as little impact of this low concentration was also seen using phosphate buffered water, and several others studies have shown the influence of the chemical characteristics of the solution on AgNP aggregate size [14, 20]. Based on current knowledge about the aggregation of nanoparticles in different electrolyte solutions, water containing a low concentration of divalent ions should be used to prepare the silver solution used to coat filters.

Recommendations resulting from this research include: 1) factories should use AgNP rather than Ag^+ due to higher retention within the filters: Ag^+ is not recommended for filter application as it can lead to a silver concentration exceeding health standards in the filtered water; 2) factories could increase the AgNP concentration to 0.3 mg/g (approximately 640 g/filter) to achieve improved microbiological performance without compromising the quality of the effluent from the filter; and, 3) although this study did not show significant differences in terms of

performance with water chemistry, there is evidence from other studies that organic and inorganic compounds present in natural water can affect AgNP performance.

We recognize that these results and recommendations will have an impact on factories. Ag^{+} is locally available and significantly cheaper in some countries (and in some cases information about quality or concentration may be unavailable); and, importing AgNP can be a challenge. Therefore, the recommendation to use only AgNP and to increase AgNP concentration by 10 times the current recommendation will add a cost burden to the manufacturers. While the manufacture of high quality filter material will remain important in achieving high performing filters, silver application improves filter effectiveness; however, silver application at lower concentrations does not appear to have lasting effectiveness and therefore is not cost effective.

We also note that previous research has not always documented sufficient detail required to compare research results including type of silver, silver concentration, dilution and throughput water characteristics. In some cases this may be attributable to a lack of documentation or information about silver type or concentration. Previous research should therefore be compared with caution.

The limitations in this study include the use of a controlled 5.4 L/hr flow rate, which is about 2-3 times the flow rate used in the field. This flow rate was selected to achieve throughput equivalent to represent long-term operation in a short period of time. The results likely overestimate biofilm formation and underestimate microbiological performance due to faster water velocity, constant pressure, and reduced contact time between silver and bacteria. This study design was such to

challenge the materials and therefore, silver would likely be more effective at the household level than measured in this study.

This study identified several key parameters that require more detailed studies, such as silver concentration and the effects of various influent water characteristics and the nature of clay and other manufacturing variables. Further research recommendations include: 1) evaluation of higher concentrations of AgNP under a selection of water chemistry conditions to evaluate nanoparticle aggregation and silver particle size distribution in filter effluent; 2) evaluate effects of water characteristics both on silver dilution and filter use (influent solutions); and, 3) evaluate physicochemical interaction between clay and AgNP or Ag^{+} on silver sorption and LRV and the influence of these properties and the pore size distribution of the porous matrix.

REFERENCE

1. WHO/UNICEF, *Progress on Drinking Water and Sanitation: 2012 Update*. 2012.
2. Clasen, T. and A. Bastable, *Faecal contamination of drinking water during collection and household storage: the need to extend protection to the point of use.* Journal of Water and Health, 2003. **1**(3): p. 109-115.
3. Boschi-Pinto, C., L. Velebit, and K. Shibuya, *Estimating child mortality due to diarrhea in developing countries.* World Health Organization Bulletin, 2008. **86**(9): p. 710-717.
4. Lantagne, D.S., *Investigation of the potters for peace colloidal silver impregnated ceramic filter. Report 1: Intrinsic Effectiveness*, USAID, Editor. 2001.
5. van Halem, D., *Ceramic silver impregnated pot filters for household drinking water treatment in developing countries*. 2006: Delft, The Netherland.
6. Brown, J. and M.D. Sobsey, *Microbiological effectiveness of locally produced ceramic filters for drinking water treatment in Cambodia.* Journal of Water and Health, 2010. **8**(1): p. 1-10.
7. WHO, *Guidelines for drinking-water quality, 2nd edition*, WHO, Editor. 1997: Geneva, Switzerland.
8. Brown, J., M.D. Sobsey, and D. Loomis, *Local drinking water filters reduce diarrheal disease in Cambodia: a randomized, controlled trial of the ceramic water purifier.* American Journal of Tropical Medicine and Hygiene, 2008. **79**(3): p. 394-400.

9. Oyanedel-Craver, V.A. and J.A. Smith, *Sustainable colloidal-silver-impregnated ceramic filter for point-of-use water treatment.* Environmental Science & Technology, 2008. **42**(3): p. 927-933.

10. Kallman, E., V. Oyanedel-Craver, and S. J, *Ceramic Filters Impregnated with Silver Nanoparticles for Point-of-Use Water Treatment in Rural Guatemala.* Journal of Environmental Engineering-ASCE, 2011. **137**(6): p. 407-415.

11. Rayner, J., B. Skinner, and D. Lantagne, *Current practices in manufacturing locally-made ceramic pot filters for water treatment in developing countries.* Journal of Water, Sanitation and Hygiene for Development (in press), 2013.

12. CMWG, *Best Practice Recommendations for Local Manufacturing of Ceramic Pot Filters for Household Water Treatment*. 2011: Atlanta, GA, USA.

13. Zhang, H. and V. Oyanedel-Craver, *Evaluation of the disinfectant performance of silver nanoparticles in different water chemistry conditions.* Journal of Environmental Engineering-ASCE, 2011. **138**: p. 56-66.

14. Zhang, H., J.A. Smith, and V. Oyanedel-Craver, *The effect of natural water conditions on the anti-bacterial performance and stability of silver nanoparticles capped with different polymers.* Water Research, 2012. **46**: p. 691-699.

15. Fabrega, J., et al., *Silver nanoparticle impact on bacterial growth: effect of pH, concentration, and organic matter.* Environmental Science & Technology, 2009. **43**(7285-7290).

16. USEPA. *http://water.epa.gov/drink/contaminants/index.cfm*. 2011.

17. Vigeant, M.A., et al., *Reversible and irreversible adhesion of motile Escherichia coli cells analyzed by total internal reflection aqueous fluorescence microscopy.* Applied and Environmental Microbiology, 2002. **68**(2794-2801).

18. Duocastella, M.d.M. and K. Morrill, *Particle size distribution analysis for ceramic pot water filter production*. 2012, Potters without Borders: Enderby, British Columbia, Canada.

19. Matsumura, Y., K. Yoshikata, and T. Tsuchido, *Mode of bactericidal action of silver zeolite and its comparison with that of silver nitrate.* Applied and Environmental Microbiology, 2003. **69**(7): p. 4278–4281.

20. Li, X.A., J.J. Lenhart, and H.W. Walker, *Dissolution-Accompanied Aggregation Kinetics of Silver Nanoparticles.* Langmuir, 2010. **26**(22): p. 16690-16698.

CHAPTER 6

COMPARISON OF THE BACTERIAL REMOVAL PERFORMANCE OF SILVER NANOPARTICLES AND A POLYMER BASED QUATERNARY AMINE FUNCTIONALIZED SILSESQUIOXANE COATED POINT-OF-USE CERAMIC WATER FILTERS

By

Hongyin Zhang and Vinka Oyanedel-Craver*

is submitted to Journal of Hazardous Materials

Department of Civil and Environmental Engineering, University of Rhode Island,

Bliss Hall 213, Kingston, RI 02881

1 Abstract

This study compares the disinfection performance of ceramic water filters impregnated with two antibacterial compounds: silver nanoparticles and a polymer based quaternary amine functiaonalized silsesquioxane (Poly (trihydroxysilyl) propyldimethyloctadecyl ammonium chloride (TPA)). These compounds were evaluated using ceramic disks (6.5 cm) manufactures with clay obtained from a ceramic filter factory located in San Mateo Ixtatan, Guatemala. Results showed that TPA can achieve a log bacterial reduction value of 10 while silver nanoparticles reached up to 2 log reduction using a initial concentration of bacteria of 10^{10}-10^{11} CFU/ml . Similarly, bacterial transport experiment through section of ceramic water filters demonstrated that ceramic filter disks painted with TPA achieved a bacterial log reduction value of 6.24, which is about 2 log higher than the values obtained for disks painted with silver nanoparticles (bacterial log reduction value: 4.42). The release of both disinfectants from the ceramic materials to the treated water was determined measuring the effluent concentrations in each test performed. Regarding TPA, about 3% of the total mass applied to the ceramic disks was released in the effluent over 300 min, which is slightly lower than the release percentage for silver nanoparticles (4%). This study showed that TPA provides a comparable performance than silver nanoparticles in ceramic water filter. Another advantage of using TPA is the cost as the price of TPA is considerable lower than silver nanoparticles. In spite of the use of TPA in several medical related products, there is only partial information regarding the long health risk of this compound. Additional long-term toxicological information

for TPA should be evaluated before their future application in ceramic water filters is considered.

2 Introduction

Ceramic filters impregnated with silver nanoparticles (AgNP) are a promising point-of-use water treatment technology in the developing world that can be applied with local materials and labor. Currently, ceramic water filters (CWFs) are manufactured by pressing and firing a mixture of clay and a combustible material such as flour, rice husks, or sawdust prior to treatment with AgNP. The filter is formed using a filter press, after which it is air-dried and fired in a flat-top kiln, increasing the temperature gradually to about 900 ˚C during an 8-h period [1]. This forms the ceramic material and burns off the sawdust, flour, or rice husk in the filters, making it porous and permeable to water. After firing, the filters are cooled and impregnated with a silver solution (either AgNP or silver nitrate) by either dipping the filters in the silver solution or painting the silver solution onto the filters.It has been demonstrated that the silver compounds add disinfection properties to the CWFs [1, 2], increasing the bacteria removal and therefore increasing the water quality [3]. Also, it has been hypothesized that the use of the silver solution extends the useful life of the ceramic filters by preventing the formation of biofilm inside the ceramic matrix [1-3].

The silver compounds are added to the CWFs as the disinfectant in three different ways: 1) they can be painted on the CWFs, 2) the CWFs can be dipped in the silver solution, and 3) the silver compounds, in powder form (AgNP or $AgNO_3$) can be mixed with clay, sawdust and water. Rayner [4] estimated that 56% of the factories painted the silver solution onto the CWF, 33% dipped the CWFs into the silver

solution, and the remaining 11% mixed the silver in powdered form with the clay and sawdust. About 83% of factories use AgNP, while other 17% use silver nitrate.

The prices of noble metals have increased significantly in the past few years. The price of silver has increased by almost a factor of three since 2005 [5], threatening the sustainability of the current application of colloidal silver in CWFs. Therefore, alternative disinfectant compounds are needed to ensure the efficacy of these systems. One candidate compound is 3-(trihydroxysilyl) propyldimethyloctadecyl ammonium chloride (TPA), a polymer that compounds silane with a quaternary ammonium species. Similar to AgNP, TPA exhibits excellent antimicrobial properties in dissolved solutions and has long-term durability. A recent report indicated that 0.25 w/w% TPA exhibited a 99.99% inhibitory effect on *Escherichia coli* while 1% silver zeolite can only achieve 41.18% inhibition [6].TPAis usually applied as an antibacterial or anti-mold reagent. Current TPA applications include impregnation into thermoplastics or thermoset resins; dissolution in water and other solvents for use in coating, as caulk or as adhesive formulations; and application asa surface treatment for disinfection purposes [6]. The price of pure TPA powder is about $222/kg, which is much lower than the price of silver (about $1024/kg)[5, 7]. The high disinfection performance and lower price makes TPA a potential disinfectant alternative to AgNP.

To the author's knowledge, no study has compared the disinfection performance of TPA and AgNP in CWFs. In this work, the potential application of TPA as a disinfectant in CWFs was evaluated. TPA was chosen because it is a non-toxic, non-irritating, biocompatible, thermally stable, and environmental friendly polymer. Compared with similar quaternary ammonian silane compounds, TPA has the

advantageous property of non-leaching because reactive silanol groups within the TPA can either react with the treated materials to form covalent bonds or form strong hydrogen bonds [6, 8]. The deactivation efficacies of AgNP and TPA were measured using a manometric technique that determines the overall activity of active bacteria and has advantage of avoiding miscounting compared to the traditional plate-count method. Bacteria were transported through the CWFs to compare the initial disinfectant performance of CWFs impregnated with AgNP and TPA. The release of AgNP and TPA from ceramic materials was also measured so that potential manufacturers could be informed regarding the best management practices to minimize the exposure of workers to the hazardous materials.

3 Materials and methods

3.1 Ceramic disks manufacturing

The composition of the ceramic disks consisted of 40% Guatemalan clay, 10% flour and 50% (grog) pottery residues by weight. This selected combination of materials was the optimum combination because CWFs with higher percentages of flour were weak and can be broken easily, while CWFs with higher clay content has low hydraulic conductivity resulting in low flow rates [1]. The clay, flour and grog were homogeneously (244 g) mixed after which 75 mL of DI water were added [1]. The mixture was molded using a cylindrical mold (with a diameter of 6.5 cm) and compressed for 1 min at a pressure of 1000 psi. The disks were air-dried at room temperature for three days and then fired in a furnace with the temperature increasing at a rate of 150^0C/h until a temperature of 600^0C was reached. Then, the rate was increased to 300^0C/h until the temperature reached 900^0C, where it was maintained for

3 h. The obtained CWFs were cut into small water filter disks of 1.5 inches in diameter. The porous structure of the disks was confirmed by scanning electron microscopy (SEM).

3.2 Preparation and characterization of AgNP and TPA

Commercial AgNP (70.37% w/w Ag^0) stabilized with casein was obtained from Argenol laboratories (Zaragoza, Spain). Commercial TPA (0.5 w/w% TPA) was obtained from BIOSAFE, Inc. (Pittsburgh, USA). The surface charge and average size distribution of AgNP and TPA in 10% phosphate buffer solution (PBS) were determined in triplicate by zeta potential and dynamic light scattering (DLS) using a Zetasizer (Nano ZS, ZEN 3600, Malvern) at 25 ^{0}C.

3.3 Microbial cultures

A non-pathogenic wild strain of *E.coli* provided by IDEXX laboratories (Westbrook, USA) was used for the bacteria-transport experiments. This organism was selected because of its use as a specific indicator of fecal contamination in drinking water and its extensive use in several studies of AgNP[1, 9, 10], which will allowed us to compare our results with previously published work. The bacteria were grown as described by Vigeant et al. [11]. Cells were re-suspended in a sterilized solution prepared with the respective water samples and synthetic water solution to a concentration of 10^{10}-10^{11} CFU/ml. Determination of the *E. coli* concentration was performed using the membrane filtration technique, applying m-FC with Rosolic Acid Broth (Millipore) and incubation at 44.5^{0}C for 24 h[11].

3.4 Evaluation of the antibacterial activity

Batch tests of the deactivation of the bacteria by AgNP and TPA (concentration range: 6-45 mg/L) were performed in duplicates during 20 h using the manometric respirometric technique described by Zhang et al. [9, 10].

3.5 Tracer and bacteria transport experiment

Transport experiments were performed with the CWFs under two conditions.1) without AgNP/TPA, and 2) after being painted with the two compounds. The CWFs were placed in holders connected to a Masterflex pump that maintained a flow rate of 0.5 mL/min. NaCl was used as the conservative tracer. The flow rate of 0.5 mL/min through a filter disk is estimated at approximately 5.4 L/h using the dimension of a full-sized water filter. One milliliter of NaCl (10 g/L) was injected, and DI water was used as the inflow solution. Samples were collected over time, and an electric conductivity (EC) meter was used to determine the NaCl concentrations. Before the bacteria transport experiment, the CWFs were saturated with 10% PBS inflow solution (consist of 1.12 g/L K_2HPO_4, 0.48 g/L KH_2PO_4, and 2 mg/L Ethylenediaminetetraacetic acid (EDTA); pH: 7.3) for 12 h. Then, the CWFs were dried in an incubator for 12 h. One milliliter of *E. coli* (10^{10}-10^{11} CFU/mL) was passed through the CWFs, and effluent samples were collected over time to determine the breakthrough of the *E. coli*. Then, the CWFs were heated in an oven at 500 ^{0}C for 30 min and then cooled to room temperature. The CWFs were painted with AgNP and TPA using brushes according to the total mass applied as described by Oyanedel-Craver and Smith [1]. After drying for 24 h, one milliliter of *E. coli* solution was passed through the CWFs, and the concentration of the bacteria in the effluent was determined. Meanwhile, the rate of decay of the bacteria in the 10% PBS also was

measured as a control using the same bacterial concentration and inflow conditions. The CXTFIT program (Riverside, USA) was used to simulate the obtained breakthrough curves. The advection-dispersion equation with first-order decay is:

$$R\frac{\partial c}{\partial t} = D\frac{\partial^2 c}{\partial x^2} - v\frac{\partial c}{\partial x} - \mu c$$

The initial and boundary conditions [1] were:

$c(x,0)=0$

$c(0, t)=c_0$ for $t<t_0$

$c(0, t)=0$ for $t>t_0$

$$\frac{\partial c(L,t)}{\partial x} = 0$$

Where R is the retardation coefficient, c is the concentration of NaCl or *E. coli* (CFU/ml), t is time (min), t_0 is the tracer or bacteria pulse injection time (min), D is the dispersion coefficient (cm^2/min), μ is the first-order decay coefficient (min^{-1}), v is the linear velocity (cm/min), and L is the thickness of the CWF. The model assumes local equilibrium sorption.

The concentration of AgNP in the effluent was measured as total silver (ICP-MS, X series, Thermo Elemental, Waltham, USA). TPA concentration was measured as quaternary ammoniumcompounds (QAC) concentration using a QAC test kit (HACH, Loveland, USA) and a DR 2100 spectrophotometer (HACH).

4 Result and discussion

4.1 Characterization of the manufactured ceramic and the disinfectants

Figure 6-1 shows the SEM analysis of the manufactured ceramic. The SEM images clearly showed the porous structure of the disks. The pores in the disk are

formed due to the volatilization of the burn off material at high temperature and the subsequent shrinkage of the clay due to vitrification.

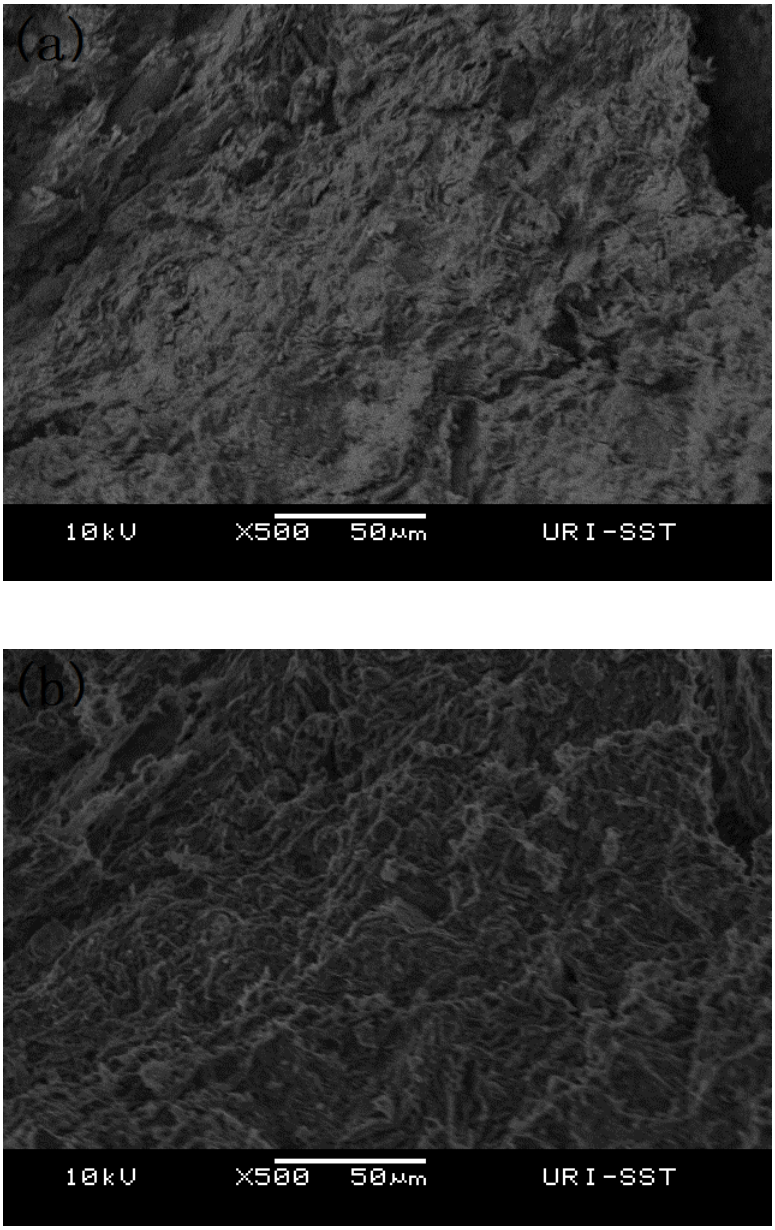

Figure 6-1 SEM analysis of the manufactured ceramic using Back scattered mode (a) and Secondary electron mode (b)

Figure C-1 (Supplementary information) shows the size distribution, average size, and ζ-potential of AgNP and TPA. The average particle size of the AgNP (69.5 ±2.6 nm) was smaller than that of TPA (247 ±27.8 nm). Further analysis was performed to compare the size distribution of AgNP and TPA. The comparison displayed that the

TPA exhibited a wider size distribution than AgNP. However, it was noticed that the ζ-potential of the AgNP was much smaller than that of TPA. AgNP shows negative ζ-potential value (-25.6±0.75 mV). In DI water condition, previous studies showed that AgNP has negative ζ-potential values because an $Ag(OH)_2^-$like species at the surface can be formed due to the oxidation of metallic silver by O_2 presence in water. In water matrices containing ions, adsorption of anions can also impart a negative surface charge. On the contrary, the positive ζ-potential value of TPA (27 ±0.95 mV) was due mainly to the positively-charged quaternary ammonia groups in the TPA compound. Similarly, Cumberland and Lead [12] found that AgNP show a ζ-potential value of -25.8 ±5 mVin solutions containing HNO_3 or NaOH (pH in the range of 5 to 8). A ζ-potential value of 28.29 mV was found for 3-(trimethoxysilyl) propyldimethyloctadecyl ammonium chloride that was very similarto that of TPA in the DI water condition[13]. Since most of the observed ζ-potentials of ceramic surfaces are negative [14], the ζ-potential values implied that the surface of the CWFs could adsorb TPA preferentially over the AgNP, which was supported by the results from the AgNP/TPA release experiment presented in Table 6-2 and Figure 6-4. Our study also investigated the ζ-potential of *E. coli* (-6.46 ±0.43 mV) in a 10% PBS, which indicates that *E. coli* may preferentially contact TPA rather than the AgNP due to the adverse ζ-potential values for TPA and *E. coli*.

4.2 Bulk Antimicrobial activity of AgNP and TPA

Figure 6-2 presents the antimicrobial activity of AgNP and TPA determined using a manometric respirometric method. The figure shows that the antimicrobial ability of both compounds increases with increasing concentration. It is noteworthy that TPA

exhibited higher antimicrobial ability (54%) than AgNP (30%) at lower concentration and similar antimicrobial ability at higher concentration (AgNP: 99%; TPA: 100%). The mechanism of the antimicrobial activity of AgNP has been attributed to the damage of bacteria by pitting the cell membrane, lysis of cells caused by silver ion release, or damage of the cell by the reactive oxygen species formed on the surface of the nanoparticles [15, 16]. The toxicity of TPA is determined mainly by the positively charged ammonium groups and octadecyl groups. Kim et al [17] suggested that the interactions between TPA and the cytoplasmic membrane of *E. coli* can be enhanced by the positively charged ammonium groups. In addition, octadecyl groups can also increase the hydrophobic interaction with the cytoplasmic membrane and then cause cell disruption and leakage of the membrane. The value of ζ-potential for *E. coli* in 10% PBS was also determined (-6.46 $\pm$ 0.43 mV), which indicates that 1) attraction forces could exist between the negatively charged *E. coli* membrane and the positively charged TPA, and 2) electrostatic repulsion forces could exist between the negatively charged *E. coli* membrane and the negatively charged AgNP. This may explain why TPA has better disinfection performance than AgNP at similar low concentrations. In addition, high ionic strength in PBS may also account for the lower antimicrobial property of AgNP. Liu and Hurt [18] reported a decreased concentration of silver ion released from AgNP in solutions with high ionic strength. As silver ion release was proposed as an important factor that could affect the antimicrobial properties of AgNP, decreasing silver ion release could result in a lower antimicrobial property. Zhang and Oyanedel-Craver [9] observed an increasing particle size of AgNP with increasing ionic strength and indicated a negative correlation between particle size and

antimicrobial property.

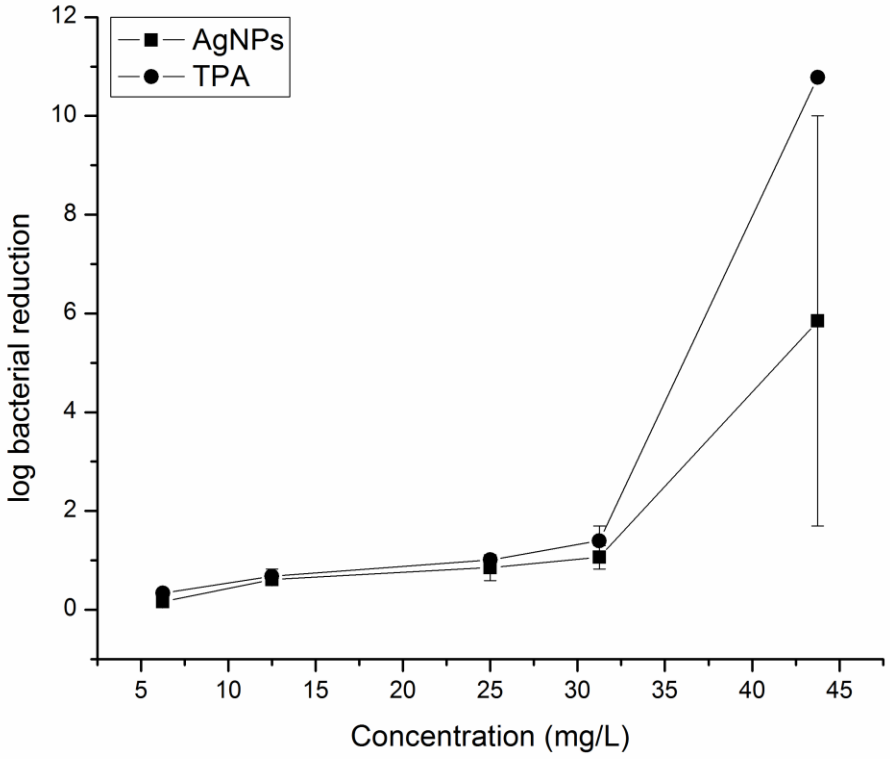

Figure 6-2 Disinfection performances of AgNP and TPA in 10% PBS; Duration: 20 h.

4.3 Tracer and bacteria transport

Table 6-1 Parameters of tracer and bacteria transport experiment and the percentages of total bacteria removal.

	Linear velocity v (cm/min)	Coefficient of dispersion D (cm^2/min)	Retardation factor R	First-order decay coefficient μ (min^{-1})	Log removal of *E.coli*
Tracer test	0.1115	0.02304	1	0	N/A
CWF_1 (without painting AgNP)	0.1115	0.02304	0.5764	0	4.22
CWF_1 (painted with AgNP)	0.1115	0.02304	0.5764	0.0258	4.42
CWF_2 (without painting TPA)	0.1115	0.02304	0.5383	0	4.34
CWF_2 (painted with TPA)	0.1115	0.02304	0.5383	1.783×10^{-8}	6.24

N/A: not available

The CXTFIT program was used to provide optimum fits for the tracer and bacteria transport data. Linear velocity *v* and dispersion coefficient *D* were determined with $R = 1$ and $\mu = 0$ using the conservative tracer transport experiment data. R and μ were determined from the bacteria transport experiment. The fitted parameters and the percentages of bacteria removal are listed in Table 6-1. The simulated concentrations of NaCl and bacteria agree well with the observed concentrations.

Figure 6-3 (a) presents the results of the tracer transport experiment. NaCl was used as a conservative tracer after the CWF had been washed with DI water for 48 h until the conductivity of the effluent became constant (< 8 μS/cm). NaCl recovery was 98.9% during the collection of the effluent sample. The figure also shows that breakthrough occurred at 10 min during the conservative tracer test.

Figure 6-3 (b) and 6-3 (c) present the bacteria transport using CWFs with/without painted AgNP and TPA, respectively. The breakthrough for *E. coli* occurred at 5 min. After the injection of *E. coli* bacteria, removals of up to 99.4% (bacterial log reduction value, LRV: 4.22) (CWF_1) and 99.55% (LRV: 4.34) (CWF_2) (Table 1) were achieved using CWFs without any AgNP or TPA. This indicates that CWFs themselves remove the bacteria effectively. After painting the CWFs with the AgNP, improved percentages of bacteria removal were obtained. The results (Table 6-1) showed that a higher percentage of bacteria removal was achieved using CWF_2 (painted with TPA) (>99.999%; LRV: 6.24) than CWF_1 (painted with AgNP) (99.89%; LRV: 4.42). It also was found that AgNP and TPA exhibited 82.3% and 99.6% bacteria removal, respectively, using the following equation:

$$\text{Bacterial removal} = \frac{N - N'}{N} \times 100\%$$

where$N$ is the number of viable bacteria in the effluent without AgNP/TPA coated on the CWFs, and N' is the number of viable bacteria in the effluent with AgNP/TPA coated on the CWFs. The results indicate that TPA had a higher antimicrobial activity than AgNP at the experimental conditions used. The results of the bacteria transport experiment agreed with those obtained in the bulk antimicrobial activity test.

Similar results were observed in earlier work [1]. The main mechanism for the removal of bacteria by CWFs before applying AgNP or TPA was size exclusion [1]. Bacteria passing through CWFs can be retained by the small pores of the CWFs and pass through the large pores preferentially. However, there is an alternative mechanism that suggests that the bacteria possibly could be retained in the CWF by a reversible sorption process [1]. However, if a reversible sorption process is occurring, the breakthrough of bacteria should appear after the breakthrough of NaCl. It is noteworthy that the peak of the observed NaCl breakthrough occurred after the peak of the bacteria breakthrough when comparing Figure6-3 (a) with Figures 6-3 (b) and 6-3 (c). Similar results were observed for bacteria transport in CWFs and natural soils [1, 19-21]. It was also observed that effluent bacteria-concentration peaks occurred before the tracer peaks.

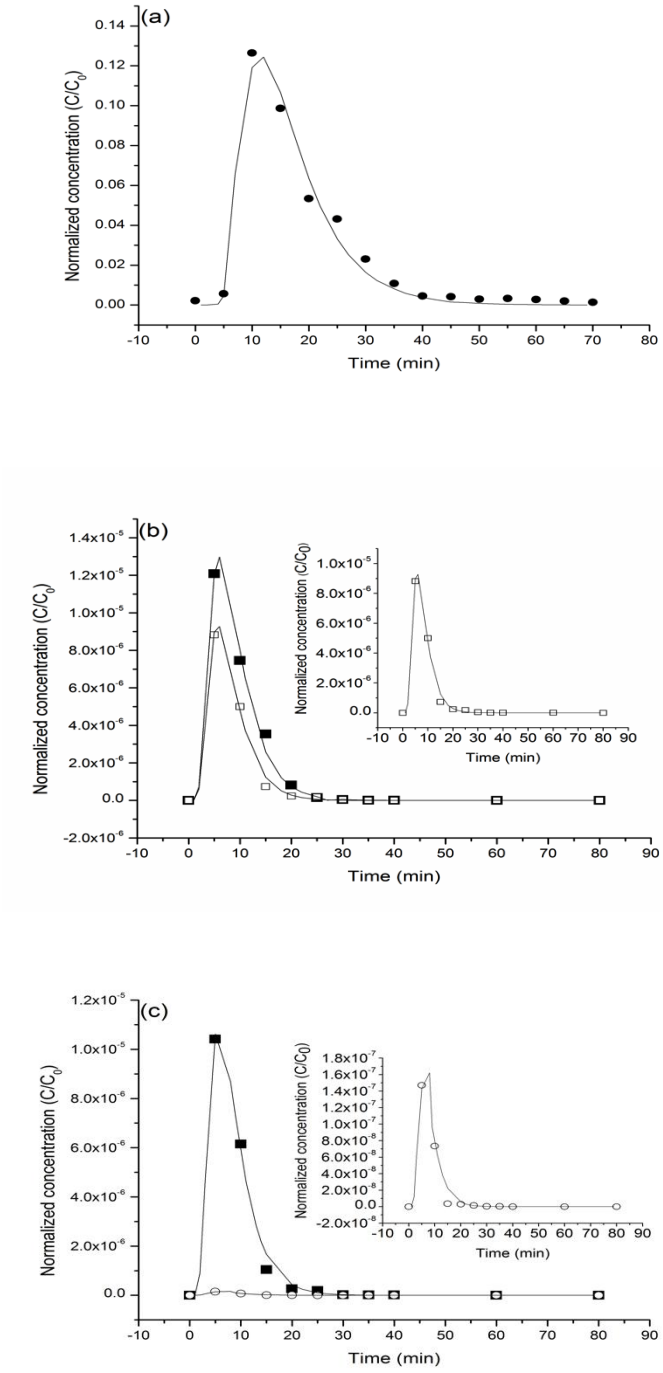

Figure 6-3 (a) Effluent NaCl concentrations normalized to the influent pulse concentration as a function of time for CWF. (b) Effluent *E. coli* concentrations normalized to the influent pulse concentration as a function of time for CWF

with/without painting AgNP. (c) Effluent *E. coli* concentrations normalized to the influent pulse concentration as a function of time for CWF with/without painting TPA. Inflow condition: 10% PBS; Solid circles: normalized NaCl concentration; Solid squares: normalized *E. coli* concentration using CWFs; Empty squares: normalized *E. coli* concentration using AgNP painted CWF; Empty circles: normalized *E. coli* concentration using TPA painted CWF; Lines: optimized solute-transport model fits

4.4 AgNP and TPA concentrations in effluent water

Table 6-2 Total release and percentage of AgNP and TPA retained in the CWFs

	Total mass released in the effluent over 300 min	Mass percentage retained in CWFs
AgNP	0.04 mg	96%
TPA	0.03 mg	97%

Table 6-2 and Figure 6-4 show the amount of AgNP and TPAretained in the CWFs and their concentrations in the effluent water. The concentrations of AgNP in the effluent decreased over time. According to the drinking water guidelines of the U.S.Environmental Protection Agency (EPA), the total concentration of silver in the water should not exceed 0.1 mg/L. However, it was observed that the initial concentration of silver in the effluent was 0.23 mg/L. Consequently, we recommend that the CWFs should be rinsed for at least 100 min before point-of-use application. Similarly, the concentration of TPA in the effluent decreased over time. Currently, no specific regulatory information has been listed for TPA. As comparison, a similar quaternary ammonium silane product, 3-(trimethoxysilyl) propyldimethyloctadecyl ammonium chloride (Oral LD_{50}>5000 mg/kg; Dermal LD_{50}>2000 mg/kg; Inhalation

LC_{50}>2.0 mg/L), has been documented by the U.S. EPA which shows a lack of toxicological effects at dose level up to and including a limit dose (i.e. 1000 mg/kg/day) [22]. We recommend that CWFs should be washed at least 300 min to minimize any possible adverse health effect.

One of the adverse health effects associated with exposure to silver is Argyria, an irreversible skin condition. The Occupational Safety and Health Administration (OSHA Washington, USA) and the National Institute for Occupational Safety and Health (NIOSH, Atlanta, USA) have established an exposure limit of 0.01 mg/m^3 (in air) for metallic and soluble silver compounds. However, although the exposure limit and health effects of silver have been studied extensively [23], the threshold exposure limit of TPA still is not available. Studies related to the exposure threshold and health effects of TPA on animals and humans are needed in future studies.

Table 6-3 Some toxicological parameters of silver and TPA

	Acute oral toxicity (LD_{50})	Acute dermal toxicity (LD_{50})	Acute inhalation toxicity (LC_{50})	Oral reference dose (RfD)
Silver	100 mg/kg (AgNP) 129 mg/kg ($AgNO_3$)	No mortality observed (AgNP)	$>7.5\times10^{-4}$ mg/L (AgNP)	0.005 mg/kg/day
TPA	>5000 mg/kg	>5050 mg/kg	>2.19 mg/L	N/A

N/A: not available. Data is obtained from Korani et al. [24]; Sung et al. [25]; U. S. EPA [26]; Venugopal and Luckey [27].

Table 6-3 shows some of the toxicological data that have been published for silver and TPA. These data indicate that silver has a higher acute oral toxicity than TPA. However, Table 6-3 suggests that acute dermal toxicity and acute inhalation toxicity are low for both AgNP and TPA. The oral reference dose (RfD) of AgNP has been

determined. However, the RfD for TPA is not available because it is an emerging disinfectant. Future studies are needed to determine the RfD of TPA to assess its chronic health effects.

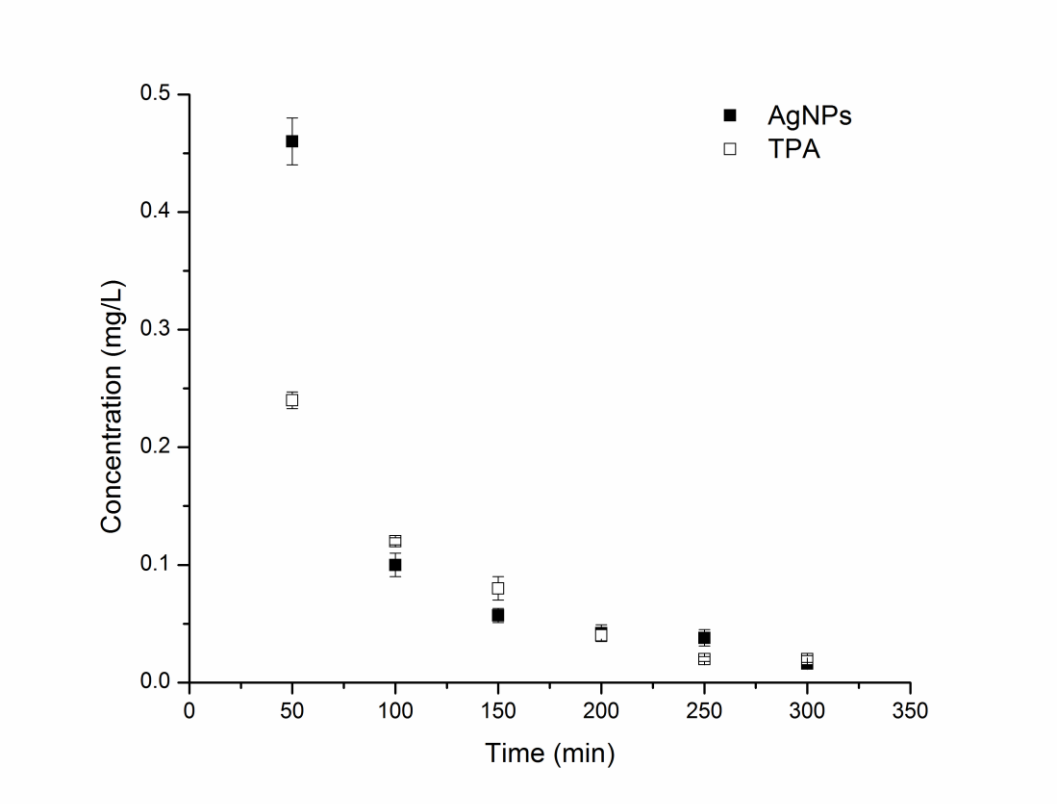

Figure 6-4 Concentrations of total silver and total TPA in the effluent water during 300 min.Inflow condition: 10% PBS; Original concentration of AgNP or TPA in CWFs: 0.03 mg/g

5 Conclusion

Conclusively, this study showed that TPA is a viable alternative to AgNP in ceramic disks due to its high antimicrobial properties. Additionally, due to its lower price compared with AgNP, the application of TPA lowers the cost of CWFs. This could benefit to manufactures that will be using a product with a market value less

variable and could economically benefit the CWF users due to a lower cost of the product.

TPA can achieve higher bacterial reduction than AgNP in both aqueous solution and ceramic disks, suggesting that TPA could be an alternative disinfectant agent for this particular technology. The concentration of both AgNP and TPA released to the effluent are similar and decrease over time, indicating that similar amount of AgNP and TPA was retained inside disks. Considering the current toxicological information of TPA, the release of TPA may not have an acute impact on human health. However, more information regarding the long-term health effects of TPA is still needed to support the application of this product to ceramic water filters.

REFERENCES

1. Oyanedel-Craver, V.A. and J.A. Smith, *Sustainable colloidal-silver-impregnated ceramic filter for point-of-use water treatment.* Environ. Sci. Technol., 2008. **42**: p. 927-933.
2. Bielefeldt, A.R., K. Kowalski, and R.S. Summers, *Bacterial treatment effectiveness of point-of-use ceramic water filters.* Water Res., 2009. **43**(14): p. 3559-3565.
3. van Halem, D., et al., *Assessing the sustainability of the silver-impregnated ceramic pot filter for low-cost household drinking water treatment.* Phys. Chem. Earth, 2009. **34**(1-2): p. 36-42.
4. Rayner, J., *Current practices in manufacturing of ceramic pot filters for water treatment*. 2009, Loughborough University.
5. Silverprice. *http://goldprice.org/silver-price.html*. 2011 [cited 2012 Nov. 11]; Available from: http://goldprice.org/silver-price.html.
6. Getman, G.D., *An advanced non-toxic polymeric antimicrobial for consumer products*, in *Rubber World* 2011. p. 22-25.
7. Biosafe. *www.biosafe.com*. 2011; Available from: www.biosafe.com.
8. Kimble, E., et al. *Quaternary functional silsesquioxanes for use in personal care: polysilsesquioxane steardimonium chloride*. in *SCC Technical Showcase*. 2012. New York City, NY.
9. Zhang, H. and V. Oyanedel-Craver, *Evaluation of the disinfectant performance of silver nanoparticles in different water chemistry conditions.* J. Environ. Eng., 2012. **138**: p. 58-66.

10. Zhang, H., J.A. Smith, and V. Oyanedel-Craver, *The effect of natural water conditions on the anti-bacterial performance and stability of silver nanoparticles capped with different polymers.* Water Res., 2012. **46**(3): p. 691-699.

11. Vigeant, M.A., et al., *Reversible and irreversible adhesion of motile Escherichia coli cells analyzed by total internal reflection aqueous fluorescence microscopy.* Appl. Environ. Microbiol., 2002. **68**: p. 2794-2801.

12. Cumberland, S.A. and J.R. Lead, *Particle size distributions of silver nanoparticles at environmentally relevant conditions.* J. Chromatogr. A, 2009. **1216**(52): p. 9099-9105.

13. Song, J., H. Kong, and J. Jang, *Bacterial adhesion inhibition of the quaternary ammonium functionalized silica nanoparticles.* Colloids Surf. B 2011. **82**(2): p. 651-656.

14. Mullet, M., et al., *A simple and accurate determination of the point of zero charge of ceramic membranes.* Desalination, 1999. **121**: p. 41-48.

15. Feng, Q.L., et al., *A mechanistic study of the antibacterial effect of silver ions on Escherichia coli and staphylococcus aureus.* J. Biomed. Mater., 2000. **52**(4): p. 662-668.

16. Sondi, I. and B. Salopek-Sondi, *Silver nanoparticles as antimicrobial agent: a case study on E. coli as a model for Gram-negative bacteria.* J. Colloid Interface Sci., 2004. **275**(1): p. 177-182.

17. Kim, H.W., B.R. Kim, and Y.H. Rhee, *Imparting durable antimicrobial properties to cotton fabrics using alginate–quaternary ammonium complex nanoparticles.* Carbohydr. Polym., 2010. **79**(4): p. 1057-1062.

18. Liu, J. and R.H. Hurt, *Ion release kinetics and particle persistence in aqueous nano-silver colloids.* Environ. Sci. Technol., 2010(44): p. 2169-2175.

19. Fontes, D.E., et al., *Physical and chemical factors influencing transport of microorganism through porous media.* Appl. Environ. Microbiol., 1991. **57**: p. 2473-2481.

20. Jewett, D.G., et al., *Bacterial transport in laboratory columns and filters: influence of ionic strength and pH on collision efficiency.* Water Res., 1995. **7**: p. 1673-1680.

21. Kretzschma, R., et al., *Experimental determination of colloid rates and collision efficiencies in natural porous media.* Water Res., 1997. **33**: p. 1129-1137.

22. EPA, U.S. *http://www.epa.gov/oppsrrd1/REDs/trimethoxysilyl-quats-red.pdf*. . 2007 [cited 2012 Nov. 09]; Available from: http://www.epa.gov/oppsrrd1/REDs/trimethoxysilyl-quats-red.pdf. .

23. Drake, P.L. and K.J. Hazelwood, *Exposure-related health effects of silver and silver compounds: a review.* Ann. Occup. Hyg., 2005. **49**(7): p. 575-585.

24. Korani, M., et al., *Acute and subchronic dermal toxicity of nanosilver in guinea pig.* Int. J. Nanomed., 2011. **6**: p. 855-862.

25. Sung, J.H., et al., *Acute inhalation toxicity of silver nanoparticles.* Toxicol. Ind. Health, 2011. **27**(2): p. 149-154.

26. EPA, U.S. *http://www.epa.gov/iris/subst/0099.htm*. 1987 [cited 2012 Nov. 11]; Available from: http://www.epa.gov/iris/subst/0099.htm.

27. Venugopal, B. and T.D. Luckey, *Metal toxicity in mammals: chemical toxicology of metals and metalloids*. 1978, Academic Press: New York. p. 32-36.

CHAPTER 7

CONCLUSIONS AND FUTURE WORK

7.1 Conclusions

To achieve the three main goals presented in Chapter 1, a systematic investigation on the physicochemical properties and antimicrobial performance of AgNP in electrolyte solutions and natural water conditions was conducted. Studies on the application of AgNP in CWFs manufactured with different clay and burn-out materials as well as application of TPA in CWFs were also conducted.

Various techniques, such as DLS, membrane ultrafiltration and ultrafiltration, and ICP were applied to quantify the particle size, aggregation kinetics, surface charges, and dissolution of AgNP. Antimicrobial performance on *E. coli* and MS2 bacteriophage were evaluated with a nano-metric respirometric technique and double layer technique, respectively. Our results showed that AgNP can achieve up to 90% antibacterial activity. However, negligible antiviral effects of AgNP were observed. The stability of AgNP varies due to the different stabilizers applied. PVP-coated AgNP are most stable compared with casein- and dextrin-coated AgNP. The abovementioned physicochemical properties and antibacterial properties change in different water chemistry conditions.

To apply the antimicrobial property of AgNP in drinking-water treatment, AgNP have been coated on CWFs to purify drinking water. This research also focused on establishing the silver application guidelines for CWF manufacturing. Silver concentration in the effluent of CWFs has been measured to make sure the effluent

concentration is below the U.S. EPA MCL (0.1 ppm) to minimize the negative health impacts of silver. Simple POU CWFs manufactured with different materials and different concentrations of two types of silver (AgNP and Ag^{+}) were studied. Bacterial removal and biofilm formation inside the disks were dose-dependent on the amount of silver applied. However, neither water chemistry conditions nor burn-out material showed an effect on any of the abovementioned parameters evaluated at the silver concentration tested. This study recommends applying a high concentration of AgNP (≥0.3 mg/g) on CWFs to achieve improved antimicrobial performance.

Investigation on the antimicrobial performance of AgNP and TPA showed that TPA-coated CWFs outperformed AgNP in a phosphate buffer solution. Amounts of AgNP or TPA released from CWFs are similar. Our results also showed that the disinfectant performance of TPA-applied CWFs exceeded AgNP-applied CWFs, indicating that TPA can be considered as a good alternative to AgNP.

7.2 Future work

1. Our research on the environmental fate of AgNP has elucidated the dissolution behavior of AgNP in different water chemistry conditions. However, the chronic environmental ecotoxicity of AgNP is still unknown. Future studies are recommended to cover the knowledge gap of their long-term (such as experimental duration in months or longer) toxicological effect on different microorganisms (such as algae and protozoa) and higher organisms (such as small fish embryos) in different water chemistry conditions.

2. In the application of AgNP on CWFs, instead of using CWFs applied with 0.003 mg/g AgNP, we recommend to conduct studies on higher concentrations of AgNP

(such as 0.3 mg/g) under a selection of water chemistry conditions to evaluate nanoparticle aggregation and silver particle size distribution in filter effluence. It is also recommended to evaluate physicochemical interaction between clay and AgNP or Ag^{+} on silver adsorption and LRV and the influence of these properties and the pore size distribution of the porous matrix.

3. Although our study indicated that TPA can be considered as a good alternative to AgNP in CWF applications, more information regarding the long-term health effects of TPA is still needed. As our study focused on bacterial removal performances using a phosphate buffer solution, natural water conditions are recommended to evaluate the practicality of TPA-applied CWFs. Finally, we recommend the spectrum of water-borne pathogens (such as viruses and protozoa) that contribute to waterborne diseases be broadened. Future research on other quaternary ammonia functionalized silane species is also suggested.

APPENDIX A

Table 2-1 Ion composition and pH across various water chemistry conditions

	Cation	Anion		
	Conc.(mg/L)	Conc.(mg/L)	Ionic strength (mM/L)	pH
Ca^{2+} (Cl^-)	1000	1775	75	5.84
	500	887.5	37.5	6.11
	250	443.8	18.8	6.43
	50	88.8	3.8	6.76
	10	17.8	0.8	6.81
Ca^{2+}(NO_3^-)	1000	3100	75	6.13
	500	1550	37.5	6.16
	250	775	18.8	6.27
	50	155	3.8	6.38
	10	31	0.8	6.6
Na^+(Cl)	648	1000	28.2	6.76
	324	500	14.1	6.76
	162	250	7.05	6.77
	32.4	50	1.41	6.79
	6.5	10	0.3	6.79
Na^+(HCO_3^-)	377	1000	16.4	9.26
	188.5	500	8.2	9.16
	94.3	250	4.1	8.78
	18.9	50	0.82	7.5
	3.77	10	0.164	7
K^+(NO_3^-)	629	1000	16.1	6.92
	314.5	500	8.05	6.92
	157.3	250	4	6.92
	31.5	50	0.81	6.91
	6.3	10	0.16	6.91
K^+(SO_4^{2-})	812.5	1000	31.2	7
	406.3	500	15.6	6.99
	203	250	7.8	6.98
	40.6	50	1.56	6.9
	8.1	10	0.3	6.9
Mg^{2+}(SO_4^{2-})	1000	4000	166.8	6.25
	500	2000	83.4	6.34

	250	1000	41.7	6.39
	50	200	8.34	6.42
	10	40	1.7	6.54
Humic acid	20	n/a	n/a	6.5
	10	n/a	n/a	6.65
	2	n/a	n/a	6.66
	1	n/a	n/a	6.66
	0.2	n/a	n/a	6.65

APPENDIX B

1 Natural water sample collection and synthetic water preparation

Water samples were collected in Rhode Island from Thirty Acre Pond (Latitude: +41.489220, Longitude: -71.546375) (surface water), Card Ponds (brackish water) (Latitude: +41.371779, Longitude: -71572486), and Scarborough State Beach (seawater) (Latitude: +41.385189, Longitude: -71.475431). The ground water was obtained at the University of Rhode Island's Kingston campus (Latitude: +41.487122, Longitude: -71.526361). The water samples were transported to the laboratory where they were filtered using filter paper (medium retention, cut-off size: 8 μm, Whatman) to remove suspended solids. Then, the samples were autoclaved for 30 min at 121 ^{0}C to eliminate microbiological contamination. Naturally occurring ions (Ca^{2+}, Mg^{2+}, Na^{+}, K^{+}, Cl^{-}, SO_4^{2-}, and NO_3^{-}) were analyzed using ion chromatography (IC) techniques (DX-120, Dionex). Total alkalinity was determined by phenolphthalein and methyl orange titration. Dissolved natural organic matter (NOM) was measured as total organic carbon (TOC) via a TOC analyzer (Apollo 9000, Tekmar Dohrman). Table S1 summarizes the compositions of all natural water tested. Synthetic water solutions containing $MgCl_2$, $CaCl_2$, and NaCl were prepared by adjusting the cation concentrations to 1,000 mg/L (ionic strength: $MgCl_2$, 125 mmol/L; $CaCl_2$, 75 mmol/L; and NaCl, 43.5 mmol/L) to study the influence of different cations on the disinfection performance and physicochemical characteristics of the nanoparticles. The concentration of 1,000 mg/L was selected because it mimics the concentration of the dominant divalent cation species Mg^{2+} in seawater, in which the AgNP solution exhibited the lowest toxicity[1]. A humic acid solution (TOC: 5 mg/L) was also prepared to study the influence of NOM on the

disinfection properties of AgNP. All salts and other reagents were ACS reagent grade and used as received.

2 Microbial cultures

A non-pathogenic, wild strain of *E. coli* provided by IDEXX laboratories was used for bacteria disinfection experiments. *E. coli* was selected because of its use as a specific indicator of fecal contamination in drinking water and because of its extensive use in several studies on AgNP [2-4].This allows the comparison of our results with the results of previously published work. Bacteria were grown as described by Vigeant et al. (2002) [5]. Cells were re-suspended in a sterilized solution prepared with the respective water samples and synthetic water solution to a concentration of $(1 \pm 0.4) \times 10^{10}$ CFU/mL. Determination of the *E. coli* concentration was performed using the membrane filtration technique, applying m-FC with Rosolic Acid Broth (Millipore) and 24-h incubation at 44.5 ^{0}C.

3 Determination of critical coagulation concentration

In brief, the initial aggregation rate of AgNP in different electrolyte solutions is proportional to the change of particle radius (nm) over time (s) ($\frac{dr}{dt}$)

$$k_{11} \propto \frac{1}{N}\frac{dr}{dt} \quad \text{(eq.1)}$$

Where $k_{11}$is the initial aggregation rate of AgNP; N is the initial nanoparticle concentration.

When the electrolyte concentration in AgNP solution is low, the strong repulsion forces between AgNP will cause a low degree of aggregation, which is termed as slow aggregation. After the added electrolyte solution reaches a certain concentration, the

aggregation of AgNP falls into the rapid aggregation regime, where the aggregation energy barriers are completely removed and the aggregation rate is independent of the increasing electrolyte concentration [6].

The attachment efficiency " α ", also defined as the inverse stability ratio (1/W), was determined by calculating the ratio of a given k_{11} over the $(k_{11})_{rapid}$, which is the normalized k_{11} value in the rapid aggregation regime.

$$\alpha = \frac{1}{W} = \frac{k_{11}}{(k_{11})_{rapid}} = \frac{\frac{dr}{dt}}{(\frac{dr}{dt})_{rapid}} \quad \text{(eq.2)}$$

Critical coagulation concentration (CCC) is defined as the estimate of the minimum electrolyte concentration required to reach the rapid aggregation regime. It is determined by the intersection of the extrapolations between the slow and rapid aggregation regime [6]. In this study, CCC was determined as x-axis coordinate of the point of intersection between the linear regression line of attachment efficiencies in the rapid aggregation regime and the linear regression line of attachment efficiencies in the slow aggregation regime.

For all the aggregation kinetics experiments, the same concentration of AgNP as used in the antibacterial assay was applied (11.5 mg/L). DLS measurements of AgNP solutions recorded the hydrodynamic radius as a function of time at 10 s time intervals. The initial aggregation rate of AgNP was calculated by conducting a linear least-squares regression analysis of hydrodynamic radius over time. Electrolyte solutions including monovalent salt (NaCl) solution (Na^+ concentration: 4,000-80,000 mg/L) and divalent salt ($CaCl_2$) solution (Ca^{2+} concentration: 100-8,000 mg/L) were prepared to compare the effect of valence on the CCC values of AgNP. Humic acid (HA) solution (TOC: 5 mg/L)

mimicking the NOM was chosen to compare the aggregation kinetics in presence and absence of HA.

4 Anti-bacterial assay

Different water samples and synthetic water solutions with monovalent salts, divalent salts, and humic acid were prepared. Bacteria deactivation batch tests were performed in duplicate using manometric respirometric equipment (OxiTop control system, WTW Weilheim, Germany). An OxiTop control system includes a sample bottle sealed with a measuring head, a small container for CO_2 absorbent fixed at the neck of the bottle, and an OxiTop controller for data recording. The test was based on automated pressure measurements conducted via piezoresistive electronic pressure sensors in a closed bottle at constant temperature. The anti-bacterial assay was conducted as described by Zhang and Oyanedel-Craver. (2011) [7]. Different amount of electrolytes solutions, DI water, and 10 mL *E. coli* (total 100 mL mixture, *E. coli* concentration: 10^{10} CFU/mL) were inoculated into sample bottles. The sample bottles were sealed with the measuring heads and placed in the incubator at 25 ^{0}C. The endogenous respiration was determined by measuring the pressure drop within 2-3 h without adding carbon source or nanoparticles. Then, 0.5 mL glucose of a 70 g/L was injected to determine the oxygen uptake rate (OUR) without AgNP. Previous tests demonstrated that the amount of glucose used was not fully consumed during the time length the tests were conducted (data not shown). Finally, after about 2-3 h, 0.25 mL AgNP stock solution was injected into the bottles to determine the alteration of the OUR due to the reduction of bacteria. The total duration of the experiments was 20 h. The percentage of the bacteria reduction using a modified equation from Tzoris et al. (2005) [8] was calculated using equation 1:

$$\text{Disinfection Performance}(\%) = \left(\frac{P_c - P}{P_t - P}\right) \times 100 \quad \text{(eq.3)}$$

Where P_c is the OUR after the injection of glucose, P_t is the OUR after the injection of AgNP, and P is the OUR during the endogenous respiration without the addition of carbon source or nanoparticles. Figure A-1 presents a typical respiration curve. The control groups without applying AgNPwere used to measure the toxicity of different water conditions on *E. coli*. Natural water samples or electrolyte solutions were mixed with10 mL *E. coli* (prepared in the same water condition) to a total 100 mL mixture, and an*E. coli* concentration of 10^{10} CFU/mL. The endogenous respiration was determined by measuring the pressure drop within 2-3 h without adding a carbon source. Then, 0.5 mL of a 70 g/L aqueous glucose solution was injected to determine the OUR without AgNP.The intrinsic bacteria decayat the different water conditionshave already been subtracted leaving the pure disinfection performance of AgNP on *E. coli*. Compared to conventional deactivation methods based on microbial growth (such as plate count methods), the manometric respirometric method determines the activity of all active bacteria (not only those that are able to grow). Other advantage is that this method is based on the total oxygen uptake rate of all bacteria while the plate count method could miscount colonies grown from bacteria aggregates because it considers them as individual bacteria. A typical respiration curve in DI water is shown in Figure A-1:

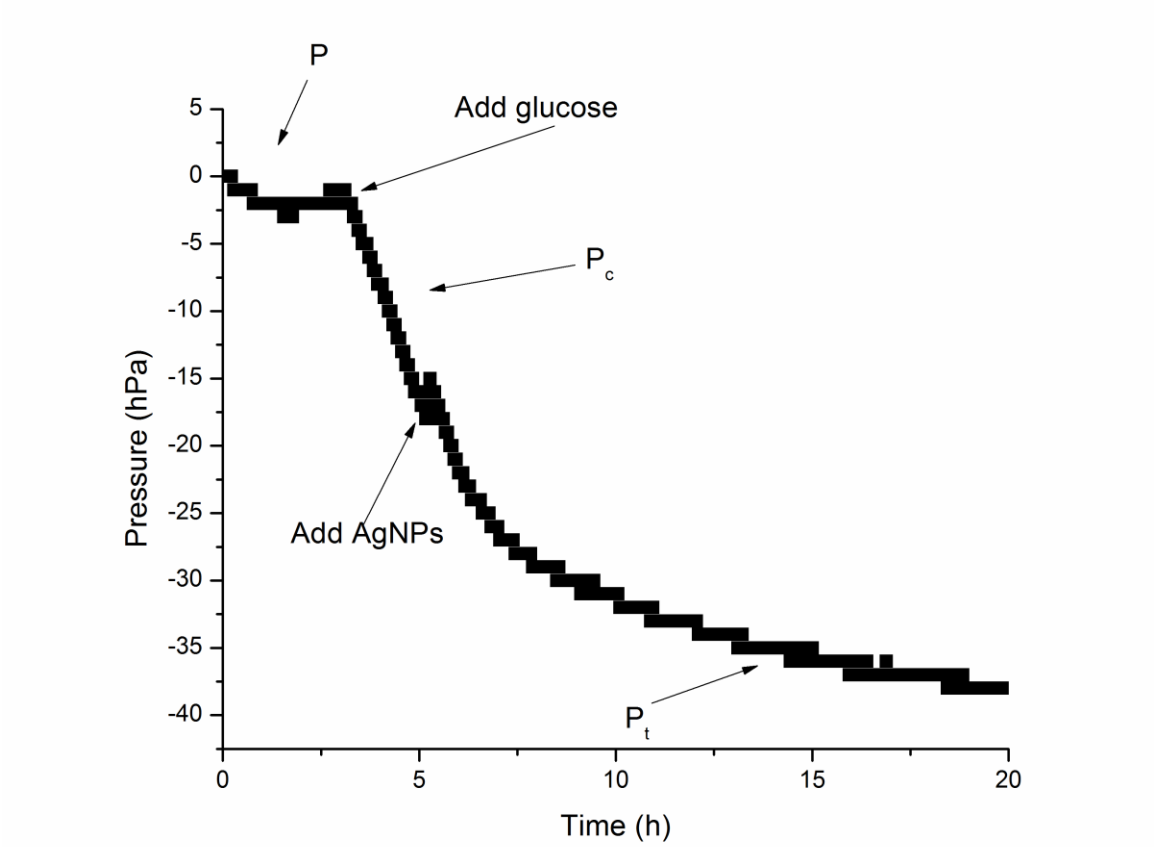

Figure B-1. A typical respiration curve after 20 h of incubation at 25 ^{0}C with glucose injection: 35 mg and AgNP concentration: 11.5 mg/L. P: Oxygen uptake rate during endogenous respiration; P_c: Oxygen uptake rate after the injection of glucose; P_t: Oxygen uptake rate after injection of AgNP.

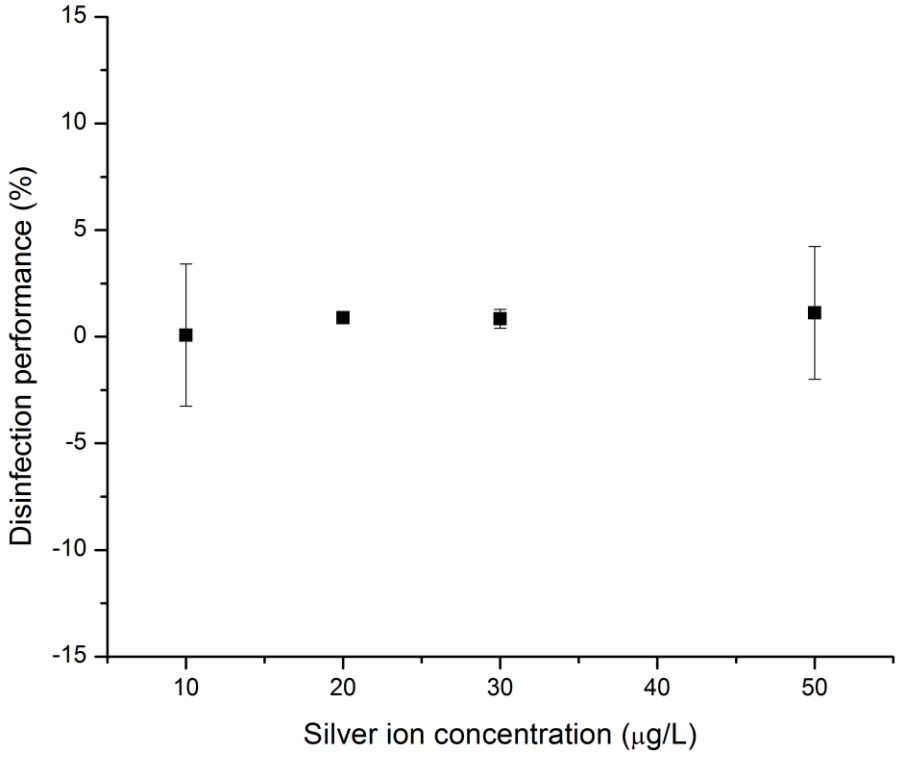

Figure B-2 Effect of silver ion concentration on the disinfection performance.

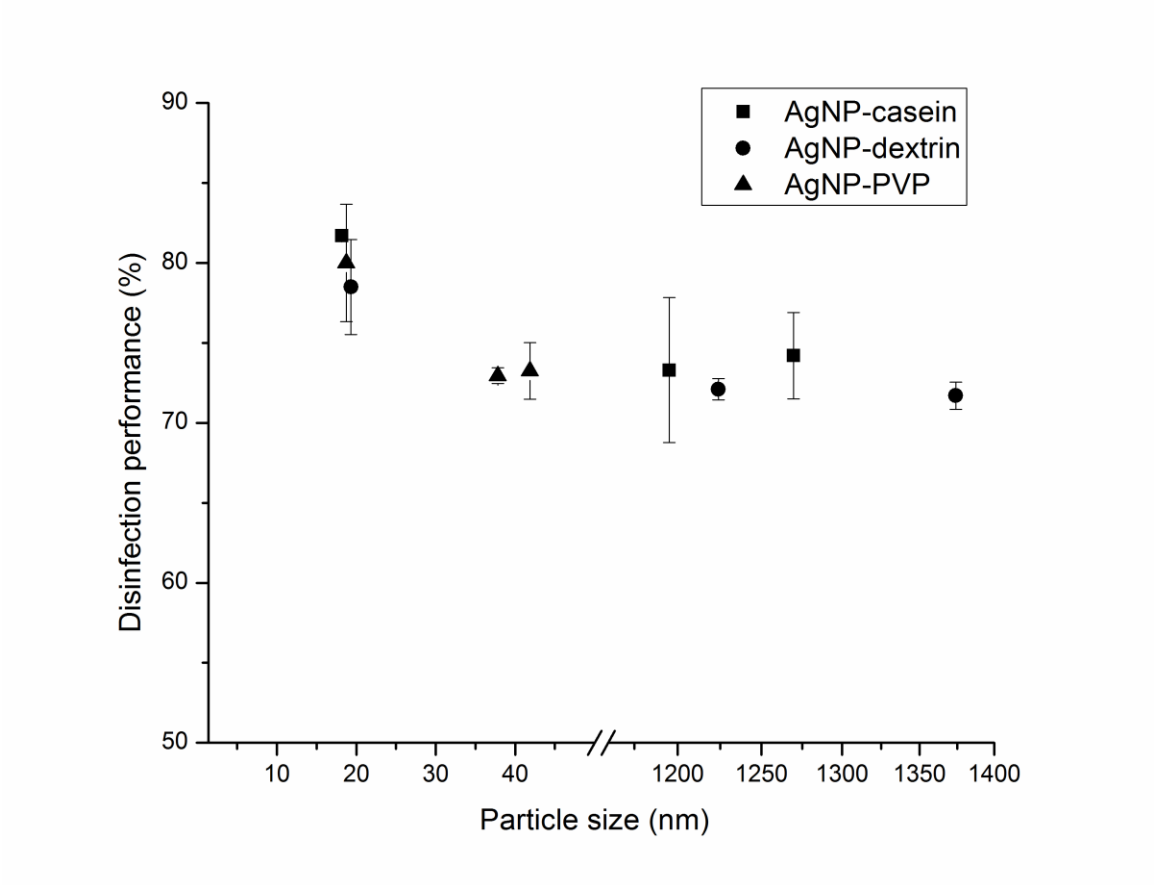

Figure B-3 Correlation of disinfection performance with particle size in the synthetic water conditions without NOM content ($MgCl_2$, $CaCl_2$ and NaCl solutions). The general trends show that the disinfection performance of the individual AgNP decreases with increasing particle size.

Table B-1 Solution chemistries of natural water samples

DL: Detection limit

Water samples	TOC (mg/L)	Alkalinity ($mgCaCO_3/L$)	Total Ag (μg/L)	Major ions (mg/L)							Ionic Strength (mmol/L)
				Na^+	K^+	Mg^{2+}	Ca^{2+}	Cl^-	NO_3^-	SO_4^{2-}	
Ground water	<DL	80	0.077	22	3	3	26	43	2	12	2.93
Surface water	5.7	25	0.127	14	3	2	6	25	<DL	9	1.35
Brackish water	7.8	33	0.1	300	12	30	14	520	<DL	76	18.7
Seawater	2.5	150	0.343	10,100	400	1,100	340	18,300	<DL	2,500	642

Table B-2 Comparison of particle sizes measured by DLS and TEM

Methods / AgNP	Average DLS sizes (nm)	Average TEM sizes (nm)
AgNP-casein	58.0 ±2.6	12.6 ±5.7
AgNP-dextrin	27.9 ±0.3	11.6 ±4.4
AgNP-PVP	29.64 ±1.7	13.1 ±5.4

Table B-3 CCC values of AgNP in $CaCl_2$ and NaCl solutions in the absence and presence of HA

CCC of AgNP / Solutions	CCC of AgNP-dextrin (mg/L)	CCC of AgNP-casein (mg/L)	CCC of AgNP-PVP (mg/L)
$CaCl_2$ solutions (TOC: 0 mg/L)	365	517	2,087
$CaCl_2$ solutions (TOC: 5 mg/L)	863	986	4,799
NaCl solutions (TOC: 0 mg/L)	8,043	34,183	59,090
NaCl solutions (TOC: 5 mg/L)	14,203	51,045	80,420

Table B-4 Correlation matrix of experimental parameters

		Disinfection performance	Particle Size	ZetaPotential	Silver ion Release	Cl^- concentration	TOC	DivalentCation concentration
Disinfection performance	Pearson Correlation	1	-.306	-.609**	.779**	-.544**	-.463*	-.595**
	Sig. (2-tailed)		.121	.001	.000	.003	.015	.001
Particle size	Pearson Correlation	-.306	1	.496**	-.237	.247	-.322	.641**
	Sig. (2-tailed)	.121		.008	.233	.214	.102	.000
Zeta potential	Pearson Correlation	-.609**	.496**	1	-.485*	.420*	.015	.635**
	Sig. (2-tailed)	.001	.008		.010	.029	.941	.000
Silver ion release	Pearson Correlation	.779**	-.237	-.485*	1	-.254	-.216	-.364
	Sig. (2-tailed)	.000	.233	.010		.201	.280	.062
Cl^- concentration	Pearson Correlation	-.544**	.247	.420*	-.254	1	-.078	.777**
	Sig. (2-tailed)	.003	.214	.029	.201		.700	.000
TOC	Pearson Correlation	-.463*	-.322	.015	-.216	-.078	1	-.296
	Sig. (2-tailed)	.015	.102	.941	.280	.700		.134
DivalentCation concentration	Pearson Correlation	-.595**	.641**	.635**	-.364	.777**	-.296	1
	Sig. (2-tailed)	.001	.000	.000	.062	.000	.134	

**. Correlation is significant at the 0.01 level (2-tailed).

*. Correlation is significant at the 0.05 level (2-tailed).

Table B-5 Correlation matrix between disinfection performance and particle size

		Disinfection performance	Particle size
Disinfection performance	Pearson Correlation	1	-.891**
	Sig. (2-tailed)		.000
Particle size	Pearson Correlation	-.891**	1
	Sig. (2-tailed)	.000	

**. Correlation is significant at the 0.01 level (2-tailed).

REFERENCES

1. Gao, J., et al., *Dispersion and toxicity of selected manufactured nanomaterials in natural river water samples: effects of water chemical composition.* Environ Sci Technol, 2009. **43**: p. 3322-3328.
2. Choi, O., et al., *The inhibitory effects of silver nanoparticles, silver ions, and silver chloride colloids on microbial growth.* Water Res, 2008. **42**(12): p. 3066-3074.
3. Morones, J.R., et al., *The bactericidal effect of silver nanoparticles.* Nanotechnology, 2005. **16**(10): p. 2346-2353.
4. Oyanedel-Craver, V.A. and J.A. Smith, *Sustainable colloidal-silver-impregnated ceramic filter for point-of-use water treatment.* Environ Sci Technol, 2008. **42**: p. 927-933.
5. Vigeant, M.A., et al., *Reversible and irreversible adhesion of motile Escherichia coli cells analyzed by total internal reflection aqueous fluorescence microscopy.* Appl Environ Microbiol, 2002. **68**: p. 2794-2801.
6. Huynh, K.A. and K.L. Chen, *Aggregation kinetics of citrate and polyvinylpyrrolidone coated silver nanoparticles in monovalent and divalent electrolyte solutions.* Environ Sci Technol, 2011. **45**(13): p. 5564-5571.
7. Zhang, H. and V. Oyanedel-Craver, *Evaluation of the disinfectant performance of silver nanoparticles in different water chemistry conditions.* Journal of Environmental Engineering, 2012. **138**: p. 58-66.

8. Tzoris, A., V. Fernandez-Perez, and E.A.H. Hall, *Direct toxicity assessment with a mini portable respirometer.* Sensors and Actuators B: Chemical, 2005. **105**(1): p. 39-49.

APPENDIX C

Table C-2 Physical properties of ceramic disks manufactured with different materials

Clay source and Burn-out material	Advection coefficient (cm/min)	Dispersion coefficient (cm^2/min)	Geometric Porosity (%)
Indo-sawdust	0.06 ±0.01	0.01 ±0.01	57 ±1.5
Tanz-sawdust	0.06 ±0.01	0.01 ±0.00	59 ±1.8
Nica-sawdust	0.09 ±0.01	0.05 ±0.03	54 ±1.5
Indo-rice husk	0.05 ±0.01	0.01 ±0.00	54 ±0.5
Tanz-rice husk	0.06 ±0.01	0.01 ±0.00	54 ±1.3
Nica-rice husk	0.10 ±0.01	0.09 ±0.05	49 ±1.6

Table C-3 Silver concentration in effluent over time from disks coated with different concentrations of silver

Disk material	Silver type	Concent-ration (mg/g)	Silver in effluent (ppb) over time (min) and equivalent time (days) and throughput (Liters) in full-sized filter			
			100 min <1 day 9 L	200 min <2 days 18 L	300 min ~2.5 days 27 L	1440 min ~12 days 130 L
Indo-Sawdust	AgNP	0.003	86	73	4	ND
		0.03	314	139	14	1
		0.3	456	407	165	27
	Ag^+	0.003	223	36	2	ND
		0.03	887	449	52	42
		0.3	20935	3368	1063	797
Tanz-Sawdust	AgNP	0.003	141	67	24	ND
		0.03	198	78	28	ND
		0.3	2377	634	59	46
	Ag^+	0.003	187	84	14	6
		0.03	1816	209	127	51
		0.3	27705	5404	1751	1414
Nica-Sawdust	AgNP	0.003	155	32	17	ND
		0.03	236	130	75	31
		0.3	2927	1517	946	198
	Ag^+	0.003	181	323	94	17
		0.03	2842	1206	218	65
		0.3	25528	22321	7688	2698
ND: not detected						

Table C-4 Silver concentration in effluent over time using different influent water characteristics

Disk material	Silver type	Water characteristic	Silver in effluent (ppb) over time (min) and full-sized filter equivalent time (days) and throughput (L)			
			100 min <1 day 9 L	**200 min <2 days 18 L**	**300 min ~2.5 days 27 L**	**1440 min ~12 days 130 L**
Indo-Sawdust	AgNP	NaCl	109	48	10	4
		$CaCl_2$	121	31	6	ND
		HA	113	58	19	7
	Ag^+	NaCl	138	34	29	26
		$CaCl_2$	120	61	44	10
		HA	196	44	22	8
Tanz-Sawdust	AgNP	NaCl	132	34	22	ND
		$CaCl_2$	124	35	18	ND
		HA	171	49	22	2
	Ag^+	NaCl	189	52	16	ND
		$CaCl_2$	50	36	10	5
		HA	173	82	27	5
Nica-Sawdust	AgNP	NaCl	161	68	19	5
		$CaCl_2$	197	43	15	2
		HA	184	52	23	6
	Ag^+	NaCl	130	85	42	3
		$CaCl_2$	184	63	32	13
		HA	239	112	47	10
Indo-Rice husk	AgNP	NaCl	103	65	41	5
		$CaCl_2$	141	29	14	8
		HA	160	33	26	3
	Ag^+	NaCl	141	45	4	4
		$CaCl_2$	118	66	10	8
		HA	110	49	36	16
Tanz-Rice husk	AgNP	NaCl	127	33	30	<1
		$CaCl_2$	103	54	46	9
		HA	135	49	32	ND
	Ag^+	NaCl	132	51	30	8
		$CaCl_2$	193	46	23	ND
		HA	234	114	40	5
Nica-Rice husk	AgNP	NaCl	152	80	30	8
		$CaCl_2$	147	78	40	11
		HA	133	90	57	ND
	Ag^+	NaCl	194	65	39	5
		$CaCl_2$	189	42	24	ND
		HA	263	160	25	19
ND: not detected						

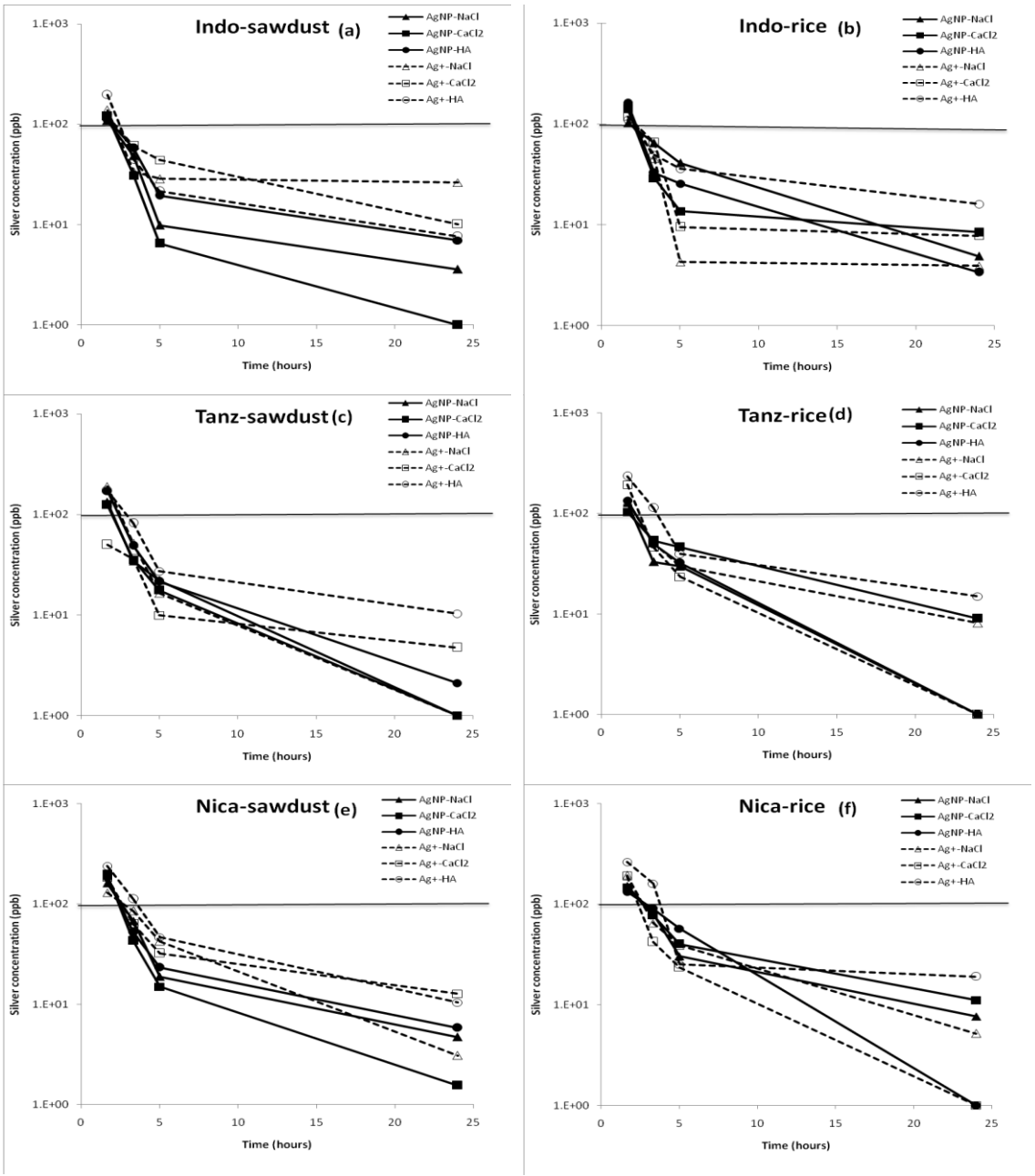

Figure C-4Concentration of silver in effluent (ppb) as a function of time (hours) from disks manufactured with Indonesian clay and sawdust (a) or rice husk (b), Tanzanian clay and sawdust (c) or rice husk (d), and Nicaraguan clay and sawdust (e) or rice husks (f) as burn-out material using different influent water chemistry conditions.

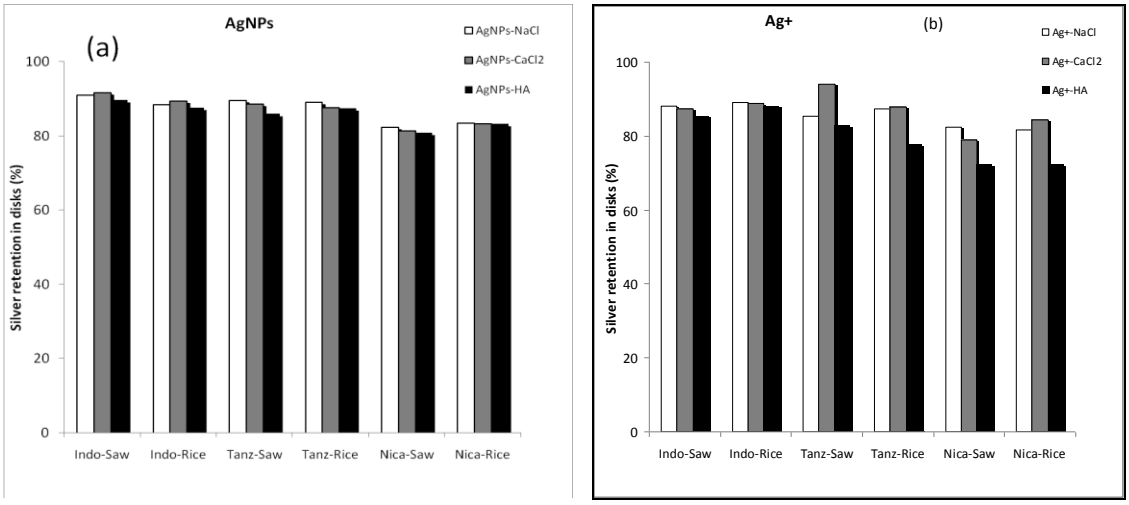

Figure C-5 Percent silver retention in disks manufactured with clay from Indonesia, Tanzania or Nicaragua and Sawdust (saw) or rice husk (rice) as burn-out material coated with 0.003 mg/g of AgNP (a) or Ag+ (b) using different influent water chemistry conditions

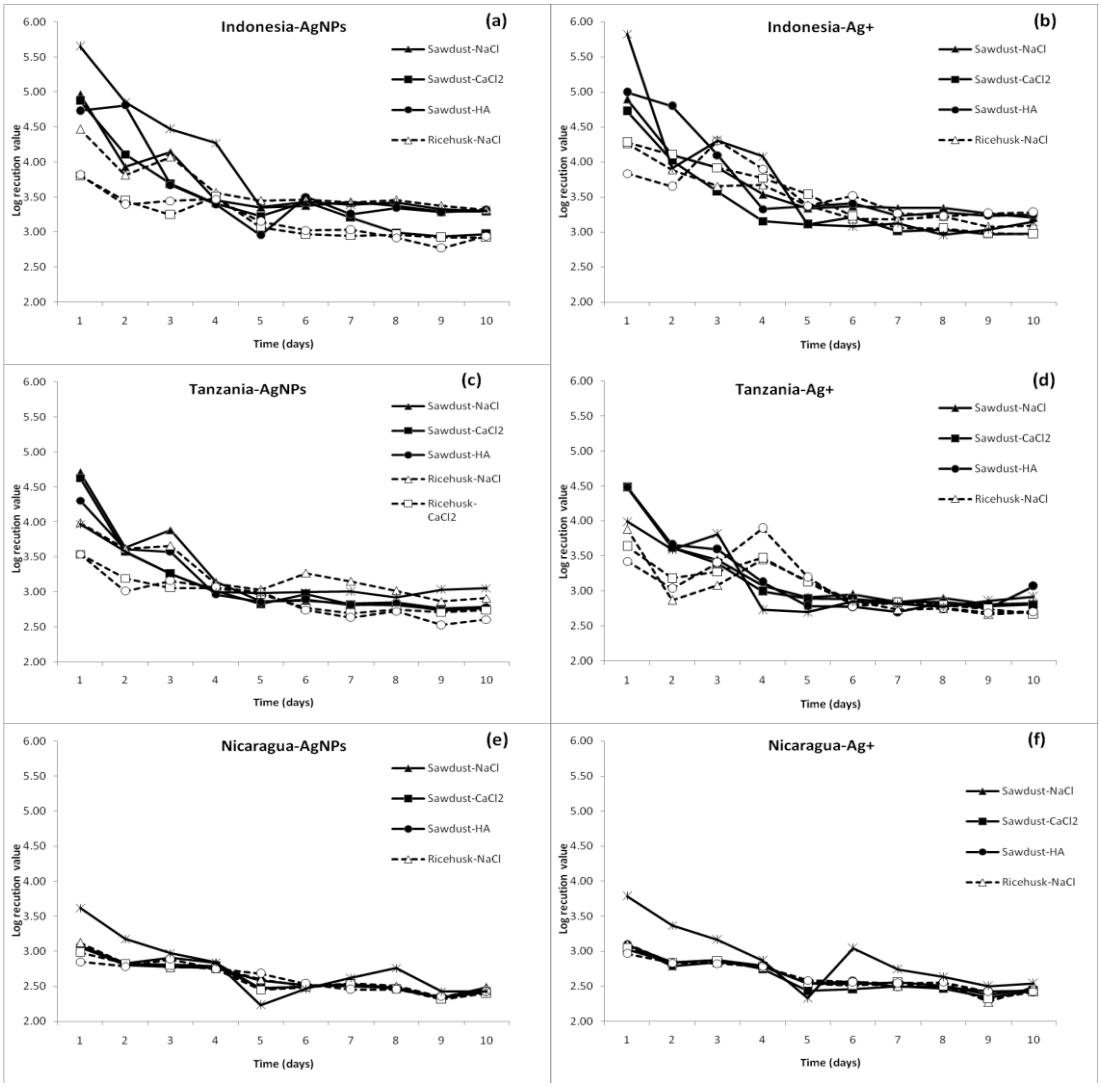

Figure C-6 LRV of disks made with sawdust and Indonesian clay with AgNP (a) or Ag+ (b), Tanzanian clay with AgNP (c) or Ag+ (d) and Nicaraguan clay with AgNP (e) or Ag+ (f) using different influent water chemistry conditions

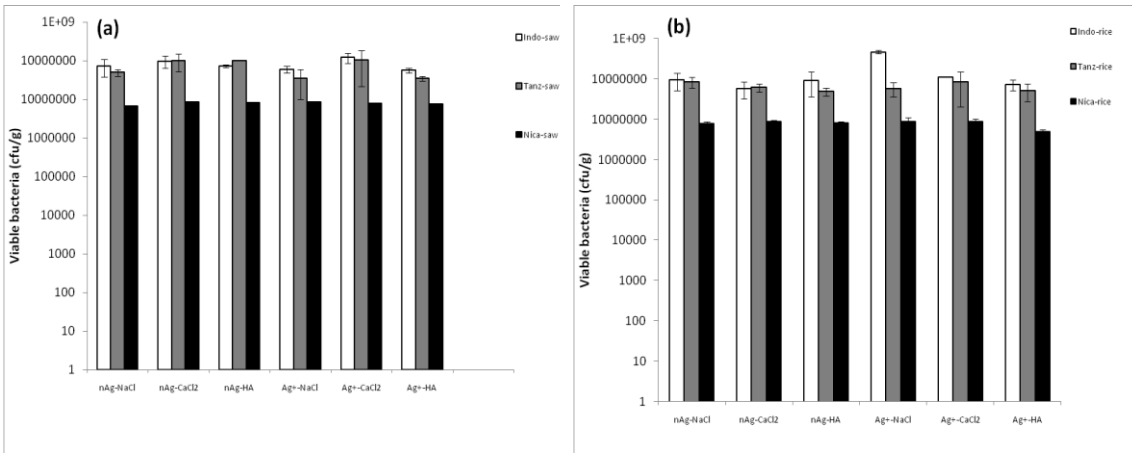

Figure C-7 Viable bacteria detected in disks coated with 0.003 mg/g of AgNP or Ag^+ manufactured with various clays and sawdust (saw) (a) or (b) rice husk (rice) as burn-out material using different influent water chemistry conditions.

APPENDIX D

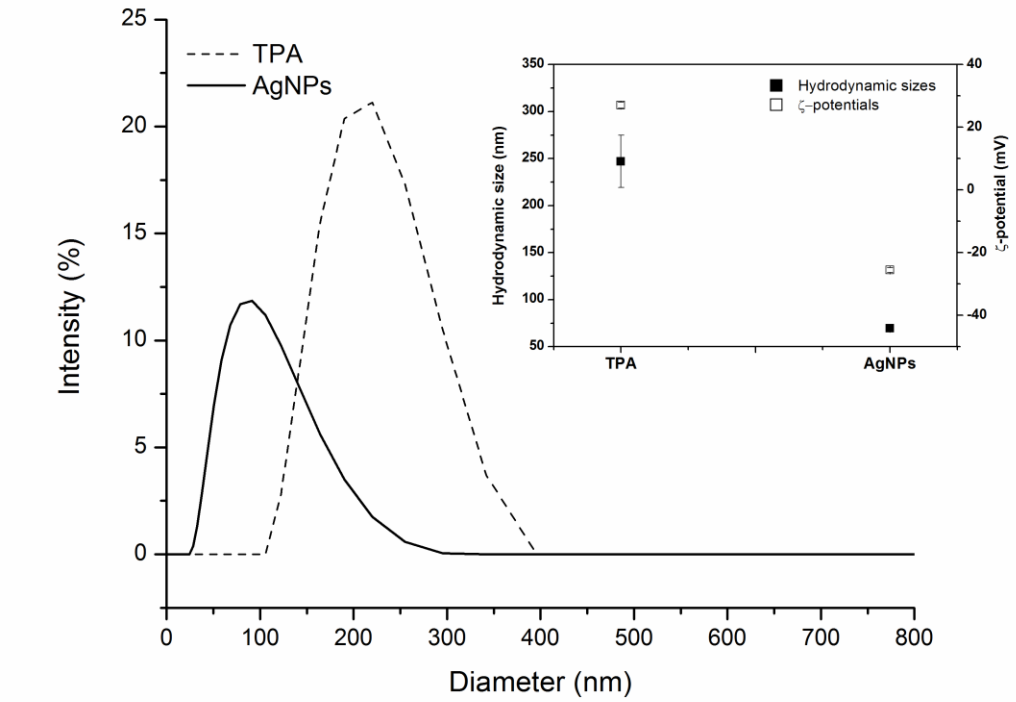

Figure D-1 Average particle sizes, ζ-potentials, and particle size distribution of AgNP and TPA 10% phosphate buffer solution.